The Mononuclear Molybdenum Enzymes†

Russ Hille

Department of Medical Biochemistry, The Ohio State University, Columbus, Ohio 43210-1218

Received March 28, 1996 (Revised Manuscript Received August 7, 1996)

Contents

Russ Hille was born in Tyler, TX, in 1951. He received a B.S. in Chemistry from Texas Tech University in 1974 and a Ph.D. in Biochemistry from Rice University in 1979. After postdoctoral work at the University of Michigan, in affiliation with the Department of Biological Chemistry and the Michigan Society of Fellows, he took a faculty position in the Department of Medical Biochemistry at The Ohio State University, where he is now Professor. His principal research interests concern the mechanism of action of molybdenum- and flavin-containing enzymes and biological electron transfer.

I. Introduction

Molybdenum is widely available to biological systems due to the solubility of its high-valent oxides in water and is found in two basic forms: as an integral component of the multinuclear M center of nitrogenases[1,2] and as the mononuclear active sites of a much more diverse group of enzymes that in general function catalytically to transfer an oxygen atom either to or from a physiological acceptor/donor molecule. It is on the basis of this commonly encountered aspect of catalysis that these enzymes are frequently referred to as oxotransferases,[3] although no mechanistic connotation is intended in using the term. Similarly, the vast majority of these enzymes possess a Mo═O unit in their active sites and are often referred to as oxomolybdenum enzymes.[4] Neither of these terms is strictly applicable to the entire class of enzymes, however, as some (polysulfide reductase, for example, and possibly formate dehydrogenase) do not catalyze oxygen atom transfer, and others do not possess a Mo═O unit. Here the term mononuclear molybdenum enzymes will be used in order to be as generic as possible. These mononuclear molybdenum enzymes constitute a fairly large class of enzymes that can be divided into two subcategories on the basis of the reaction catalyzed. The first of these is a quite large family of enzymes whose members catalyze the oxidative hydroxylation of a diverse range of aldehydes and aromatic heterocycles in reactions that necessarily involve the cleavage of a C−H bond. These enzymes are properly considered hydroxylases,[5] although product tautomerization in reactions involving heterocyclic substrates usually results in the keto rather than enol form predominating in aqueous solution. The second category includes enzymes that typically catalyze proper oxygen atom transfer reactions to or from an available electron lone pair of substrate and can itself be subdivided into two families. The first of these consists of well-known enzymes such as sulfite oxidase and the assimilatory nitrate reductases (*i.e.*, those enzymes whose physiological function is to reduce nitrate to nitrite in the first step of its reduction to ammonia for utilization by the cell). The second is a family made up of bacterial enzymes such as DMSO reductase and biotin-*S*-oxide reductase, as well as the bacterial dissimilatory (or respiratory) nitrate reductases: those periplasmic or membrane-associated enzymes that function as terminal respi-

† This review is dedicated to Professor R. C. Bray in recognition of his 40 years of contribution to the study of molybdenum-containing enzymes.

S0009-2665(95)00061-6 CCC: $25.00

ratory oxidases. From a simple spectroscopic standpoint, the distinguishing feature that sets the DMSO reductase family apart from that exemplified by sulfite oxidase is the presence of a long-wavelength charge-transfer band ($\lambda_{max} > 700$ nm) in the electronic spectrum of the molybdenum centers of the former enzymes.

The purpose of the present account is to provide a comprehensive survey of the literature concerning the structure and function of the mononuclear molybdenum enzymes. The emphasis, however, will be on more recent results, particularly with regard to structural and mechanistic aspects of these enzymes.

II. Overview of the Mononuclear Molybdenum Enzymes

A. Structure and Biosynthesis of the Pterin Cofactor

In all known cases the enzymes considered here possess a pterin cofactor having the following basic structure:

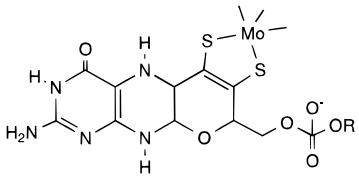

This structure has been established crystallographically in the molybdenum-containing aldehyde oxidoreductase from *Desulfovibrio gigas* and DMSO reductase from *Rhodobacter sphaeroides*.[6,7] The basic pterin ring structure and dithiolene side chain had been elucidated previously by chemical analysis of several modified or inactivated forms of the cofactor extracted from purified enzymes[8−11] and corroborated by chemical synthesis of the metabolic degradation product urothione,[12,13] but the pyran ring had gone undetected and was established crystallographically. Indeed, the identical three-ring system had previously been observed in the tungsten-containing aldehyde oxidoreductase from *Pyrococcus furiosus*,[14] a protein that possesses the same type of pterin cofactor as the molybdenum enzymes[15] and appears to have an active-site structure loosely related to that of the DMSO reductases and related enzymes (see below).

In both the molybdenum enzymes whose structures have been determined crystallographically,[6,7] as well as the one tungsten enzyme similarly defined,[14] the cofactor is found to be coordinated via its dithiolene side chain to the metal (in the case of the molybdenum-containing DMSO reductase from *Rhodobacter sphaeroides* and the tungsten-containing aldehyde: ferredoxin oxidoreductase from *Pyrococcus furiosus*, two molecules of the cofactor are bound; see below), with a twist of approximately 40° in the pyran ring so that the structure of the enzyme-bound cofactor is distinctly nonplanar.[6,14] It is significant that the pterin nucleus itself does not coordinate directly to the metal. Inorganic complexes of molybdenum possessing coordinated pterin species have been a synthetic goal for the past decade or more,[16−18] but while such complexes have interesting chemistry in their own right, it appears unlikely on the basis of the protein structures that this chemistry will prove to be directly relevant to the reaction mechanism of the molybdenum-containing enzymes. It should be borne in mind that although the pterin cofactor is frequently referred to by the trivial name molybdopterin,[10] it has been found in a variety of tungsten-containing enzymes as well,[15,19] and the term in any case refers to the metal-free organic cofactor only. In the present account, this organic component of the molybdenum centers of these enzymes will simply be referred to as the pterin cofactor.

In enzymes from eukaryotic systems the pterin cofactor possesses the structure shown above, but in enzymes from prokaryotic sources it can be found as the dinucleotide of guanine,[20] cytosine,[21] adenine,[22] or hypoxanthine.[22] In the molybdenum-containing aldehyde oxidoreductase from *Desulfovibrio gigas*, the pterin cytosine dinucleotide found in this enzyme is bound in a fully extended form,[6] and it is likely that the cofactor in other enzymes possessing a dinucleotide form will be found to bind in a similar fashion.

In 1964 Pateman and co-workers discovered a family of pleiotropic mutations in *Aspergillus niger* that resulted in nonfunctional forms of both nitrate reductase and xanthine dehydrogenase, and inferred that these resulted from the inability of the mutant strains to synthesize a cofactor common to the two enzymes.[23] Since that time the biosynthesis of the pterin cofactor in several organisms has been actively investigated, both from the standpoint of establishing the genes involved in the biosynthetic pathway and the chemical nature of precursors.[24,25] In *E. coli*, the proteins required for biosynthesis of the pterin cofactor are encoded in the *moa-mog* gene systems (formerly designated *chlA*−*G*).[26] The enzymes responsible for biosynthesis of the mononucleotide form of the pterin cofactor are encoded by the *moa* and *moe* operons and are discussed further below. The *mob* locus consists of at least two genes,[27] *mobA* and *mobB*,[28] the first of which encodes a pterin guanine dinucleotide synthase that adds GMP (using GTP as donor) to the molybdenum-complexed pterin cofactor[29] (called Protein FA in earlier work[28]). The role of the second gene product of *mob* is not known at present; it appears not to be strictly essential for biosynthesis of the pterin cofactor, but does enhance the activity of the dinucleotide synthase under some conditions.[30] The *modABCD* gene products, on the other hand, have been known for some time to be involved in uptake of molybdate by the organism.[31−34] The complete operon has recently been sequenced[35,36] and the ModA gene product over-expressed and characterized.[37] The protein is found to be a 28.6 kDa periplasmic protein that appears to be the initial molybdate-binding protein of the transport system, with relatively high affinity for both molybdate and tungstate (4 and 7 μM, respectively).[37] It is thought to deliver bound molybdate to ModB (24.9 kDa), localized on the periplasmic side of the inner membrane of *E. coli*, which in conjunction with ModC internalizes the molybdate.[36] ModC possesses an

Scheme 1

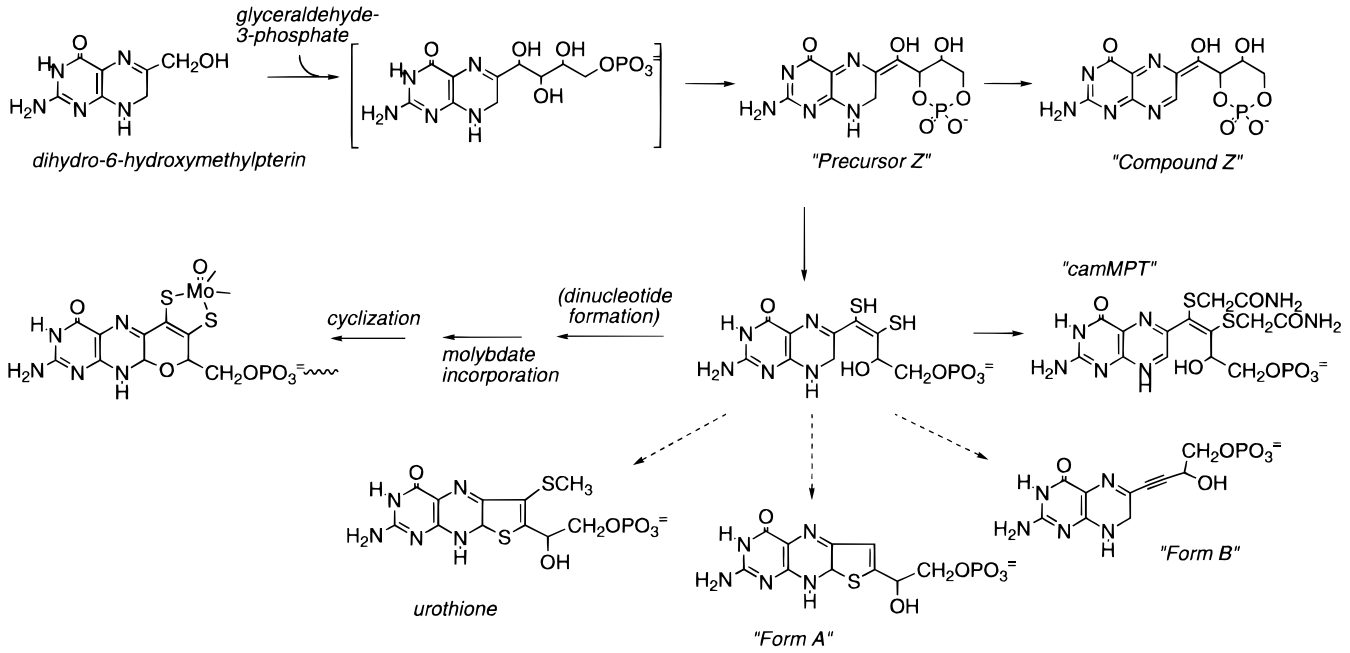

ATP-binding motif and presumably couples internalization of molybdate with ATP hydrolysis. No function in molybdate uptake has yet been assigned to ModD, and indeed deletion of *modD* produces no phenotype characteristic of impaired molybdate uptake.[37] The gene products of the *E. coli modABC* locus exhibit 23−43% sequence identity with the corresponding *mod* loci of *Azotobacter vinelandii*[38] and *Rhodobacter capsulatus*.[39]

The *moa* operon of *E. coli* encodes five proteins: *moaA*−*E*,[40] which correspond to *chlA1*−*chlA5* in the older designation. The *moaA* gene encodes a protein of M_r 37 300 having the N-terminal sequence (M)-ASQLTDAFAR...; from a sequence comparison with the *cnxB* gene product of *Arabadopsis thaliana*, it is evident that *moaA* possesses an internal motif common to guanine-binding proteins.[41] *moaB* encodes a protein having M_r = 18 700, with the N-terminal amino acid sequence (M)SQVSTEFIPT..., and *moaC* one of M_r 17 200 with an N-terminal sequence of (M)-SQLTHINAAG... These three proteins are thought to be involved in very early stage(s) of the biosynthesis of a metabolic intermediate to the mature cofactor designated precursor Z (see below).[40] It is of interest that *moaB* possesses a folate-binding motif[40,42] and may represent an intracellular carrier protein. A *molR* gene product is required for effective function of the *moa* operon,[43] presumably as a regulatory element that may mediate repression of the *moa* operon by the mature pterin cofactor. The *mog* gene product exhibits some homology to that for *moaB* and has been implicated in presenting molybdenum to the mature cofactor prior to insertion in enzymes;[42] it has also been implicated in the process of molybdenum incorporation into apoprotein, and may be homologous to a cofactor carrier protein termed Mop that has been characterized from *Chlamydomonas reinhardtii*.[44]

The final step in the biosynthesis of the pterin cofactor proper is catalyzed by molybdopterin synthase (known as "converting factor" in earlier work[45,46]), a heterodimer of M_r 27 000 having subunits of M_r 10 000 and 16 000.[45] On the basis of protein and gene sequence comparisons, it is clear that the larger subunit is the gene product of *moaE* (formerly *chlA5*). The gene encoding the smaller subunit has apparently not yet been identified by direct sequence comparison, but is thought to be *moaD* (formerly *chlA4*).[25] This conclusion is supported by the observation that a *chlM* mutation (old nomenclature) mapping to *moaD* is known to result in loss of synthase activity and accumulation of the precursor[26] and that of the open reading frames of the *moa* operon only *moaD* encodes a putative protein of the correct molecular weight for the smaller subunit of the synthase.[25] The sulfur atoms that become incorporated into the dithiolene moiety of the mature cofactor have been shown to arise directly from the smaller subunit of the synthase.[46] The protein responsible for charging the smaller subunit of the synthase with sulfur is encoded by the *moeB* genes (*chlN* in the old designation), possibly with the involvement of the *moeA* gene product (formerly *chlE*),[46] but the chemical nature of the labile sulfur of the charged synthase has not yet been elucidated. The pterin substrate for the synthase, which has been given the name "precursor Z", has been examined by mass spectrometry and NMR and possesses a 2′,4′ phosphodiester as its side chain, but lacks the dithiolene moiety that coordinates the molybdenum[47] (see Scheme 1). It has been suggested that the pterin ring of the precursor is in the dihydro oxidation state, but is readily (and reversibly) oxidized to a fluorescent species designated "compound Z" that possesses a fully oxidized pterin ring.[48,49] This latter species is relatively stable and accumulates in substantial amounts in mutant strains of *E. coli* that are defective in molybdopterin synthase activity.[48]

The crystal structure of the aldehyde oxidoreductase from *D. gigas* indicates the presence of a glycine residue, Gly623, in the molybdenum-binding portion of the protein that is conserved among the hydrox-

ylase family of mononuclear molybdenum enzymes.[6] Although not particularly close to the molybdenum center (it is approximately 11 Å away, quite near the solvent access channel to the active site), a G1011E mutant at the comparable position of the *Drosophila melanogaster* xanthine dehydrogenase has been analyzed, and its molybdenum center found to possess unusual properties. The mutant as isolated has an intact but nonfunctional molybdenum center that is incapable of oxidizing xanthine, but can be irreversibly activated upon treatment with a strongly oxidizing cocktail of ferricyanide, phenazine methosulfate, and cytochrome *c*.[50] The results have been interpreted as indicating that a species having a reduction potential in the range +80 to +250 mV, possibly the pterin ring of the cofactor, must be oxidized for development of full catalytic activity.[50] It has been suggested that the pterin cofactor is incorporated into the protein as an inactive tetrahydro ring-opened derivative, which undergoes pyran ring closure (and development of full catalytic activity) only after having been oxidized to the level of dihydropterin.[50] It is thus possible that the form of the cofactor incorporated into these enzymes in fact possesses the structure originally proposed by Kramer *et al.*[11] in which the side chain is not cyclized but found as the ring-opened free hydroxyl derivative (but at the oxidation level of tetrahydropterin).

Earlier steps in the biosynthesis of the pterin cofactor are at present less clear, and there is apparent disagreement in the literature on the point as to whether the pathway leading to the mature cofactor shares common steps with known metabolic pathways or whether it represents a new pathway altogether. Irby and Adair,[51] investigating cofactor biosynthesis in the yeast *Pichia canadensis*, found that label arising from either [7-^{14}C]neopterin or [6,7,1-^{14}C]hydroxymethylpterin, both of which are assimilated at known stages of the folate biosynthetic pathway, was incorporated into a well-characterized oxidation product of the cofactor designated "dephospho Form A", as well as into folate. Use of [6-^{14}C]-glucose led to incorporation of label into this same oxidation product of the pterin cofactor (but not into folate), and it was suggested that the glycolytic intermediate glyceraldehyde 3-phosphate might be the source of the 3-carbon unit whose incorporation into 6-(hydroxymethyl)pterin yields a side chain possessing the correct number of carbons. These workers have concluded that biosynthesis of the pterin cofactor shares steps with the folate biosynthetic pathway up to the point of (dihydroxymethyl)-pterin (Scheme 1) and that condensation with glyceraldehyde 3-phosphate may represent the first committed step of pterin cofactor biosynthesis. By contrast, Wuebbens and Rajagopalan[52] have concluded from similar labeling studies in *E. coli* that the early steps in cofactor biosynthesis represent a new metabolic pathway altogether. The key observation in this work is that label from [8-^{14}C]guanosine was essentially quantitatively retained in the pterin ring of compound Z. These authors concluded that guanosine cyclohydrolase, which catalyzes the first step in the folate biosynthetic pathway in a manner that results in loss of the C-8 carbon of guanosine, is not involved in the utilization of guanosine to synthesize the pterin cofactor and that the pathway must therefore represent a totally new metabolic route. Interestingly, it is found that the retained label originating at C-8 is lost upon formation pterin-6-carboxylate, a side-chain-shortened species generated from purified compound Z by treatment with alkaline permanganate.[52] This suggests that the C-8 carbon of guanosine is retained in compound Z as one of the three distal carbons of the pterin side chain. Given that these two studies involved quite different organisms, the results are not directly contradictory. In *Pichia*, at least, it appears that biosynthesis of the pterin cofactor proceeds via the pathway shown in Scheme 1, in which steps leading from guanosine to dihydro-6-(hydroxymethyl)pterin are shared with the folate biosynthetic pathway. Incorporation of glyceraldehyde 3-phosphate into the pterin side chain has been suggested to take place via an aldolase reaction, after which cyclization and oxidation yield precursor Z.[51] The gene products of *moaA−C* are presumably involved in this step of the metabolic sequence. The metabolic pathway for the biosynthesis of the pterin cofactor has important clinical implications because in humans genetic lesions resulting in an inability to properly synthesize the pterin cofactor lead to a combined sulfite oxidase and xanthine oxidase deficiency that is manifested by serious neurological abnormalities and mental retardation (presumably associated with the systemic accumulation of sulfite).[53,54]

The role of the pterin cofactor in the reaction mechanisms of the mononuclear molybdenum enzymes has been the subject of considerable speculation.[24,55] Given that the stoichiometry of reducing equivalents taken up by enzymes such as xanthine oxidase in the course of catalysis are quantitatively accounted for by their canonical redox-active cofactors,[56] it is unlikely that the pterin cofactor is itself reversibly reduced in the course of catalysis. On the basis of the crystal structure of the *D. gigas* aldehyde oxidoreductase,[6] however, two quite specific roles for the cofactor can be inferred: mediation of electron transfer to other redox-active centers (but not involving a frank change in oxidation state of the pterin ring) and modulation of the molybdenum reduction potential. Quite remarkably, in aldehyde oxidoreductase the amino group of the cofactor distal to the dithiolene side chain is hydrogen bonded to one of the cysteine ligands to a 2Fe-2S center that is also present in the enzyme. It is thus extremely likely that the pterin mediates electron transfer out of the molybdenum center of the enzyme in the course of turnover, although not in such a way that it is itself transiently reduced. In support of this interpretation it is found that in the enzyme sulfite oxidase, two-electron oxidation of the native dihydropterin cofactor of the enzyme to the fully oxidized form (by reaction with ferricyanide) does not greatly compromise the reactivity of the molybdenum center toward sulfite, but does reduce significantly the ability of the enzyme to reduce cytochrome *c* (the physiological oxidant for this enzyme, which interacts with the heme center of the enzyme) at the expense sulfite.[55] These results have been interpreted as indicating that oxidation

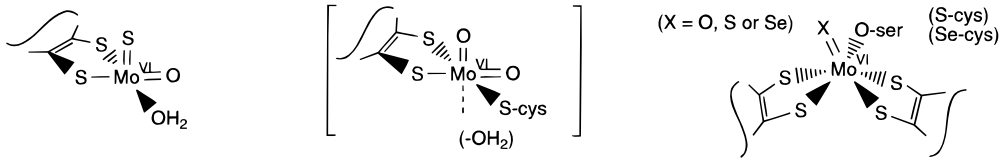

The Xanthine Oxidase Family (true hydroxylases) *The Sulfite Oxidase Family* *The DMSO Reductase Family*

Figure 1. The major families of mononuclear molybdenum enzymes. Members of the xanthine oxidase family (*i.e.*, the true hydroxylases) have molybdenum centers consisting of a single cofactor dithiolene ligand coordinated to a *fac*MoOS-(H_2O) unit. Members of the sulfite oxidase family are likely to possess a single cofactor dithiolene coordinated to a *cis* MoO_2 unit (additional coordination positions may be taken up by water and/or a cysteine residue that is conserved within the family; see the text). Members of the DMSO reductase family are distinguished by bisdithiolene coordination of the molybdenum, but this group of enzymes is likely to be more structurally diverse than the other two families. The Mo=X position may be taken up by oxygen, sulfur, or (possibly) selenium, while the sixth ligand coordination position may be occupied by serine, cysteine, or selenocysteine.

of the pterin cofactor compromises electron transfer from the molybdenum to the heme of sulfite oxidase.

A second likely role for the pterin cofactor is modulation of the reduction potential of the molybdenum center. One specific mechanism by which this is likely to occur is evident from the conformational changes that occur in the molybdenum coordination environment upon reduction of the *D. gigas* aldehyde oxidoreductase.[57] Particularly significant is the observation that the sulfur−sulfur distance of the dithiolene moiety increases from 3.0 to 3.5 Å, with the S−Mo−S bond angle also increasing considerably upon reduction of the enzyme. Given that the van der Waals radius of sulfur is 1.85 Å, the S−S distance of 3.0 Å seen in the oxidized enzyme presumably reflects considerable covalency between the two sulfurs (*i.e.*, disulfide bond formation).[58] To the extent that this occurs, the dithiolene ligand contributes considerably greater electron density to the metal and the reduction potential for the molybdenum center is expected to decrease as a result. (It is known that aldehyde oxidoreductase, xanthine oxidase, and related enzymes operate in a quite low oxidation−reduction regime.) Such a role for the pterin cofactor in modulating the molybdenum reduction potential has in fact been anticipated on the basis of the structures of relatively simple inorganic complexes of molybdenum such as L_2MoO_2(L=$SC(CH_3)_2CH_2NH(CH_3)$)[59] and $[Mo_2O_4(SC_6H_5)_4]^{2-}$.[60] In these compounds sulfur−sulfur distances of 2.8−3.0 Å are found, again indicative of partial disulfide bond character. The increased electron-donating capacity of the dithiolene ring with (partial) disulfide bond formation may also contribute to the stability of a Mo(VI) center in the enzyme that is only five-coordinate (see below).

It has been suggested previously that the pterin cofactor may act as the proximal oxo donor to substrate, specifically in the form of a pterin 4a-hydroxide species.[24,55] In general, however, pterin and flavin 4a-hydroxides are not reactive as hydroxylating species but instead simply split out water to return to the fully oxidized form. Pterin- or flavin-containing hydroxylases instead use 4a-peroxides as the hydroxylating species in their reaction mechanisms, which yield the 4a-hydroxide after transfer of the distal oxygen of the peroxide to give the hydroxylated product. Also, in the case of the aldehyde oxidoreductase (and probably also for other members of the xanthine oxidase family) a direct role for the pterin cofactor in the reaction catalyzed is unlikely since the cofactor lies on the opposite side of the metal from the clearly defined solvent access channel by which substrate undoubtedly enters the active site.[6]

B. Categories and General Structures of the Active Sites

The mononuclear molybdenum enzymes are most reasonably categorized on the basis of the structures of their molybdenum centers, and in the present discussion the enzymes will be described in the context of the three families discussed above, as exemplified by xanthine oxidase, sulfite oxidase, and DMSO reductase. As stated previously, the crystal structure for aldehyde oxidoreductase from *D. gigas*, a member of the xanthine oxidase family (the true hydroxylases), has recently been reported,[6,57] as has that for the DMSO reductase from *Rhodobacter sphaeroides*.[7] In addition, it is possible to infer several important aspects of the structure of the molybdenum center of the sulfite oxidase family, given that in some ways these enzymes may be considered to be intermediate between the xanthine oxidase and DMSO reductase families. With the caveat kept in mind that the structural features for the sulfite oxidase family presented here are somewhat speculative, the active sites of the three families of mononuclear molybdenum enzymes may be represented as indicated in Figure 1.

Considering first the xanthine oxidase family, as represented by the *D. gigas* aldehyde oxidoreductase, the molybdenum coordination sphere of the oxidized enzyme is found to possess a distorted square-pyramidal coordination geometry, with the metal lying approximately ~0.5 Å out of the equatorial plane toward the apical position.[6] As indicated above, the pterin cofactor (present as the cytosine dinucleotide) is coordinated to the molybdenum via its dithiolene side chain, which is ring closed to give a third, pyran ring in the protein. The pterin dithiolene defines the equatorial plane of the molybdenum coordination sphere. The pyran and pterin rings of the cofactor are nonplanar by some 40° and the pyrazine ring of the pterin is itself distinctly puckered, consistent with the pterin being reduced rather than oxidized. The three remaining ligand coordination positions to the metal, including the

apical position, are occupied by oxygen derived from solvent in the form of enzyme initially crystallized. There is no protein ligand to the molybdenum, although a glutamate (E869) lies sufficiently close to the metal (at 3.5 Å, and more or less *trans* to the apical position) that it might coordinate the metal with relatively minor changes in its position.

In the structure originally reported, the oxygen ligands were left undesignated, but it has been known for some time from X-ray absorption studies that the molybdenum coordination sphere of xanthine oxidase from cow's milk[61−63] and xanthine dehydrogenase[64] from chicken liver possess both an oxo and sulfido ligand to molybdenum in their oxidized forms. Both enzymes are inactivated by cyanide,[65] which results in release of the sulfur as thiocyanate and replacement of the Mo═S with a second Mo═O to give the so-called "desulfo" form of the enzymes.[62,64,65] The aldehyde oxidoreductase sample initially investigated crystallographically was known to be in the corresponding desulfo form of this enzyme, but more recently, the crystal structure has been solved with a form of the enzyme that has been resulfurated by incubation with sulfide under turnover conditions.[57] It is found that electron density at the apical position of the molybdenum coordination sphere both enlarges and moves away from the metal by approximately 0.4 Å, as expected for substitution of Mo═S for Mo═O. This result is extremely surprising since the oxo group in simple molybdenum complexes is known to predominate in the metal coordination sphere and to exert a particularly strong *trans* effect, weakening ligand coordination opposite the metal to it.[3,66] On this basis it would have been expected that the Mo═O group occupied the apical coordination position of the molybdenum in the enzyme, but this is apparently not the case. Instead, the shorter of the two Mo−O groups in the equatorial plane, that opposite the 8′-S of the cofactor dithiolene and having a Mo−O distance of ∼1.8 Å, has been assigned the Mo═O.[57] This distance is consistent with a Mo═O distance of 1.7 Å as established by X-ray absorption spectroscopy (XAS),[61−64] but surprisingly gives a coordination geometry having an oxo group *trans* to one of the dithiolene sulfurs. The other Mo−O in the equatorial plane is longer at ∼2.4 Å and has been assigned to a bound water rather than hydroxide on the basis of the long bond length. Given the present resolution of the data (2.25 Å), it is possible that this water in fact occupies a position more *trans* to the apical Mo═S, in which case the molybdenum coordination geometry is distorted from square pyramidal toward trigonal bipyramidal with the attractive result that neither of the dithiolene sulfurs is strictly *trans* to the Mo═O. In any case, the metal-bound water molecule is within hydrogen-bonding distance of Glu 869 in the crystal structure of the oxidized enzyme, and it has been suggested that the two interact, with the protonated carboxylate side chain acting as a hydrogen-bonding donor.[6] The apical Mo═S has the imidazole of His 653 as nearest neighbor (at ∼3.2 Å) and is probably hydrogen bonded to it. The Mo═O group is in a quite sterically constrained environment and has the backbone amide of Arg 533, the backbone carbonyl of Phe 421 and C_α of Gly 422 as nearest neighbors. The metal-bound water faces directly into the extended solvent channel that provides access to the active site, opposite the metal from S7′ of the pterin cofactor dithiolene. Overall, the crystal structure is quite consistent with the results of the previous XAS results with xanthine oxidase and xanthine dehydrogenase,[61−64] which had established that in addition to the Mo═O and Mo═S groups at ∼1.7 and 2.15 Å, respectively, the molybdenum coordination sphere possesses at least two thiolate ligands at a distance of approximately 2.4 Å. XAS studies have also shown that in of the reduced forms of these enzymes,[63,64] the Mo═S bond lengthens by approximately 0.3 Å, and this has been interpreted as resulting from protonation to give a Mo^{IV}−SH. There is comparable evidence in the crystal structure data for lengthening of this bond upon reduction of the aldehyde oxidoreductase.[57]

The crystal structure of DMSO reductase from *Rhodobacter sphaeroides*[7] has recently been reported, and it is found that the metal is coordinated by two molecules of the pterin cofactor (both in the guanine dinucleotide form, with the two dinucleotides extending from the active site in opposite directions). The overall molybdenum coordination geometry is distorted trigonal prismatic, as indicated in Figure 1, with a single Mo═O and a serine alkoxide ligand to the metal in addition to the four ligands contributed by the 2 equiv of pterin cofactor. The Mo═O is approximately *trans* to one of the dithiolene sulfur ligands, and upon reduction of the enzyme the Mo−S distance for this bond increases significantly, from 3.1 to 3.7 Å, indicating that the bond is essentially ruptured upon reduction of the metal.[7] In addition, the Mo═O group is lost with the result that there is a significant reduction in molybdenum coordination in going from Mo(VI) to Mo(IV). These results are generally consistent with a recent study of the *R. sphaeroides* DMSO reductase by X-ray absorption spectroscopy.[67] The oxidized enzyme is found to be a monooxo Mo(VI) center with approximately four thiolate ligands at 2.44 Å and an oxygen/nitrogen at 1.92 Å; reduction of the enzyme with dithionite results in loss of the short Mo═O at 1.68 Å and appearance of an additional Mo−O/N (possibly arising from protonation of the Mo═O of oxidized enzyme). The bis(dithiolene) coordination of the molybdenum center in DMSO reductase has also been confirmed recently by biochemical means,[68] and it is to be noted that there is abundant precedent for monooxo Mo(VI) complexes in the inorganic literature.[69] Overall, the metal coordination bears some resemblance to that seen in the tungsten site of the aldehyde:ferredoxin oxidoreductase from *Pyrococcus furiosus* in that it is also coordinated by 2 equiv of pterin cofactor[14] and possesses a single oxo group in its activated form.[70] This structural homology between the tungsten- and molybdenum-containing enzymes exists despite there being only minimal protein sequence homology between aldehyde:ferredoxin oxidoreductase[71] and DMSO reductase.[72−74]

With the above structural results for aldehyde oxidoreductase and DMSO reductase in mind, it is possible to make some statement as to the likely coordination geometry of the remaining family of

mononuclear molybdenum enzymes, that exemplified by sulfite oxidase and the assimilatory nitrate reductases. Starting with the conclusion from several X-ray absorption studies that the oxidized enzymes possess two Mo=O groups,[75−77] it is clear from a wide variety of model compound studies that these are most likely to be mutually *cis* to one another in the molybdenum coordination sphere.[3,66,78] Although there are enough remaining ligand coordination positions (assuming an octahedral geometry) for two dithiolene ligands, the XAS data indicates that there are no more than a total of three thiolates in the molybdenum coordination sphere, and MALDI-TOF mass spectral analysis yields a protein molecular weight consistent with the presence of only a single pterin cofactor.[79] Thus, as in the *D. gigas* aldehyde oxidoreductase structure described above, it appears likely that a single dithiolene ligand to molybdenum defines an equatorial plane in the case of sulfite oxidase and related enzymes. One of the Mo=O groups must then occupy an axial position and the other lie in the equatorial plane, corresponding to the positions of the Mo=S and Mo=O groups, respectively, seen in the hydroxylase family of molybdenum enzymes. The remaining coordination position(s) are most likely occupied by water and/or a cysteine thiolate, consistent with the observation of a conserved cysteine residue in the amino acid sequences of chicken sulfite oxidase and nitrate reductases from a variety of sources.[80,81] Recent site-directed mutagenesis studies of both nitrate reductase (from *Aspergillus nidulans*)[82] and sulfite oxidase (both rat and human)[83] have provided strong evidence that cysteine does in fact directly coordinate to the molybdenum as mutation of this residue (Cys 150 in nitrate reductase, Cys 207 in sulfite oxidase to alanine or serine) results in loss of activity and, in the case of the human sulfite oxidase, a significant perturbation of the absorption spectrum of the molybdenum center. In light of the structures for aldehyde oxidoreductase and DMSO reductase, it would appear likely that the molybdenum coordination environment of sulfite oxidase and related enzymes possesses either square pyramidal or octahedral coordination geometry with the cofactor dithiolene defining the equatorial plane.

Table 1 gives a list of the known molybdenum-containing enzymes for which there was information as of the end of 1995. It is seen that members of the xanthine oxidase family are broadly distributed, with eukaryotic, prokaryotic, and archaeal representatives. Members of the sulfite oxidase family, on the other hand, are largely restricted to eukaryotes while members of the DMSO reductase family have to date only been found in bacteria and archaea. The form the pterin cofactor takes in a given enzyme appears to be largely related to species of origin rather than enzyme function or classification: enzymes isolated from *E. coli*, including the organism's dissimilatory nitrate reductases, possess the guanine dinucleotide form of the cofactor, for example. All eukaryotic enzymes, including aldehyde oxidase, possess the mononucleotide form of the cofactor, but the aldehyde oxidoreductase from *D. gigas* possesses the cytidine dinucleotide form of the cofactor. It should be noted, however, that least one organism, *Hydrogenophaga pseudoflava*, is able to synthesize both the guanine and cytosine dinucleotide forms of the pterin cofactor and incorporate these specifically into its dissimilatory nitrate reductase and CO dehydrogenase, respectively.[84,85] On the other hand, the formylmethanofuran dehydrogenase isolated from *Methanobacterium thermoautotrophicum* is found to be quite indiscriminate in its preference for the cofactor, possessing the guanine, adenine, and hypoxanthine dinucleotides in the ratio 1.0:0.4:0.1.[22]

The establishment of the three principal families of mononuclear molybdenum enzymes given above has been substantively justified in a number of recent studies establishing amino acid sequence homologies among known molybdenum-containing enzymes, making it possible to identify and classify many new molybdenum-containing enzymes on the basis of sequence homologies to known molybdenum enzymes.[86] Members of the xanthine oxidase family, for example, share substantial sequence homology (typically ~25% sequence identity and 60−70% sequence similarity). It is noteworthy that unlike other members of this family, which catalyze hydroxylation reactions, CO dehydrogenase from organisms such as *Pseudomonas carboxidovorans* catalyzes the oxidation of CO to CO_2.[87] Formally, this reaction can be categorized as an oxygen atom transfer to the carbon lone pair of CO, by analogy to the reactions catalyzed by the other families of mononuclear molybdenum enzymes, but it has been clearly established that CO dehydrogenase is irreversibly inactivated by cyanide in the same manner as the other members of the xanthine oxidase family, and presumably possesses the Mo=S group that is characteristic of this family.[88]

The molybdenum hydroxylases invariably possess redox-active sites in addition to the molybdenum center and are found with two basic types of polypeptide architecture. Enzymes of the first group, including the eukaryotic xanthine oxidases, xanthine dehydrogenases, and aldehyde oxidases,[5] as well as the *D. gigas* aldehyde oxidoreductase,[6,89] are α_2 homodimers in which the several redox-active cofactors are found in distinct domains within a single polypeptide. Members of this group have in common a folding pattern that proceeds (from the N-terminus) to give a pair of discrete 2Fe-2S domains, followed by a flavin domain (absent in the aldehyde oxidoreductase of *D. gigas*) and finally the molybdenum-binding portion of the protein.[86,90,91] The remaining hydroxylases, all from bacterial and archaeal sources (including the CO dehydrogenases,[92,93] along with those enzymes metabolizing quinoline-related compounds,[94−100] and derivatives of nicotinic acid[101−104]) form a separate group in which each of the redox-active centers are found in separate subunits. Those enzymes possessing flavin subunits[94−96,102−104] are organized as $\alpha_2\beta_2\gamma_2$, with a pair of 2Fe-2S centers in the α subunit, the flavin in the β subunit and the molybdenum in the γ subunit. Those enzymes lacking a flavin unit have the makeup $\alpha_2\beta_2$, with a pair of 2Fe-2S centers again in the α subunits and the molybdenum in the β subunits. Interestingly, the recently characterized xanthine dehydrogenase from

Table 1. The Oxomolybdenum Enzymes[†]

enzyme	source	subunits	cofactor[a]
The Xanthine Oxidase Family (LMoOS-Possessing Enzymes)[‡]			
xanthine oxidase	cow's milk[b]	α_2	MPT
xanthine dehydrogenase	chicken liver[c]	α_2	MPT
	rat liver[d]	α_2	MPT
	Micrococcus lactyliticus[e]		
	Drosophila melanogaster[f]	α_2	MPT
	Chlamydomonas reinhardtii[g]		
	human[h]	α_2	(MPT)
aldehyde oxidase	rabbit liver[i]	α_2	(MPT)
	human[j]	α_2	(MPT)
	cow[k]	α_2	(MPT)
aldehyde oxidoreductase (dehydrogenase)	*Desulfovibrio gigas*[l]	α_2	MCD
	Acetobacter polyoxogenes[m]		
formate dehydrogenase	*Alcaligenes eutrophus*[n]	$\alpha\beta\gamma\delta$	
	Methylosinus trichosporum[o]	$\alpha_2\beta_2\gamma_2\delta_2$	
CO dehydrogenase (oxidoreductase)	*Pseudomonas carboxydovorans*[p]	$\alpha_2\beta_2\gamma_2$	
	Pseudomonas carboxydoflava[q]	$\alpha_2\beta_2\gamma_2$	MCD
	Oligotropha carboxidovorans[r]	$\alpha_2\beta_2\gamma_2$	MCD
quinoline-2-oxidoreductase	*Pseudomonas putida* [s]	$\alpha_2\beta_2\gamma_2$	MCD
	Rhodococcus sp. B1[t]	$\alpha_2\beta_2\gamma_2$	MCD
	Comamonas testosteroni 63[u]	$\alpha_2\beta_2\gamma_2$	MCD
isoquinoline 1-oxidoreductase	*Pseudomonas diminuta*[v]	$\alpha\beta$	MCD
quinoline-4-carboxylate-2-oxidoreductase	*Agrobacterium* sp. 1B[w]	$\alpha_2\beta_2\gamma_2$	MCD
quinaldine-4-oxidoreductase	*Arthrobacter* sp.[x]	$\alpha_2\beta_2\gamma_2$	MCD
quinaldic acid 4-oxidoreductase	*Serratia marcescens*[y]		
	Pseudomonas sp. AK-2[z]	$\alpha\beta$	
nicotinic acid hydroxylase (dehydrogenase)	*Clostridium barkeri*[aa,ab]	α_2	
	Bacillus niacini[ac]	$\alpha_2\beta_2\gamma_2$	
	Arthrobacter oxidans[ad]	$\alpha\beta\gamma$	
6-hydroxynicotinate hydroxylase	*Bacillus niacini*[ac]	$\alpha\beta\gamma$	
nicotine dehydrogenase	*Arthrobacter oxidans*[ad]	$\alpha\beta\gamma$	
	Arthrobacter nicotinovorans[ae]		
picolinate hydroxylase	*Arthrobacter picolinophilus*[af]	$\alpha_2\beta_2\gamma_2$	MCD
(2*R*)-hydroxycarboxylate oxidoreductase	*Proteus vulgaris*[ag]		
The Sulfite Oxidase Family ($LMoO_2$-Possessing Enzymes)[§]			
sulfite oxidase	bovine liver[ah]	α_2	MPT
	chicken liver[ai]	α_2	MPT
	rat liver[aj]	α_2	MPT
	human[ak]	α_2	MPT
	Thiobacillus novellus[al]	α	
nitrate reductase (assimilatory)	*Neurospora crassa*[am]	α_2	MPT
	spinach[an]	α_2	MPT
	Chlorella vulgaris[ao]	α_4	MPT
The DMSO Reductase Family (L_2MoX-Possessing Enzymes)[‖]			
DMSO reductase	*Rhodobacter sphaeroides*[ap]	α	MGD
	Rhodobacter capsulatus [aq]	α	MGD
	Escherichia coli [ar]	$\alpha\beta\gamma$	MGD
biotin-*S*-oxide reductase	*Escherichia coli*[as]		
trimethylamine-*N*-oxide reductase	*Escherichia coli*[at]	α_2	
nitrate reductase (dissimilatory)	*Escherichia coli* (NarGHI)[au]	$\alpha\beta\gamma$	MGD
	Escherichia coli (NarZYV)[av]	$\alpha\beta\gamma$	MGD
	Escherichia coli (FdoGHI)[aw]	$\alpha\beta\gamma$	MGD
	Paracoccus denitrificans (NapABCD)[ax]	$\alpha\beta\gamma\delta$	
	Haloferax volcanii[ay]		
formate dehydrogenase	*Escherichia coli* (FdhF)[az]	α	MGD
	Escherichia coli (FdnGHI)[ba]	$\alpha\beta\gamma$	MGD
	Escherichia coli (FdoGHI)[bb]	$\alpha\beta\gamma$	MGD
	Methanobacterium formicicum[bc] (*X*=*S*)	$\alpha\beta\gamma$	MGD
	Wollinella succinogenes[bd]	$\alpha\beta\gamma$	
polysulfide reductase	*Wolinella succinogenes*[be]	$\alpha\beta\gamma$	MGD
arsenite oxidase	*Alcaligenes faecalis*[bf]	α	MCD
formylmethanofuran dehydrogenase	*Methanobacterium thermoautotrophicum*[bg] (*X*=*S*)	$\alpha\beta\gamma\delta\epsilon(\zeta)$	MGD, MAD, MHD
	Methanosarcina barkeri[bh]		MGD
Unclassified Molybdenum-Containing Enzymes			
pyridoxal oxidase	*Drosophila melanogaster*[bi]		
chlorate reductase	*Proteus mirabilis*[bj]		
tetrathionite reductase	*Proteus mirabilis*[bj]		
xanthine dehydrogenase	*Clostridium* sp.[bk,ab]		
pyruvate:ferredoxin oxidoreductase	*Archaeoglobus fulgidus*[bl]		
pyrogallol transhydroxylase	*Pelobacter acidigallici*[bm]		
2-furoyl-CoA dehydrogenase	*Pseudomonas putida*[bn]		

Footnotes to Table 1

† Entries under a given enzyme name are intended to reflect species distribution and/or enzymes of a fundamentally different nature, as discussed in the text. ‡ Assigned on the basis of a documented irreversible inhibition by cyanide or extensive sequence identity with known MoOS enzymes (references indicate the initial evidence in support of assignment to this family by these criteria). MoOS units have been definitively established only for milk xanthine oxidase and chicken xanthine dehydrogenase by XAS, and the *D. gigas* aldehyde oxidoreductase by X-ray crystallography. § Enzymes are assigned on the basis of a documented insensitivity or reversible sensitivity to cyanide. Only chicken sulfite oxidase and the nitrate reductases from spinach and *Chlorella vulgaris* have been definitively assigned by XAS to possess a MoO_2 unit. ‖ Enzymes are assigned on the basis of significant sequence homology or spectral similarity to the DMSO reductases from *R. sphaeroides* and *R. capsulatus*, which have been examined by XAS and/or X-ray crystallography. Except where indicated, X=O. [a] MPT, the mononucleotide form of the pterin cofactor (molybdeopterin); MCD, molybdopterin cytosine dinucleotide; MGD, molybdopterin guanine dinucleotide; MAD, molybdopterin adenine dinucleotide; XAS, X-ray absorption spectroscopy. [b] Bray, R. C.; Malmström, B. G.; Vänngård, T. *Biochem. J.* **1959**, *73*, 193. [c] Rajagopalan, K. V.; Handler, P. *J. Biol. Chem.* **1967**, *242*, 4097. [d] Waud, W. R.; Rajagopalan, K. V. *Arch. Biochem. Biophys.* **1976**, *172*, 354. [e] Smith, S. T.; Rajagopalan, K. V.; Handler, P. *J. Biol. Chem.* **1967**, *242*, 4108. [f] Lee, C. S.; Curtis, D.; McCarron, M.; Love, C.; Gray, M.; Bender, W.; Chovnick, A. *Genetics* **1987**, *116*, 55. Keith, T. P.; Riley, M. A.; Kreitman, M.; Lewontin, R. C.; Curtis, D.; Chambers, G. *Genetics* **1987**, *116*, 67. [g] Pérez-Vicente, R.; Alamillo, J. M.; Cárdenas, J.; Pineda, M. *Biochim. Biophys. Acta* **1992**, *1117*, 159−166. [h] Ichida, K.; Amaya, Y.; Noda, K.; Minoshima, S.; Hosoya, T.; Sakai, O.; Shimizu, N.; Nishino, T. *Gene* **1993**, *133*, 279. [i] Mahler, H. R.; Mackler, B.; Green, D. E.; Bock, R. M. *J. Biol. Chem.* **1954**, *210*, 465. [j] Wright, R. M.; Vaitaitis, G. M.; Wilson, C. M.; Repine, T. B.; Terada, L. S.; Repines, J. W. *Proc. Natl. Acad. Sci. U.S.A.* **1993**, *90*, 10690. [k] Li Calzi, M.; Raviolo, C.; Ghibaudi, E.; De Gioia, Salmona, M.; Cazzaniga, G.; Kurosaki, M.; Terao, M.; Garattini, E. *J. Biol. Chem.* **1995**, *270*, 31037. [l] Romao, M. J.; Barata, B. A. S.; Archer, M.; Lobeck, K.; Moura, I.; Carrondo, M. A.; LeGall, J.; Lottspeich, F.; Huber, R.; Moura, J. J. G. *Eur. J. Biochem.* **1993**, *215*, 729. [m] Tamaki, T.; Horinouchi, S.; Fukaya, M.; Okumura, H.; Kawamura, Y.; Beppu, T. *J. Biochem.* **1989**, *106*, 541. [n] Friebald, J.; Bowein, B. *J. Bacteriol.* **1993**, *175*, 4719. [o] Meyer, O. *J. Biol. Chem.* **1982**, *257*, 1333. [p] Jollie, D. R.; Lipscomb, J. D. *J. Biol. Chem.* **1991**, *266*, 21853. [q] Krüger, B.; Meyer, O. *Eur. J. Biochem.* **1986**, *157*, 121. [r] Schübel, U.; Kraut, M.; Mörsdorf, G.; Meyer, O. *J. Bacteriol.* **1995**, *177*, 2197. [s] Tshisuaka, B.; Kappl, R.; Hüttermann, J.; Lingens, F. *Biochemistry* **1993**, *32*, 12928. [t] Peschke, B.; Lingens, F. *Biol. Chem. Hoppe-Seyler* **1990**, *372*, 1081. [u] Schach, S.; Tshusuaka, B.; Fetzner, S.; Lingens, F. *Eur. J. Biochem.* **1995**, *232*, 536. [v] Lehmann, M.; Tshisuaka, B.; Fetzner, S. L.; Röger, P.; Lingens, F. *J. Biol. Chem.* **1994**, *269*, 11254. [w] Bauer, G.; Lingens, F. *Biol. Chem. Hoppe-Seyler* **1992**, *373*, 699. [x] deBeyer, A.; Lingens, F. *Biochem. J. Hoppe-Seyler* **1993**, *374*, 101. [y] Fetzner, M.; Lingens, F. *Biol. Chem. Hoppe-Seyler* **1993**, *374*, 363. [z] Sauter, M.; Tshisuaka, B.; Fetzner, S.; Lingens, F. *Biol. Chem. Hoppe-Seyler* **1992**, *374*, 1037. [aa] Dilworth, G. L. *Arch. Biochem. Biophys.* **1982**, *219*, 565. [ab] Has been shown to possess molybdenum coordinated to acid-labile selenium, possibly as Mo=Se (see text). [ac] Nagel, M.; Andreesen, J. R. *Arch. Microbiol.* **1990**, *154*, 605. [ad] Freudenberg, W.; König, K.; Andreesen, J. R. *FEMS Microbiol. Lett.* **1988**, *52*, 13. [ae] Grether-Beck, S.; Iglio, G. L.; Pust, S.; Schilz, E.; Decker, K.; Brandsch, R. *Mol. Microbiol.* **1994**, *13*, 929. [af] Siegmund, I.; Koenig, K.; Andreesen, J. R. *FEMS Microbiol. Lett.* **1990**, *67*, 281. [ag] Trautwein, T.; Krauss, F.; Lottspeich, F.; Simon, H. *Eur. J. Biochem.* **1994**, *222*, 1025. [ah] Cohen, H. J.; Fridovich, I.; Rajagopalan, K. V. *J. Biol. Chem.* **1971**, *246*, 374. [ai] Kessler, D. L.; Rajagopalan, K. V. *J. Biol. Chem.* **1972**, *247*, 6566. [aj] Kessler, D. L.; Johnson, J. L.; Cohen, H. J.; Rajagopalan, K. V. *Biochim. Biophys. Acta* **1974**, *334*, 86. [ak] Garrett, R. M.; Bellisssimo, D. B.; Rajagopalan, K. V. *Biochim. Biophys. Acta* **1995**, *1262*, 147. [al] Toghrol, F.; Sutherland, W. M. *J. Biol. Chem.* **1983**, *258*, 6762. [am] Nicholas, D. J. D.; Nason, A. *J. Biol. Chem.* **1954**, *207*, 353. [an] Notton, B. A.; Graf, L.; Hewitt, E. J.; Povey, R. C. *Biochim. Biophys. Acta* **1974**, *364*, 45. [ao] Solomonson, L.; Lorimer, G.; Hall, R.; Borchers, R.; Bailey, J. *J. Biol. Chem.* **1975**, *250*, 4120. [ap] Satoh, H.; Kurihara, F. N. *J. Biochem.* **1987**, *102*, 191. [aq] McEwan, A. G.; Ferguson, S. J.; Jackson, J. B. *Biochem. J.* **1991**, *274*, 305. [ar] Weiner, J. H.; MacIsaac, D. P.; Bishop, R. E.; Bilous, P. T. *J. Bacteriol.* **1988**, *170*, 1505. [as] del Campillo-Campbell, A.; Campbell, D. *J. Bacteriol.* **1982**, *149*, 469. [at] Shimakawa, O.; Ishimoto, M. *J. Bacteriol.* **1973**, *86*, 1709. [au] Blasco, F.; Iobbi, C.; Giordano, G.; Chippaux; Bonnefoy, V. *Mol. Gen. Genet.* **1989**, *218*, 249. [av] Blasco, F.; Iobbi, C.; Ratouchniak, J.; Bonnefoy, V.; Chippaux, M. *Mol. Gen. Genet.* **1990**, *222*, 104. [ax] Berks, B. C.; Richardson, D. J.; Reilly, A.; Willis, A. C.; Ferguson, S. J. *Biochem. J.* **1995**, *309*, 983. [ay] Bickel-Sandkötter, S.; Ufer, M. *Z. Naturforsch.* **1995**, *50*, 365. [az] Zinoni, F.; Birkmann, A.; Stadtman, T. C.; Böck, A. *Proc. Natl. Acad. Sci. U.S.A.* **1986**, *83*, 4650. [ba] Berg, B. L.; Li, J.; Heider, J.; Stewart, V. *J. Biol. Chem.* **1991**, *266*, 22380. [bb] Blattner, F. R.; Burland, V. D.; Plunkett, G., III; Sofia, H. J.; Daniels, D. L. *Nucleic Acids Res.* **1993**, *21*, 5408. [bc] Shuber, A. P.; Orr, E. C.; Recny, M. A.; Schendel, P. F.; May, H. D.; Schauer, N. L.; Ferry, J. G. *J. Biol. Chem.* **1986**, *261*, 12942. [bd] Bokranz, M.; Gutmann, Körner, C.; Kojro, E.; Fahrenholz, F.; Lauterbach, F.; Kröger, A. *Arch. Microbiol.* **1991**, *156*, 119. [be] Krafft, T.; Bokranz, M.; Klimmek, O.; Schröder, I.; Fahrenholz, F.; Kojro, E.; Kröger, A. *Eur. J. Biochem.* **1992**, *206*, 503. [bf] Anderson, G. L.; Williams, J. W.; Hille, R. *Biol. Chem.* **1992**, *267*, 23674. [bg] Börner, G.; Karrasch, M.; Thauer, R. K. *FEBS Lett.* **1991**, *290*, 31. [bh] Karrasch, M.; Börner, G.; Enssle, M.; Thauer, R. K. *Eur. J. Biochem.* **1990**, *194*, 367. [bi] Warner, C.; Watts, D. T.; Finnerty, V. *Mol. Gen. Genet.* **1980**, *180*, 449. [bj] Oltmann, L. F.; Claassen, V. P.; Kastelein, W. N. M.; Stouthammer, A. H. *FEBS Lett.* **1979**, *106*, 43. [bk] Dilworth, G. L. *Arch. Biochem. Biophys.* **1982**, *221*, 565. [bl] Kunow, J.; Linder, D.; Thauer, R. K. *Arch. Microbiol.* **1995**, *163*, 21. [bm] Sommer, S.; Reichenbacher, W.; Schink, W.; Kroneck, P. M. H. *J. Inorg. Chem.* **1995**, *59*, 729. [bn] Koenig, K.; Andreesen, J. R. *J. Bacteriol.* **1990**, *172*, 5999.

Comamonas acidovorans is found to be unique in its subunit composition.[105] Although the enzyme possesses the identical cofactor constitution as the eukaryotic xanthine dehydrogenases (molybdenum, two 2Fe-2S and FAD), it is found to be an $\alpha_2\beta_2$ tetramer. Although it has not been conclusively demonstrated, it appears likely that the molybdenum center is found in the larger subunit, and the FAD and iron−sulfur centers together in the smaller one, thus representing a variation on the above theme of subunit organization within the hydroxylase family. Also unique is the xanthine dehydrogenase from *Pseudomonas putida*, which has been reported to possess a *b*-type cytochrome instead of a flavin center; this protein also is an $\alpha_2\beta_2$ tetramer.[106]

It should be emphasized at this point that the human aldehyde oxidoreductase was originally considered to be a xanthine dehydrogenase.[107] More recent comparisons among authentic aldehyde and xanthine dehydrogenases, however, has provided a convincing argument that the DNA sequence of Wright *et al.*[107] encodes an aldehyde- rather than xanthine-utilizing enzyme,[90,108−113] and that the sequence initially reported by Nishino and co-workers[90] represents the authentic human xanthine dehydrogenase. The criteria that are found to distinguish the amino acid sequences of the aldehyde oxidases from those of the xanthine dehydrogenases include a C-terminal shifted site of tryptic cleavage between the flavin- and molybdenum-containing domains and distinct amino acid sequences in the N-terminal portions of both the flavin- and molybdenum-containing domains, as well as the central portion of the former domain.[110] In the flavin domain, two specific regions in the center of the domain, corresponding to residues 351−369 and 391−401 of the human

aldehyde oxidase sequence, possess 12 residues that are invariant among seven authentic dehydrogenases, but are different (at several positions distinctly so) in the human and bovine aldehyde oxidase sequences (see below).[108−113]

As with the molybdenum hydroxylases, members of the sulfite oxidase family of mononuclear molybdenum enzymes also have additional redox-active centers to the MoO_2-containing molybdenum center. Sulfite oxidase has been isolated from rat, bovine, and chicken liver[114−116] as well as *Thiobacillus novellus*,[117] and the enzyme from all sources is a homodimer (∼110 kDa) possessing in each subunit a *b*-type cytochrome in addition to the molybdenum.[114−121] As with the hydroxylase family the molybdenum-containing region is found in the C-terminal portion of the sequence.[80,81] In the case of the assimilatory nitrate reductases, the molybdenum domain is at the N-terminus of the amino acid sequence,[80] with discrete flavin- and heme-containing domains following in order.[122] The flavin domain of the assimilatory nitrate reductases[123] possesses significant sequence identity with both ferredoxin reductase[124,125] and cytochrome b_5 reductase,[126,127] while the heme domain exhibits homology to both cytochrome b_5[128] and the heme domain of sulfite oxidase.[80] In the case of the chicken sulfite oxidase, the two domains can be cleaved proteolytically into separate 9.5 and 47 kDa peptides, the molybdenum domain retaining the capacity to oxidize sulfite (in the presence of a suitable electron acceptor) and the reduced heme domain the capacity to pass its electron to cytochrome *c*.[129,130] Nitrate reductase can also be cleaved by limited proteolysis to give peptides that retain many of their spectral and catalytic properties.[131,132] In addition, it has proven possible to clone and express the isolated flavin and heme domains of nitrate reductase,[133−135] which appear to fold properly, exhibit the expected spectral properties compared to their counterpart domains in the intact enzyme and retain many of their physiological activities. It is thus clear that these domains are encoded by contiguous regions in the gene sequence and that the structural genes themselves are in all likelihood the product of gene fusion events giving rise to the more complex holoenzymes.[122]

As indicated, the heme domain of sulfite oxidase[80] exhibits quite a strong sequence homology to the heme-binding domains of microsomal cytochrome b_5[128] as well as the *Arabadopsis thaliana* assimilatory nitrate reductase[123] (31% sequence identity, overall ∼50% sequence similarity). Of the four conserved histidine residues among the three sequences, His 40 and 65 of chicken sulfite oxidase correspond to His 39 and 63 in cytochrome b_5 that bind to the heme.[128] The molybdenum domain of sulfite oxidase exhibits even greater homology to the molybdenum domains of the assimilatory nitrate reductases from a variety of plant sources (38% sequence identity, ∼60% overall sequence similarity).[80,86] A considerably weaker sequence homology between the molybdenum-binding portions of sulfite oxidase and that of the molybdenum hydroxylases (*ca*. 14% sequence identity) is also observed,[86] with most of the significant homology restricted to the first of the two domains that constitute the molybdenum-binding portion of the latter proteins (see below). As indicated in section II.B, a conserved cysteine residue has been identified (Cys 207 of rat sulfite oxidase) that is a ligand to the molybdenum in both the sulfite oxidases and nitrate reductases.[81]

The final family of molybdenum enzymes, the DMSO reductases and related enzymes, also fall into two groups. The first of these, consisting of enzymes such as the DMSO reductases from *Rhodobacter sphaeroides*[136] and *R. capsulatus*,[137] and the biotin-*S*-oxide reductase from *R. sphaeroides*,[138] are soluble periplasmic proteins that are unique in having a molybdenum center as their sole redox-active center. These enzymes are not involved in proton translocation and instead appear to be involved in the dissipation of excess reducing equivalents under certain growth conditions (*i.e.*, photoheterotrophic growth on a highly reduced carbon source). The second group of enzymes include the membrane-bound bacterial DMSO reductases such as that from *E. coli*, the dissimilatory (respiratory) nitrate reductases and formate dehydrogenases from a variety of sources. In addition to a molybdenum-containing subunit exposed to the periplasm (which bears considerable sequence homology to the soluble *Rhodobacter* proteins), the *E. coli* DMSO reductase possesses a second extrinsic subunit containing four iron−sulfur centers of the bacterial ferredoxin (4Fe-4S) variety and an intrinsic membrane anchoring subunit possessing *b*-type cytochromes.[139,140] The dissimilatory nitrate reductases may be either terminal oxidases that deposit reducing equivalents generated in the course of anaerobic electron transport to nitrate or soluble periplasmic proteins which do not pump protons. The principal *E. coli* protein possesses three subunits[141,142] containing the molybdenum center (α, the *narG* gene product), a 3Fe-4S and three 4Fe-4S iron−sulfur clusters (*β*, the *narH* gene product) and a *b*-type cytochrome (*γ*, the *narI* gene product); the complex is exposed to the cytoplasm and is anchored to the inner bacterial membrane via the *γ* subunit.[143] The *E. coli* nitrate reductase has also recently been shown to possess a tightly bound equivalent of menaquinone,[144] which may function in a manner similar to the tightly bound quinone species found in certain other ubiquinone-utilizing membrane enzymes, such as the cytochrome bc_1 complex of mitochondria.

It is undoubtedly the case that molybdenum-containing enzymes possessing variations on the above structural categories will be found, and there are several quite interesting reports in the literature. For example, there is evidence that the archaeal formylmethanofuran dehydrogenases, enzymes with considerable sequence homology to DMSO reductase, possess a cyanide-labile sulfur.[145] Similarly, the formate dehydrogenase from *Methanobacterium thermoautotrophicum*, another member of the DMSO reductase family, possesses a cyanolyzable Mo═S.[146] These enzymes may represent a subgroup of this family of enzymes in which a Mo═O unit has been replaced with Mo═S. It is also significant that some of the archaeal formylmethanofuran dehydrogenases can be isolated in either molybdenum- or tungsten-

containing forms,[147] suggesting a fundamental structural relationship between some tungsten enzymes and molybdenum enzymes of the DMSO reductase class. In addition, a few molybdenum-containing enzymes have been found that possess selenium in the molybdenum coordination sphere, either as selenocysteine (as in the formate-hydrogen lyases of *E. coli*[148,149] or *Methanococcus vanielli*[150]), or in an acid-labile form that may represent Mo=Se (as in the clostridial nicotinic acid hydroxylase[101, 151−153]). The nicotinate hydroxylase from *Clostridium barkeri* has recently been purified to near-homogeneity and found to be an $\alpha_2\beta_2\gamma_2(\delta_2)$ heteromer of molecular weight 320 000 (subunit masses of 23, 33, 37, and 50 kDa, respectively, with the smallest possibly a proteolytic fragment of one of the larger subunits).[153] The enzyme bears striking similarity to other molybdenum hydroxylases in terms of the reaction catalyzed, overall makeup of its constituent redox-active centers (the enzyme possesses FAD and two 2Fe-2S centers in addition to molybdenum), and the Mo(V) EPR signals exhibited by partially reduced enzyme, including one with $g_{1,2,3}$ = 2.067, 1.982, 1.974 that possesses a general line shape quite reminiscent of the "very rapid" EPR signal of xanthine oxidase (see below). There are, however, several aspects of the protein that are at variance with the general behavior of other members of this family. The enzyme is extremely air-sensitive and is not inhibited by cyanide (but is reversibly inhibited by both selenide and sulfide), and none of the N-terminal amino acid sequences of the subunits correspond to those of known molybdenum hydroxylases.[153] At present it is unclear whether the polyselenides detected upon acid or heat denaturation of nicotinate hydroxylase are in fact derived from a Mo=Se unit in the active site, or whether the pterin cofactor itself might possess selenide in place of one of its dithiolene sulfides.

Finally, it has recently been demonstrated that a pyrogallol transhydroxylase from *Pelobacter acidigallici* is a molybdenum enzyme (possessing the guanine dinucleotide form of the pterin cofactor, as well as a number of iron−sulfur centers),[154,155] despite it catalyzing a reaction that does not strictly conform to the canonical stoichiometry for mononuclear molybdenum enzymes. The reaction catalyzed by this enzyme is given in Scheme 2, and it is possible that

Scheme 2

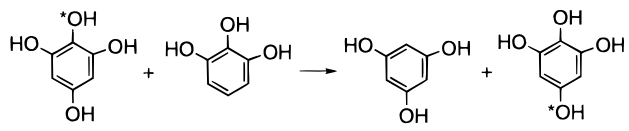

the catalytic cycle represents a "closed-cycle" dehydroxylation/hydroxylation sequence, with 1,2,3,5-tetrahydroxybenzene being dehydroxylated by reduced enzyme and pyrogallol becoming hydroxylated in subsequent reaction with the oxidized enzyme thus generated to return to reduced enzyme and complete the catalytic cycle.[155] If the enzyme in fact functions in this way, it should bear some resemblance to the xanthine oxidase family of enzymes, but it is not yet known whether this is the case.

III. The Xanthine Oxidase Family: The Molybdenum Hydroxylases

Members of the xanthine oxidase family generally catalyze hydroxylation reactions of the type shown in Scheme 3. This stoichiometry is unique among

Scheme 3

$$RH + H_2O \longrightarrow ROH + 2H^+ + 2[e^-]$$

biological systems catalyzing hydroxylation reactions in that reducing equivalents are generated rather than consumed in the course of the reaction, and water rather than dioxygen is utilized as the ultimate source of the oxygen atom incorporated into substrate.

The overall reaction mechanism of these and related enzymes is typically broken down into reductive and oxidative half-reactions of the catalytic cycle, defined from the standpoint of the enzyme. It is the reductive half-reaction in which the molybdenum center participates, with the metal becoming reduced from Mo(VI) to Mo(IV) in the course of the chemistry leading to hydroxylation.

A. The Crystal Structure of Aldehyde Oxidoreductase from *Desulfovibrio gigas*

As indicated above, the crystal structure of the aldehyde oxidoreductase from *Desulfovibrio gigas* has recently been elucidated.[6] In addition to the structural features of the molybdenum center that have been described above, the overall protein structure is interesting in many other ways, representing as it does the first to be obtained for a molybdenum hydroxylase. The protein is organized into four domains, with the polypeptide tracing out in order from the N-terminus two small 2Fe-2S domains and two much larger domains that together constitute the molybdenum-containing portion of the enzyme (Figure 2). The first iron−sulfur domain (consisting of residues 1−76) possesses the consensus CXXGX-CXXC sequence shared by the spinach ferredoxin class of iron−sulfur proteins.[156] The general polypeptide fold, consisting of a five-stranded β sheet that partially encloses an α helix, also closely resembles that seen in other members of this class of metalloprotein. The only substantive departures in secondary structure are a six-residue shorter turn between the first two strands of the sheet and the absence of a 19-residue loop toward the C-terminal end of the aldehyde oxidoreductase domain. The iron atoms of the first cluster are coordinated by cysteines 40, 45, 47, and 60, and the γ S of Cys 60 is exposed to solvent. The second iron−sulfur domain (residues 84−157) is found to possess a unique fold, a four-helix bundle with two longer, central helices flanked by shorter peripheral ones lying at a somewhat oblique angle. The metal cluster lies at the N-terminal ends of the two larger helices, coordinated by cysteines 100, 103, 137, and 139. The polypeptide trace of this domain possesses a pseudo 2-fold axis of symmetry along the Fe−Fe axis of the cluster, extending fully through the domain.

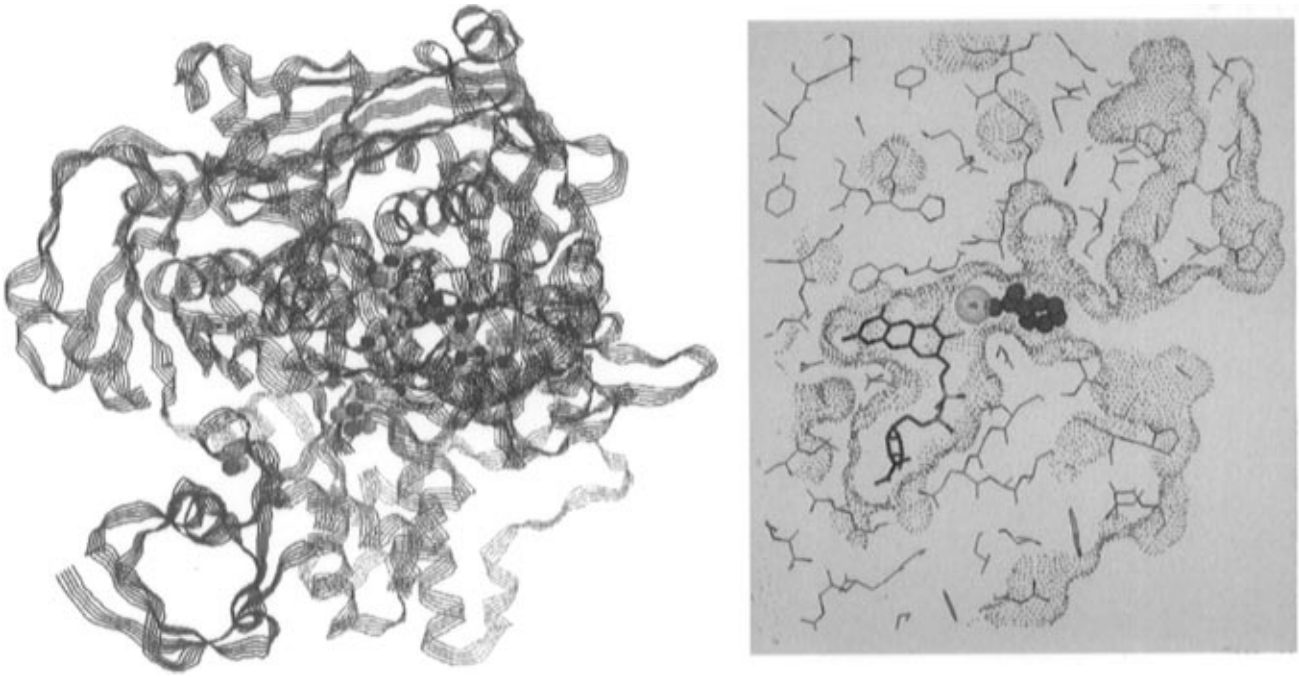

Figure 2. (a) The structure of the aldehyde oxidoreductase from *Desulfovibrio gigas*. (Left) The overall polypeptide fold of the protein, with two discrete N-terminal domains containing the two 2Fe-2S clusters of the protein (red and orange, respectively), followed by an extended meander (in gray) which connects to the two domains (designated Mo1 and Mo2 in green and blue, respectively) that together contain the molybdenum center. The molybdenum atom is represented by a gray sphere (at the interface of the Mo1 and Mo2 domains) and the extended MGD cofactor rendered in wireframe with CPK coloring. The oxygen and sulfur ligands to molybdenum are rendered in red and yellow, respectively. The iron−sulfur centers are shown with the Fe and S as orange and yellow spheres, respectively. Cys 139, which coordinates one of the iron atoms of the second Fe-S center and is also hydrogen-bonded to the amino group of the pterin cofactor, is also rendered in wireframe with CPK coloring. In this orientation, the solvent access channel to the active site extends away from the molybdenum up and to the rear of the molecule opposite S7′ of the cofactor (the left-most sulfur coordinated to the molybdenum), between Mo1 and Mo2. This figure was prepared with the RasMol software package, using the atomic coordinates of Romão *et al*.[6] with permission. (Right) A cross-section of the active site of the aldehyde oxidoreductase from *Desulfovibrio gigas*. The active site molybdenum is indicated by the orange van der Waals sphere. The binding pocket for the pterin cofactor and the solvent access channel to the active site (the latter partially occupied by salicylate from the mother liquor of the crystal) are indicated by the blue van der Waals surface. Reproduced from Romão *et al*.[6] with permission.

The second iron−sulfur domain is connected to the molybdenum-containing portion of the enzyme via an extended meander that extends some 50 Å across a generally concave region of the surface from one side of the protein to the other. The meander possesses a pair of two-turn α helices that interact with the second iron−sulfur domain, but is otherwise devoid of secondary structure. Given the considerable sequence homology between the Fe-S- and molybdenum-containing domains of the *D. gigas* aldehyde oxidoreductase and the eukaryotic xanthine dehydrogenases (approximately 52% sequence similarity in the iron−sulfur and molybdenum domains[156]), it is clear that the flavin domain of the latter group of enzymes fits into the structure of the aldehyde oxidoreductase somewhere along the meander.

The bulk of the aldehyde oxidoreductase polypeptide is taken up by two large, elongated domains that lie across one another at approximately 90° and have the molybdenum center at their interface. The first of these domains, designated Mo1 and consisting of residues 196−581, is roughly in the shape of a cylinder 28 Å thick and 72 Å long, and consists of two distinct subdomains. The larger N-terminal subdomain is made up of a seven-stranded incomplete β barrel with an α helix in its central cavity and is flanked by two other helices that are exposed at the surface of the protein. The smaller, C-terminal subdomain of Mo1 consists of a five-stranded antiparallel β sheet flanked by a pair of α helices, one of which lies on the protein surface. The polypeptide trace passes twice between these two subdomains in forming Mo1. The second molybdenum-binding domain of aldehyde oxidoreductase, Mo2, consists of residues 582 to 907 and is also organized into two subdomains, these in the general form of two wings that together span over 80 Å. Each wing is formed by a four-stranded β sheet that bends around a pair of α helices, and the two are loosely related to one another by a dyad axis of symmetry; as in Mo1, there the chain trace passes twice between the two subdomains of Mo2. Most of the polypeptide contacts with the (extended) molybdopterin cytosine dinucleotide cofactor occur along the subdomain interface of Mo2, with the metal binding site at the juncture of the subdomain interfaces of Mo1 and Mo2. Given this, it is not surprising that the polypeptide sequence of Mo2 has less homology to the eukaryotic hydroxylases (which possess the mononucleotide from of the pterin cofactor) than does the sequence of Mo1. The two iron−sulfur domains have substantial interactions with Mo2 and with one another, but there is little contact with Mo1. Although the molybdenum center lies deep within the protein, it is readily

accessible to solvent via a channel that is approximately 15 Å deep and several angstroms across at the protein surface, tapering slightly toward the metal center (Figure 2). This channel lies opposite the molybdenum from the pterin cofactor and iron−sulfur domains and has a hydrophobic surface made up of residues contributed by both Mo1 and Mo2 domains. Approximately half way in from the protein surface, the channel is constricted by two phenylalanine and two leucine residues so that, in the absence of dynamic motion in the side chains, larger aromatic substrates would be unable to gain access to the active site.

The molybdenum atom lies 14.5 Å from the nearer iron atom of the second iron−sulfur center, which lies completely buried within the protein (~15 Å at nearest approach to the protein surface, and completely inaccessible to solvent). As mentioned above, the pterin portion of the cofactor spans the region between the molybdenum and this iron−sulfur center, hydrogen bonding to the γ sulfur of Cys 139, which is one of the coordinating cysteines of the iron−sulfur center. The N-terminal iron−sulfur center lies ~27 Å from the molybdenum and 12 Å from the second iron−sulfur center; the Fe1−Fe2−Mo angle subtended by the three redox-active centers is approximately 150°. At present the assignment of the two Fe-S EPR signals exhibited by aldehyde oxidoreductase[157] to specific iron−sulfur centers in the crystal structure is problematic. Like xanthine oxidase[158,159] and the avian xanthine dehydrogenase,[160] two quite distinct Fe-S EPR signals are observed at low temperature. The first of these signals, designated Fe-S I in xanthine oxidase, is quite similar to the signal exhibited by spinach ferredoxin with $g_{1,2,3}$ = 2.02, 1.93, and 1.90 ± 0.01 for the five proteins compared, and is readily observable at temperatures up to 40 K. The second signal, Fe-S II, has $g_{1,2,3}$ = 2.10 ± 0.02, 1.98 ± 0.015, and 1.91 ± 0.01;[159] this signal exhibits substantially broader lines and is observable only below 22 K.[158] In the case of xanthine oxidase it is known that the site giving rise to the Fe-S I EPR signal interacts magnetically with the molybdenum center when the two sites are paramagnetic, with the result that at 40 K each EPR signal is split isotropically by about 11 G.[161,162] Assuming a strictly dipolar interaction between the two paramagnetic centers, this splitting has been used to estimate a distance of approximately 14 Å between Fe-S I and the molybdenum center of xanthine oxidase,[163] in very good agreement with the crystallographically determined distance between the molybdenum center and the second Fe-S center of the *D. gigas* aldehyde oxidoreductase. More recently, a more general local spin model has been used to simulate the magnetic interaction between the Mo and Fe-S I center of xanthine oxidase, arriving at a somewhat longer site−site distance of 19 Å (measuring to the center of mass of the 2Fe-2S cluster).[164] The difficulty in either case is that in the aldehyde oxidoreductase the nearer iron−sulfur center (that hydrogen-bonded to the amino group of the pterin cofactor) is found in the domain exhibiting the unique polypeptide fold, and one would have expected this *a priori* to be the center giving rise to the EPR signal exhibiting the more unusual features (high *g* values and temperature dependence). It is possible, however, that it is the solvent accessibility rather than the polypeptide fold that imparts unusual EPR features to the center designated Fe-S II, as these features ultimately relate to a much faster spin−lattice relaxation time for the paramagnetic state of the center. If this is the case, then the assignment of EPR signals is Fe-S II to the N-terminal center, and Fe-S I to the second center, consistent with the distance estimates by EPR. Single-crystal EPR of reduced aldehyde oxidoreductase would obviously be of great use in providing a definitive assignment of EPR signals to the two Fe-S clusters of the enzyme.

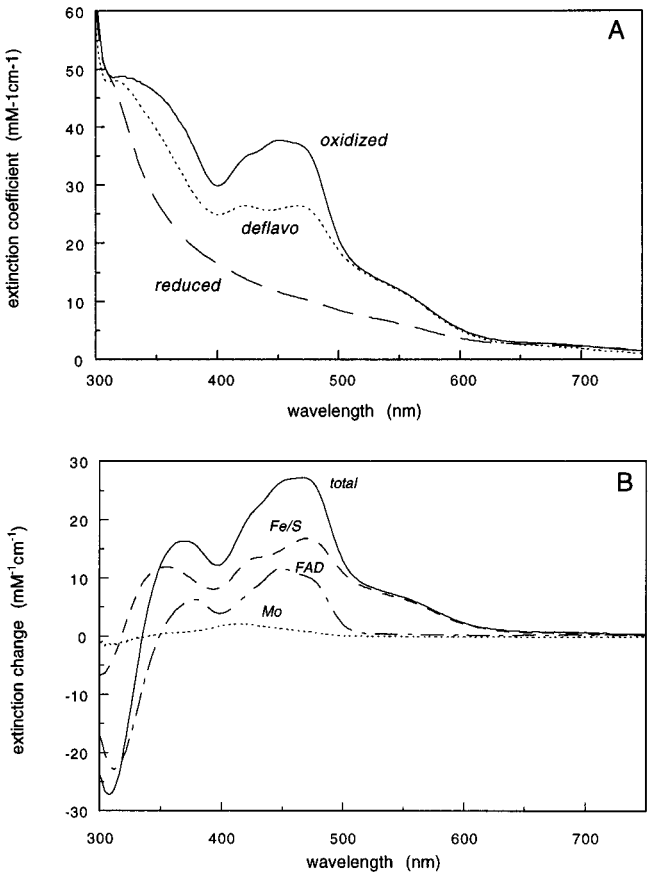

Figure 3. The absorption spectra and difference spectra seen on reduction for milk xanthine oxidase: (A) the spectra of oxidized enzyme (solid line), oxidized enzyme from which the flavin has been removed (dotted line), and reduced enzyme (dashed line); and (B) the spectral change associated with reduction of the enzyme (solid line) deconvoluted into contributions due to the iron−sulfur (dashed line), FAD (dot-dashed line), and molybdenum (dotted line) centers. After Ryan *et al.*,[166] with permission.

B. Mechanistic Studies of Xanthine Oxidase

Xanthine oxidase is a 300 kDa homodimer that possesses FAD in addition to the molybdenum and pair of 2Fe-2S centers in common with the *D. gigas* aldehyde oxidoreductase. The flavin and Fe-S centers dominate the UV/vis absorption spectrum of the oxidized enzyme and the overall spectral change associated with reduction of the enzyme (Figure 3A). The iron−sulfur contribution to oxidized enzyme includes maxima at 420 and 470 nm, and a shoulder

at 550 nm, while that of the flavin consists of the typical maxima at 360 and 450 nm.[165] Although the two iron−sulfur centers exhibit indistinguishable UV/vis and CD spectral changes on reduction,[159] they are readily distinguished on the basis of their EPR signals in the reduced state, as indicated above (Table 2). The Mössbauer features of the two centers are also distinct, particularly in the reduced enzyme, with one of the centers (tentatively designated as Fe-S I) exhibiting a more or less normal quadrupole splitting of 2.4 mm/s for its ferrous ion but the other with an unusually large quadrupole splitting of 3.2 mm/s.[159] Although largely obscured by the much larger spectral changes attributable to the iron−sulfur and flavin centers, the UV/vis absorbance and circular dichroism changes associated with reduction of the molybdenum center of xanthine oxidase have been determined recently using a double-difference technique for various forms of the enzyme complexed with the tight-binding inhibitor alloxanthine.[166] At pH 8.5, the Mo^{VI}-*minus*-Mo^{IV} difference spectrum exhibits a positive feature at 420 nm, having an extinction change of ~3000 M^{-1} cm^{-1}, as well as evidence for a negative feature below 340 nm. The deconvolution of the overall spectral change seen on reduction of xanthine oxidase is shown in Figure 3B, and it can be seen that the portion of the change attributable to the molybdenum center is not only quite small compared to the changes associated with reduction of the FAD and iron−sulfur centers of the enzyme but is also centered on an absorption minimum in the absorbance change associated with the FAD and Fe-S centers, explaining why it has avoided detection until recently. The spectral change associated with reduction of the molybdenum center is found to exhibit a marked pH dependence,[166] indicating that ionizable groups in the vicinity of the molybdenum center, perhaps within the molybdenum coordination sphere itself, are able to perturb the spectral change associated with its reduction. This spectral change provides a new and direct spectroscopic handle on the molybdenum center of the enzyme that should prove useful in a variety of studies of xanthine oxidase, particularly resonance Raman applications.

Much of the structural information concerning the *D. gigas* aldehyde oxidoreductase is in all likelihood directly relevant to xanthine oxidase and other members of the molybdenum hydroxylase family. As mentioned earlier, for example, the coordination environment of the molybdenum atom in aldehyde oxidoreductase is consistent with the XAS results obtained with both xanthine dehydrogenase and xanthine oxidase. These are summarized in Figure 4 for several of the forms of xanthine oxidase that have been examined by XAS. In addition to the XAS of the oxidized and reduced enzyme that has already been discussed, two other forms of the functional, sulfido form of xanthine oxidase have been examined using this technique. These are the complexes of reduced enzyme with violapterin[167] and alloxanthine,[167,168] and both cases the data are consistent with direct coordination of heterocycle to the metal, via the C-7 hydroxyl in the case of violapterin (Mo−O = 2.08 Å) and N-8 in the case of alloxanthine (Mo−N = 2.27 Å). The alloxanthine complex is significant because its one-electron oxidation gives an EPR signal that resembles the so-called "very rapid" signal seen transiently in the course of the reaction of enzyme with xanthine, and the violapterin complex has been shown to represent a particularly stable complex of reduced enzyme with product (see below). There is also a variety of other evidence indicating that the active sites of aldehyde oxidoreductase and xanthine oxidase are fundamentally very similar. Xanthine oxidase is known to effectively catalyze the oxidation of a wide range of aldehydes, for example,[169,170] and the molybdenum center of the aldehyde oxidoreductase exhibits many of the same types of "rapid" Mo(V) EPR signals as does xanthine oxidase and the other eukaryotic enzymes.[171] These signals, originally named on the basis of the relative rates at which they accumulate in the course of reaction of xanthine oxidase with xanthine, have been divided into categories "type 1" and "type 2" depending on the nature of the proton hyperfine splitting that is observed in the signal.[172,173] The type 1 signals exhibit hyperfine coupling to two inequivalent protons with splitting of 14 and 3.3 G, while the type 2 signals exhibit coupling to two (approximately) equivalent protons with a hyperfine splitting of 12 G. *g* values for each of these signals, and others exhibited by members of the hydroxylase family, are given in Table 2. It can be seen that the type 2 signal exhibited by the *D. gigas* enzyme upon reaction with salicylaldehyde is quantitatively very similar to that observed upon reaction of xanthine oxidase with xanthine. In the case of xanthine oxidase, these signals have been shown to arise from dead-end complexes of Mo(V) enzyme with substrate (bound at the active site but not coordinated to the molybdenum) that in all likelihood represent paramagnetic analogs of the true Michaelis complex.[174,175] As such they represent sensitive probes of the molybdenum environment in the active site (see below).

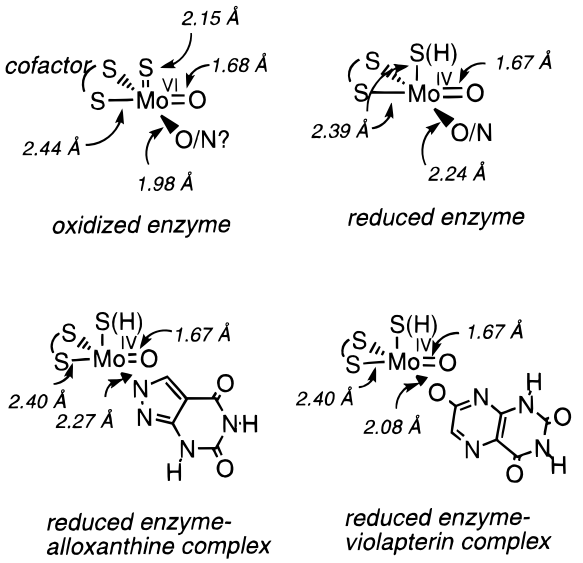

Figure 4. A summary of XAS results obtained with the several forms of xanthine oxidase shown. The coordination geometry of the molybdenum center is inferred from that for the *D. gigas* aldehyde oxidoreductase. The bond distances given are from Cramer and Hille[63] and Hille *et al.*[167]

Table 2. *g* Values for Various Mo(V) EPR Signals Seen in Biological Systems

	g																	
	milk xanthine oxidase			avian xanthine dehydrogenase			rabbit aldehyde oxidase			*D. gigas* aldehyde oxidoreductase			nitrate reductase[h]			sulfite oxidase[i]		
	x	*y*	*z*	*x*	*y*	*z*	*x*	*y*	*z*	*x*	*y*	*z*	*x*	*y*	*z*	*x*	*y*	*z*
"rapid type 1"	1.9654	1.9707	1.9906	1.966	1.970	1.991												
	xanthine[a]			xanthine[c]														
"rapid type 2"	1.9616	1.9712	1.9951				1.9622	1.9700	1.9891	1.9643	1.9702	1.9882						
	xanthine[b]						purine[d]			salicylaldehyde[f]								
Fe-S I	1.894	1.932	2.022	1.925	1.939	2.026	1.981	1.930	2.018[e]	1.93	1.94	2.02[g]						
Fe-S II	1.902	1.991	2.110	1.92	2.00	2.08	1.915	2.003	2.106[f]	1.89	ND	2.06[g]						
Mo^V													1.9628	1.9855	1.9989	1.9658	1.9720	2.0037

[a] Bray, R. C.; Barber, M. J.; Lowe, D. J. *Biochem. J.* **1978**, *171*, 653. [b] Gutteridge, S.; Tanner, S. J.; Bray, R. C. *Biochem. J.* **1978**, *175*, 869. [c] Barber, M. J.; Bray, R. C.; Lowe, D. J.; Coughlan, M. P. *Biochem. J.* **1976**, *153*, 297−307. [d] Bray, R. C.; George, G. N.; Gutteridge, S.; Norlander, L.; Stell, J. G. P.; Stubley, C. *Biochem. J.* **1982**, *203*, 263. [e] Barber, M. J.; Coughlan, M. P.; Rajagopalan, K. V.; Siegel, L. M. *Biochemistry* **1982**, *21*, 3561−3568. [f] Turner, N. A.; Barata, B.; Bray, R. C.; Deistung, J.; Legall, J.; Moura, J. J. G. *Biochem. J.* **1987**, *243*, 755. [g] Moura, J. J. G.; Xavier, A. V.; Cammack, R.; Hall, D. O.; Bruschi, M.; Gall, J. L. *Biochem. J.* **1978**, *173*, 419−425. [h] Vincent, S. P.; Bray, R. C. *Biochem. J.* **1978**, *171*, 639−647. [i] Lamy, M. T.; Gutteridge, S.; Bray, R. C. *Biochem. J.* **1980**, *185*, 397−403.

Scheme 4

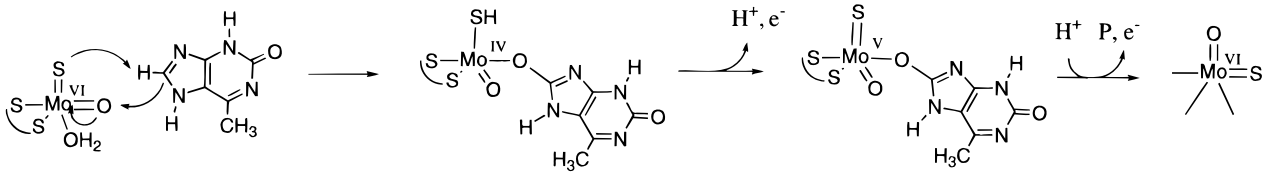

It has been known for some time that the source of oxygen incorporated into substrate by the molybdenum hydroxylases, as exemplified by xanthine oxidase, is derived from water.[176] Under single-turnover conditions, however, it has been shown that the oxygen atom incorporated into product is derived from a catalytically labile site on the enzyme,[177] which must then be regenerated with oxygen from water for subsequent turnover. On the basis of the demonstrated lability of Mo=O bonds in relatively simple coordination complexes,[3] and the appreciation that the molybdenum coordination sphere of the enzyme possessed such a group, it has been suggested that the catalytically labile site of xanthine oxidase is in fact the Mo=O of the enzyme.[177] A mechanism has been proposed in which catalysis proceeds via deprotonation of the C-8 position of xanthine, followed by nucleophilic attack of the resultant carbanion on the Mo^{VI}=O group to give a Mo^{IV}−OR species (Scheme 4).[177,178] Similar chemistry involving nucleophilic attack on an electrophilic Mo=O group had been proposed previously for the reaction of $Mo^{VI}O_2$ species with phosphines (to give the corresponding phosphine oxide and Mo^{IV}=O) on the basis of the large, negative entropy of activation associated with the reaction.[179] With regard to the enzyme mechanism, however, it must be remembered that the XAS results obtained with the complexes of reduced enzyme with violapterin[167] and alloxanthine[167,168] (thought to represent an authentic catalytic intermediate and a particularly stable analog, respectively) indicate that both species possesses a Mo=O group. Thus, if the Mo=O group of oxidized enzyme is in fact the catalytically labile oxygen, then it must be regenerated (from solvent) early in the course of the catalytic sequence. In light of the crystal structure of the *D. gigas* aldehyde oxidoreductase, it is possible that this might be accomplished by deprotonation of a metal-complexed water rather than directly from bulk solvent (but see below).

It has been pointed out[177] that the chemistry shown in Scheme 4, involving abstraction of the C-8 proton by the Mo=S group, is consistent with the known acidity of this position of xanthine (with a pK_a of ∼14 it is sufficiently acidic to exchange with solvent under relatively mild conditions[180]) and the observation that the Mo=S group (rather than the Mo=O) is sufficiently basic as to protonate upon reduction of the enzyme. Thus, in considering the MoOS unit alone, it appears that a reaction initiated by proton abstraction followed by carbanion attack on Mo=O,[177,178] rather than a hydride attack on Mo=S[181] is the more likely reaction pathway (*i.e.*, a clockwise rather than counterclockwise motion of electrons in the first step of Scheme 4). In the context of a mechanism based on an electrophilic Mo=O group, the greater basicity of Mo=S relative to Mo=O (as reflected in protonation of the former group rather than the latter on reduction of the molybdenum center) provides a rationale for the catalytic requirement of a sulfido group in the molybdenum hydroxylases whose reactions involve C−H bond cleavage. It is to be noted that substrate need not coordinate to the molybdenum in order for the chemistry of Scheme 4 to proceed, and the crystallographic data for the *D. gigas* aldehyde oxidoreductase suggests quite strongly that in fact substrate does not coordinate to the metal.[57] Consistent with the mechanism shown in Scheme 4, it is known that the isotope-sensitive step of the reductive half-reaction with [8-^{2}H]xanthine (*i.e.*, formation of the Mo^{IV}−OR intermediate) is much faster than the rate-limiting step of the reaction (thought to be product dissociation, either from Mo^{IV} or Mo^V).[182] In addition, it has been shown in single-turnover acid-quench experiments with both xanthine[182] and 2-hydroxy-6-methylpurine[183] that the

Scheme 5

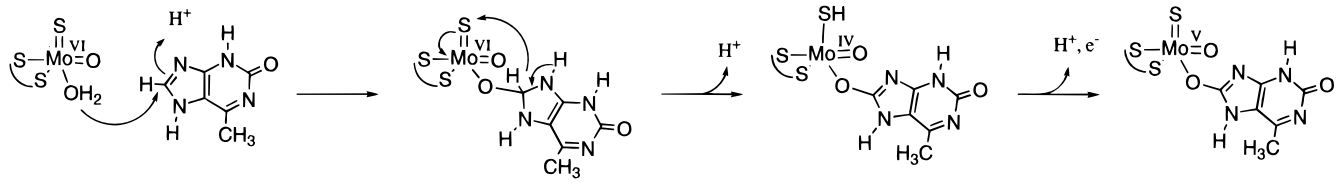

C−O bond of the product forms with a rate constant comparable to that for formation of the initial intermediate formed in the reaction.

The above notwithstanding, in light of the demonstration by crystallography of a molybdenum-bound water in the active site of the *D. gigas* aldehyde oxidoreductase the possibility must be considered that this group rather than the Mo=O represents the catalytically labile oxygen,[57] being activated for nucleophilic attack on substrate by coordination to the molybdenum in a manner comparable to the zinc activation of water in enzymes such as carboxypeptidase A. In fact, Wedd and co-workers have previously suggested that a metal-bound hydroxide might represent the catalytically labile oxygen on the basis of ^{17}O-EPR studies of model compounds relevant to the enzyme active sites.[184] A mechanism involving the metal-coordinated water has recently been proposed for the aldehyde oxidoreductase,[57] and the comparable mechanism for xanthine oxidase is shown in Scheme 5. This mechanism is consistent with much that is known about the reductive half-reaction of xanthine oxidase. The reaction is initiated by nucleophilic attack on C-8 of substrate by (presumably deprotonated) water to give a transient tetrahedral intermediate. This breaks down as shown by hydride transfer to the Mo=S group, with resultant reduction of the molybdenum to the Mo(IV) valence state. It should be noted that just as the pK_a for the C-8 position of purines is known to be relatively low, this same position is also known to be susceptible to nucleophilic attack of the type envisioned in Scheme 5.[185] Using a homologous series of substituted quinazoline derivatives that are hydroxylated by xanthine oxidase, for example, Skibo and co-workers have demonstrated that under conditions of rate-limiting chemistry in the overall mechanism, the reaction exhibits a negative Hammett correlation.[186] This result is consistent with a mechanism based on either nucleophilic attack on or proton abstraction from the position to become hydroxylated; in both cases, the purine nucleus accommodates negative charge accumulation at C-8 by delocalization onto the keto oxygens of the pyrimidine subnucleus, as indicated in Scheme 6.

Scheme 6

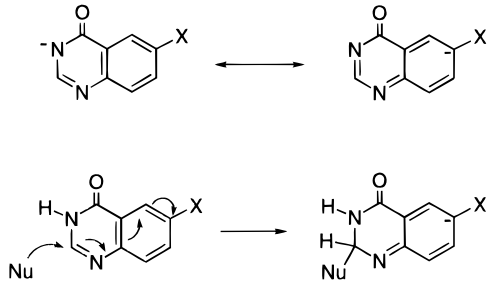

Yet another mechanism for xanthine oxidase has been suggested by Coucouvanis and co-workers, who in studying inorganic complexes of the type CpMo(O)(μ-S)$_2$Mo(O)(S) (Cp = cyclopentadienyl anion) have noted the ability of unsaturated hydrocarbons to add across Mo=S bonds.[187] As shown in Scheme 7, this mechanism involves the addition of the C_8−H bond across the Mo=S of oxidized enzyme to give a Mo−SH species with a molybdenum−C_8 bond. This then incorporates hydroxide from solvent to yield the same initial intermediate as in the two mechanisms considered above. A variation on the mechanism shown in Scheme 6 has recently been proposed by Bray and co-workers,[188] in which the molybdenum−carbon bond persists in intermediates downstream from the first chemical step of the reaction mechanism; this new mechanism is fundamentally very different from the others described here and will be considered further below. Yet another reaction mechanism has been considered by Pilato and Stiefel[18] in which the N-7/C-8 double bond adds across the Mo=O directly in a 2 + 2 cycloaddition, to give the intermediate shown in Scheme 8, which breaks down by hydride transfer to give a species differing from that proposed to form directly in the mechanism shown in Scheme 4 in that it lacks a Mo=O group. In light of the XAS

Scheme 7

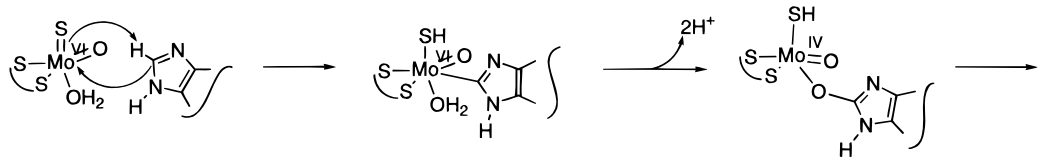

Scheme 8

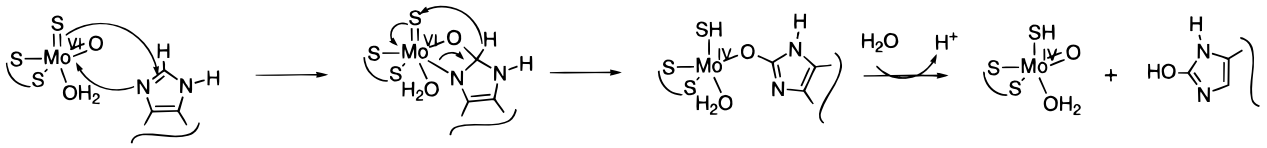

results with the violapterin complex of xanthineoxidase, indicating that the Mo=O group is present in this intermediate, the mechanism in Scheme 8 shares the same difficulty as that shown in Scheme 4 in that the Mo=O group must be regenerated immediately in the catalytic sequence if it is indeed the catalytically labile oxygen. Again, the molybdenum-bound water could conceivably serve such a purpose.

Apart from the mechanistic difficulty concerning regeneration of the Mo=O, if it is in fact the catalytically labile oxygen atom of the molybdenum hydroxylases, there are other reasons to question whether the Mo=O group indeed plays the mechanistic role indicated in Scheme 4. In studying the metathesis of olefins, Goddard has pointed out the importance of the so-called "spectator oxygen" effect in the molybdenum and chromium coordination complexes that catalyze these reactions.[189,190] This phenomenon refers to the ability of metal oxo groups to drive chemistry in the metal coordination sphere in which it does not participate directly. In complexes possessing two oxo groups, for example, one oxo group can render the other susceptible to olefin addition in a manner analogous to the mechanisms shown in Schemes 7 and 8. The driving force for the reaction is the creation of a substantially stronger M=O bond in the monooxo product metal complex (formally a triple bond with two d orbitals participating in π-back-bonding interactions with the oxygen, rather than a double bond with a single d orbital available for π interaction as required by the geometry of the *cis* dioxo complex). The enthalpy gain due to such effects can be in excess of 100 kJ mol^{-1} for dioxomolybdenum complexes in which the remainder of the metal coordination sphere is occupied by highly electronegative ligands such as chloride or alkoxides.[189] The very ionic character of these other ligands in fact plays a large role in determining the overall chemical properties of the complexes examined, and substitution with less electronegative ligands (which have more covalent bond character as ligands to the metal) results in more ionic character in the Mo=O bond, with the result that the spectator effect is much diminished. Given the preponderance of sulfur in the molybdenum coordination sphere of the molybdenum hydroxylases, it would therefore appear questionable as to whether a spectator oxo effect plays a prominent role in the mechanism of these enzymes. The coordination geometry of the xanthine oxidase and DMSO reductase families also make it unlikely that this is an important consideration. In the latter case, there is only a single oxo group in the oxidized enzyme. In the former case, while it is conceivable that a "spectator sulfido" effect could be important in activating the equatorial Mo=O, for example, the nature of the initial product of aldehyde or purine addition across the Mo=O bond is problematic.

By way of addressing the early steps of the catalytic sequence of xanthine oxidase, the reaction of enzyme with xanthine has been probed by examining the pH dependence of the steady-state kinetic parameter k_{cat}/K_m and the corresponding kinetic parameter k_{red}/K_d from the reductive half-reaction.[191] These kinetic parameters correspond to the second-order rate constants for reaction of enzyme with substrate in the low-[substrate] regime and reflect the chemistry occurring up through the first irreversible step of the reaction. It is found that both kinetic parameters exhibit a bell-shaped pH dependence, indicating the requirement for the deprotonated form of an ionizable group having a pK_a of 6.6 and the protonated form of an ionizable group having a pK_a of 7.4 for the reaction to proceed. The latter pK_a agrees very well with the first pK_a for xanthine (at N_5, reflecting the prototropic equilibrium between neutral and monoanionic species),[192] indicating that it is the neutral form of substrate that is acted upon by enzyme. This result is consistent with either an electrophilic Mo=O or nucleophilic Mo$-H_2O$ mechanism: in the former case, formation of the monoanion of substrate would make it more difficult to deprotonate the C-8 position (creating a transient dianion); in the latter case, negative charge accumulation on the heterocycle would be expected to render it less susceptible to nucleophilic attack. The ionizable group having a pK_a of 6.6 identified in this study must be on the enzyme, and may be either the Mo=S (in an electrophilic Mo=O mechanism such as that shown in Scheme 4) or the Mo$-H_2O$ (in a nucleophilic Mo$-H_2O$ mechanism as in Scheme 5).

The same pH dependence is observed in the reaction of enzyme with lumazine (2,6-dihydroxypteridine), the advantage being that the reduced enzyme−product complex formed in the course of the reaction exhibits a characteristic long-wavelength absorbance that provides a unique opportunity to follow its formation directly.[193,194] The pH profile of k_{lim}/K_d, determined from the dependence of the kinetics of the formation of this intermediate on the lumazine concentration, is again bell-shaped: the acidic limb of the pH profile is governed by a group having a pK_a of 6.5 and the basic limb of the pH profile by an ionizable group having a pK_a of 7.8 rather than 7.4 (consistent with the moderately higher pK_a for lumazine relative to xanthine).[191] The fact that the pH profile for k_{lim}/K_d in this experiment is the same as that for the steady-state parameter k_{cat}/K_m strongly suggests that formation of the reduced enzyme−product complex seen here represents the first irreversible step in the overall reaction. This conclusion is consistent with the interpretation of the original kinetic work done with lumazine as substrate, in which the intermediate was taken to represent a true catalytic intermediate in the hydroxylation reaction whose breakdown was rate limiting for turnover.[194] The identical species is obtained upon anaerobic addition of violapterin (2,6,7-trihydroxypteridine, the product of enzyme action on lumazine) to a solution of dithionite-reduced enzyme, and the complex is indefinitely stable so long as the enzyme is kept reduced.[193] This complex has been investigated by resonance Raman spectroscopy[195] as well as the previously cited XAS study,[167] and both sets of results have been interpreted in the context of direct coordination of product to the molybdenum via the hydroxyl ligand that has been introduced by the catalytic action of the enzyme, as previously suggested.[193] As stated above, the XAS results indicate that the molybdenum center possesses both Mo=O and Mo−SH, and there is (somewhat weaker)

evidence for a Mo—O at a distance (2.08 Å) appropriate for an alkoxy ligand to the metal. The resonance Raman spectrum of the complex exhibits resonance enhancement of a number of vibrational modes throughout the Raman shift range 250−1600 cm^{-1} when exciting at 676.4 nm (well within the charge-transfer absorption envelope),[195] providing strong evidence that the long-wavelength electronic transition that characterizes the complex is charge transfer rather than d−d in nature. When the Raman sample is prepared in $H_2{}^{18}O$, modes at 1469, 853, 517, and 325 cm^{-1} shift 5−12 cm^{-1} to lower frequency; this has been interpreted as reflecting strong vibrational coupling of Mo−O−C internal modes to ring modes of the hetercycle proper, effectively diluting the 25−50 cm^{-1} shift expected for $^{18}O/^{16}O$ substitution on the basis of simple harmonic oscillator calculations for Mo−O and O−C bonds.[195] Discouragingly, there was no evidence in the data for isotope-sensitive Mo═O stretching modes, expected in the region 850−1050 cm^{-1}, and it was simply concluded that these must be orthogonal to the transition dipole of the charge-transfer transition and therefore not resonance-enhanced by excitation within the charge-transfer absorption envelope.

The absorption features of the Mo^{IV}−product complex formed in the course of the reaction of xanthine oxidase with lumazine are not unique to this substrate. Indeed, uric acid binds to reduced xanthine oxidase to form a stable complex with absorption maxima at 360 and 550 nm,[196] and with both xanthine[197] and 2-hydroxy-6-methylpurine,[183] intermediates develop transiently in the course of the reaction with enzyme that exhibit discrete absorption features. Although the spectral changes observed exhibit substantially smaller extinction coefficients (500−800 M^{-1} cm^{-1} as compared with 4000 M^{-1} cm^{-1} observed for the violapterin complex) and the absorption maxima occur at ∼470 nm rather than 650 nm, they are nevertheless likely to arise from the same kind of interaction between purine and molybdenum center as is seen with violapterin. It thus appears that small spectral changes at the molybdenum center are in fact a characteristic feature of the reductive half-reaction of xanthine oxidase, although these are frequently difficult to resolve from the much larger spectral changes associated with reduction of the iron−sulfur and flavin centers of the enzyme that occur under most reaction conditions.

Studies of the reaction of enzyme with 2-hydroxy-6-methylpurine have proven particularly informative in examining the chemistry of the reductive half-reaction of xanthine oxidase.[183] This substrate has been known for some time to react relatively slowly with enzyme, turning over on a second rather than millisecond time scale, but to transiently accumulate substantial amounts of the Mo(V) species that gives rise to the so-called "very rapid" EPR signal in the course of the reaction when carried out at high pH.[198] This signal is one of several exhibited by the molybdenum center of xanthine oxidase, as indicated in Figure 5, and is thought to arise from a true intermediate in the catalytic sequence. The signal has $g_{1,2,3}$ = 2.0252, 1.9550, 1.9494 and is readily distinguished from the "rapid" family of Mo(V) EPR

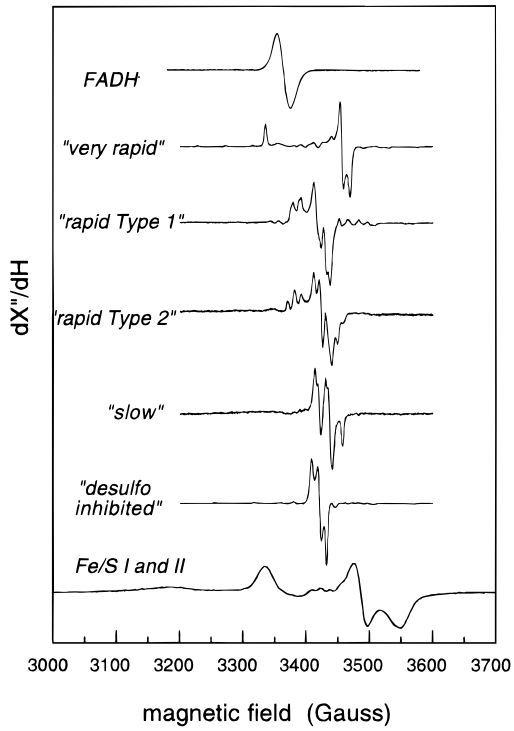

Figure 5. EPR signals exhibited by xanthine oxidase: (from top to bottom) flavin semiquinone, "very rapid", "rapid type 1", "rapid type 2", "slow" ("desulfo"), "desulfo inhibited", and the signals arising from the two iron−sulfur centers when reduced. After Bray,[4] with permission.

signals of xanthine oxidase in lacking obvious proton hyperfine structure.[172] In the course of the reaction of enzyme with xanthine at pH 10, this EPR signal accumulates maximally some 10 ms after mixing.[199−202] With 2-hydroxy-6-methylpurine, on the other hand, the reaction is not only slowed to the extent that the signal accumulates maximally at 40 s, but the relative magnitudes of the rate constants for formation and decay of the signal-giving species (1.3 and 0.11 s^{-1}, respectively at 25 °C) are such that approximately 80% of the enzyme molybdenum accumulates at maximum in the form of the signal-giving species.[183] Because the reaction is so slow, it is possible to perform the experiment under aerobic conditions with the significant advantage that reducing equivalents do not accumulate to any significant degree in the iron−sulfur centers and flavin of the enzyme, and these centers therefore do not contribute to the spectral changes observed in the course of the reaction. It is found that an initial intermediate, absorbing maximally (relative to oxidized enzyme) at 470 nm forms and subsequently decays to a second species exhibiting absorbance (again relative to oxidized enzyme) at 540 nm. The kinetics of the formation and decay of this second intermediate correspond within experimental error to the formation and decay of the "very rapid" EPR signal, and the 540 nm absorbance has been attributed to the UV/vis spectral signature of the EPR-active Mo(V) species.[183] In acid quench experiments, it is found that product 2,8-dihydroxy-6-methylpurine accumulated on a time scale comparable to that for formation of the first intermediate, indicating that the C−O bond of product is formed in the first step of the observed reaction.

Under the experimental conditions used in the above experiment, reducing equivalents departing the molybdenum center pass rapidly to the flavin center via intramolecular electron transfer, then on to molecular oxygen to form superoxide ion quantitatively.[204,205] The superoxide can be scavenged by cytochrome c^{III}, a reaction that can be conveniently monitored at 550 nm, making it possible to follow the rate-limiting decay of the Mo(IV)−product complex kinetically. It has been demonstrated in this way that the generation of the "very rapid" EPR signal is accompanied by the release of one reducing equivalent, with its subsequent decay giving rise to a second.[183] These results demonstrate that, from the standpoint of the molybdenum center, generation of the Mo(V) state is an oxidative event, and that the preceding intermediate in the reaction mechanism must be a Mo(IV) species. This EPR-silent state preceding the species giving rise to the "very rapid" EPR signal had in fact been anticipated on the basis of several lines of kinetic evidence.[193,202] The results are not consistent with a radical-based mechanism for formation of the "very rapid" EPR signal,[206] in which the "very rapid" species is generated directly by transfer of a single electron from substrate to Mo(VI). Instead, the evidence indicates that the initial chemical step of the catalytic sequence of xanthine oxidase is the two-electron reduction of Mo(VI) to Mo(IV), consistent with the results cited above with lumazine as substrate.

The species giving rise to the "very rapid" EPR signal has been extensively studied using a variety of techniques. In a series of incisive studies, Bray and co-workers utilized a variety of isotope substitution experiments to examine the nature of this species. When the EPR signal was generated using [8-^{13}C]xanthine, strong, approximately isotropic splitting of 3.2 G was observed, demonstrating that the purine nucleus of substrate was an integral component of the signal-giving species.[207] When the signal was generated using enzyme labeled with ^{33}S (by inactivating the enzyme with cyanide,[65] then reactivating with labeled sulfide[208]), strong and anisotropic coupling was observed, providing the initial evidence to suggest that the catalytically essential sulfur was a Mo=S group.[209,210] Similarly, when the signal was generated in $H_2{}^{17}O$, strong but approximately isotropic splitting of approximately 14 G was observed.[211] The signal-giving species was concluded to possess a Mo−OR group, representing the now hydroxylated product coordinated to the molybdenum via the newly introduced hydroxyl group. Although subsequent analysis left open the possibility that the strongly coupled oxygen observed in the "very rapid" EPR signal was due to Mo=O,[212] the original interpretation has been corroborated in more recent model compound studies.[184,213] This work, involving EPR studies of crystallographically well-defined model compounds possessing $LMo^{V}OS$ and $LMo^{V}(OH)S$ units (L = *N*,*N*′-dimethyl-*N*,*N*′-bis(2-mercaptophenyl)-1,2-diaminoethane), has shown that ^{17}O is weakly coupled when present as Mo=O group but much more strongly coupled when present as Mo−OH.[184] For example, coupling to two ^{17}O nuclei is observed in the Mo(V) model $LMo^{17}O(^{17}OH)$, with $a_{1,2,3}$ = 7.6, 3.3, 14.3 G and $a_{1,2,3}$ = 1.2, 3.1, 3.1 G.[184] Coupling in $LMo^{17}O(SH)$ or $LMo^{17}OS$, on the other hand, is substantially weaker and approximately isotropic ($a_{av} \approx$ 2.5 G), indicating that the more strongly coupled oxygen in the MoO(OH) complex is the hydroxyl group and not the terminal oxo. The results are thus consistent with a Mo−OR assignment for the strongly coupled ^{17}O in the "very rapid" enzyme species. This conclusion is also consistent with the observation that in the EPR signal elicited by the alloxanthine complex, which bears a striking resemblance to the "very rapid" EPR signal, no ^{17}O coupling is observed even by ENDOR[188] despite the fact that the signal-giving species is known to possess a Mo=O group.[167,168] In all, the EPR data from both ^{17}O-[184,213] and ^{33}S-labeled[214] models are entirely consistent with a *fac*-Mo(V)OS(OR) species in the enzyme giving rise to the "very rapid" EPR signal.

The "very rapid" EPR signal has also been analyzed using enzyme that has been isotopically labeled with molybdenum.[212] The natural abundance of molybdenum includes two isotopes, ^{95}Mo (15.7%) and ^{97}Mo (9.5%), possessing $I = {}^5/_2$; ^{97}Mo also has a substantial nuclear quadrupole. Data has been obtained with the "very rapid" signal generated using enzyme enriched in ^{95}Mo ($I = {}^5/_2$; $Q \approx 0$) and ^{97}Mo ($I = {}^5/_2$; Q = 1.1b) to ascertain the molybdenum hyperfine interaction in the signal-giving species.[212] (Isotopically enriched enzyme is obtained by isolating enzyme from cows that have been treated with an oral or intravenous dose of a neutral molybdate solution of the appropriate isotope over a period of several days. Although orally administered molybdate is moderately toxic to cattle, the dose can be kept well below the lethal limit; the procedure yields essentially complete isotopic enrichment in a protein from a very large eukaryote.) For the "very rapid" signal seen with 2-hydroxy-6-methylpurine, the molybdenum hyperfine splitting is quite anisotropic, $A_{1,2,3}$ = 141.6, 60.1, 63.4 MHz for ^{95}Mo, and the **g** and **A** tensors are distinctly noncoincident with α and β Euler angles of 7 and 42°, respectively, indicating that the signal-giving species possesses low molecular symmetry or none at all. In the spectrum obtained with ^{97}Mo-enriched enzyme, the introduction of a significant molybdenum quadrupole moment results in orbital mixing that substantially reduces the forbiddenness of $\Delta M_I \neq 0$ transitions that contribute appreciably to the observed EPR signal (and even to that of the natural-abundance enzyme).[212]

The "very rapid" EPR signal has also been examined recently by electron spin echo[215] and ENDOR spectroscopy.[188] In the former work, the electron spin−echo envelope modulation (ESEEM) of the "very rapid" EPR signal generated with 2-hydroxy-6-methylpurine was examined and compared with that for the so-called "desulfo-inhibited" EPR signal of the enzyme. This latter signal is prepared in substantial amounts by inactivation of the enzyme with cyanide, reduction with sodium dithionite, and treatment with ethylene glycol, followed by air oxidation.[216] By contrast with the ESEEM exhibited by this signal, that of the "very rapid" signal exhibits strong coupling to at least two nitrogen nuclei, and it has been concluded that the detected nitrogens

Scheme 9

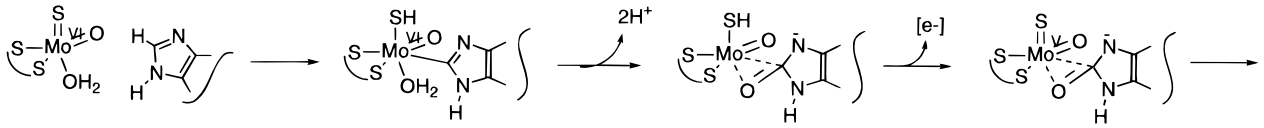

derive from the purine nucleus of substrate. The molybdenum coordination sphere is otherwise devoid of nitrogen-containing ligands (*e.g.*, histidine or the pterin nucleus of the cofactor coordinated directly to molybdenum via nitrogen). This interpretation is consistent with independent ENDOR studies[217] and has subsequently been substantiated by the crystal structure of the *D. gigas* aldehyde oxidoreductase.[6] Although coupling to protons is not evident in the normal EPR of the "very rapid" signal, weak coupling to several solvent-exchangeable protons is observed in the ESEEM of this signal. By using a deuterium-ratioing technique, it has proven possible to estimate a distance of 3.2 Å to the nearest of these protons, a distance considered consistent with it being the $N_\epsilon-H$ of the imidazole subnucleus of product coordinated to the molybdenum via its C-8 hydroxyl group, assuming a bent rather than linear Mo−O−C geometry.[215]

In recent ENDOR studies, Bray and co-workers have investigated several EPR-active states of the molybdenum center of xanthine oxidase using isotope probes. The signals examined have included the "inhibited" signal,[218] as well as the "very rapid" signal formed with both xanthine and 2-hydroxy-6-methylpurine and the "very rapid"-like signal obtained upon partial reoxidation of the complex of alloxanthine with reduced enzyme.[188] In the case of the "inhibited" signal generated by reaction of functional enzyme with doubly labeled $^2H_2{}^{13}CO$, ENDOR spectra recorded throughout the EPR absorption envelope permit assignment of the ^{13}C-hyperfine coupling tensor, with $A_{1,2,3}$ = 52.5, 40.6, 40.6 MHz being determined. The anisotropy of this coupling can be used in the context of a point dipole approximation for the magnetic interaction to yield a Mo−C distance. With a correction applied to account for electron density on the carbon p orbitals (which accumulates due to π bonding with the valence d_{xy} orbital of the Mo(V)), a distance of 1.9 Å has been determined, and it has been concluded that the signal-giving species possesses a Mo−C bond. When the same procedure is applied to the "very rapid" EPR signal generated by reaction of enzyme with [8-^{13}C]-xanthine, the components of the hyperfine tensor are found to be $A_{1,2,3}$ = 7.6, 11.1, 7.6 MHz and a $Mo-C_8$ distance of <2.4 Å is obtained, again interpreted to reflect a direct Mo−C bond in the signal-giving species. In this work, caveats were emphasized concerning the applicability of the point−dipole approximation and the approximate nature of the various corrections made owing to uncertainties in the exact electronic structure of the molybdenum center. These follow in large part to the substantial extent (~40%) to which the unpaired spin density in the species giving rise to the "very rapid" EPR signal is delocalized onto the Mo=S group.[212] These concerns notwithstanding, it was felt that the data provided reasonable support for a Mo−C bond in the species giving rise to the "very rapid" EPR signal.

When the "very rapid" EPR signal observed in the course of the reaction of enzyme with 2-hydroxy-6-methylpurine is generated in $H_2{}^{17}O$, a strongly coupled oxygen is observed in the ENDOR spectrum ($A_{1,2,3}$ = 32.4, 34.7, 35.4 MHz) that has been assigned as the oxygen of the C_8-hydroxyl of nascent product. No evidence for a second, more weakly coupled, oxygen is found that might be assigned as the Mo=O group present in the signal-giving species, even when the signal is generated using enzyme that has previously turned over in labeled water. Similarly, no coupling to ^{17}O is observed at all in the "very rapid"-like EPR signal observed with alloxanthine-complexed enzyme. Particularly in the case of the "very rapid" signal, it is expected that the Mo=O group would have become labeled in the course of this experiment were it the catalytically labile oxygen, and on the basis of the failure to observe a second, weakly coupled oxygen in addition to the strongly coupled oxygen of the Mo−O−C unit, it has been concluded that the Mo=O group does not represent the catalytically labile oxygen.[188] However, the possibility cannot be excluded that the Mo=O has in fact become labeled under turnover conditions in these experiments, but is not detected owing to intrinsically weak coupling of ^{17}O to the electron spin of the Mo(V) species (in agreement with model compound studies[184,213]) and/or significant line broadening due to quadrupolar interactions with the ^{17}O nucleus. To the extent that either of these alternatives are possible, the data do not exclude a mechanism based on oxygen atom transfer from the Mo=O.

In light of the above ENDOR results, a new mechanism for the initial step in the reaction of xanthine oxidase has been proposed (Scheme 9).[188] This mechanism involves insertion of the C_8-H bond across the Mo=S of the molybdenum center in a fashion comparable to that considered by Coucouvanis above,[187] but in a way that does not lead directly to reduction of molybdenum. Instead, subsequent reaction with a "buried" oxygen (perhaps the water coordinated to the molybdenum) yields a Mo−O−C three-membered ring in which substantial Mo−C bond character remains; oxidation of this species by one electron is proposed to yield the species giving the "very rapid" EPR signal and having the structure given in Scheme 7. It is not clear, however, how substantive the differences in physical structure are for the two quite different electronic structures for the product of the initial step of the catalytic sequence given in Scheme 7, on the one hand, and Schemes 4 or 5 on the other. It is undoubtedly the case that the oxygen of the $Mo^{IV}-OR$ species of Scheme 4 is sp^3 hybridized, with the result that the Mo−O−R bond angle will be on the order of 107° and the Mo−C distance will be substantially shorter than the sum of the Mo−O and O−C bonds. Although the Mo−C distance cannot be made as small as 2.4 Å

simply by making the Mo−O−C angle more acute, it must be kept mind that there is considerable uncertainty regarding the value for the Mo−C distance estimated from the ENDOR experiments. Furthermore, the extent to which the geometry of the species must actually change to accommodate a η^2 bond of the type envisioned in the mechanism shown in Scheme 7 is also not obvious, and the Mo−O and Mo−C distances are almost certainly unequal. What is substantively different in the first intermediate formed in the mechanisms of Schemes 4 and 5, on the one hand, and Scheme 7 on the other, is the formal oxidation state of the molybdenum, being Mo(IV) in the former cases and Mo(VI) in the latter. (Although bonding from the coordinated purine can possibly reduce the formal positive charge on the molybdenum in the structure shown in Scheme 7, from the standpoint of a formal valence count the electrons involved belong to the ligand. It is also clear that the purine nucleus clearly has not been oxidized at this stage of the reaction. It is further to be noted that η^2 bonds of the type shown are typically found only in complexes of highly reduced metals (*e.g.*, Mo(III)) as back-bonding by d electrons is required to stabilize the complex.) The mechanism in Scheme 9 is also difficult to reconcile with the kinetic and structural results obtained with the lumazine/violapterin system. As discussed above, the long-wavelength absorbing intermediate observed transiently in the course of the reaction of enzyme with lumazine[194] can also be formed upon addition of product violapterin to enzyme that has been reduced with a reagent such as sodium dithionite.[193] The EXAFS of this species clearly demonstrates the presence of a Mo=O group but no evidence for carbon at so short a distance as 2.4 Å (although it must be said that such a weak scatterer as carbon could easily have been missed in the EXAFS analysis), and the near-edge data indicates that the oxidation state of the molybdenum is IV not VI.[167] Given that the formation of this intermediate in all likelihood represents the first committed step of catalysis, the conclusion seems inescapable that at the stage of the first intermediate encountered in the catalytic sequence the molybdenum center has become formally reduced from the VI to the IV valence state. Clearly, more work is required in light of the new ENDOR data to ascertain the extent to which the alternate electronic representations for this intermediate as represented in Schemes 4 and 7 more accurately represent the structure of this critical intermediate and the chemistry by which it arises.

The above differences in interpretation of the ESEEM and ENDOR data notwithstanding, it is significant that in neither study is evidence found for coupling of the molybdenum to phosphorus. It has previously been proposed on the basis of ^{31}P NMR that a phosphoserine residue is present in the active site of xanthine oxidase and that this may act as a nucleophile in initiating the chemistry leading to hydroxylation of substrate.[219] The reproducibility of the NMR result has been called into question, however,[220] and no evidence for an active site phosphoserine has been obtained by ^{31}P ENDOR[221] In addition, careful quantitation of the phosphate in highly purified xanthine oxidase indicates that the enzyme possesses only three phosphate groups (constituents of the pterin cofactor and FAD) and the presence of a phosphoserine residue in the active site of xanthine oxidase has become controversial.[220,221] The absence of apparent ^{31}P coupling in the catalytically relevant "very rapid" species studied by ESEEM[215] and ENDOR[188] argues against any catalytic role for a phosphoserine residue, even if one is present in the enzyme. It is worth noting that the *D. gigas* aldehyde oxidoreductase whose crystal structure has been determined does not possess a phosphoserine residue in either its desulfo[6] or sulfido[57] forms. While Ser 698 of this protein is found near the active site with its −OH group approximately 5.8 Å from the molybdenum atom, it is clear from the electron density that this residue is not phosphorylated.

Regardless of the form that the first intermediate of the reaction takes, in both mechanisms it possesses the C_8−H proton of substrate bound as Mo−SH.[222−224] This proton must be lost on forming the species giving rise to the "very rapid" EPR signal, as this signal possesses no strong coupling to protons, and the Mo−SH proton would certainly be expected to be evident were it present. In addition, breakdown of the "very rapid" species must involve reprotonation in order to yield the neutral form of product. The pH dependence and solvent isotope sensitivity of these latter stages of the reaction have been examined to test this, and the results are found to be fully consistent with the expected behavior.[191] By contrast with the bell-shaped pH dependence of its formation (discussed above), decay of the complex of reduced enzyme with violapterin (presumably via a Mo(V) intermediate[194]) is found to be a base-catalyzed process governed by an ionizable group having a pK_a ≥ 11. It has been suggested that it is ionization of the Mo^{IV}−SH group itself that is responsible for the observed rate acceleration at high pH, as depicted in Scheme 10.[191] Similarly, the pH dependence of the

Scheme 10

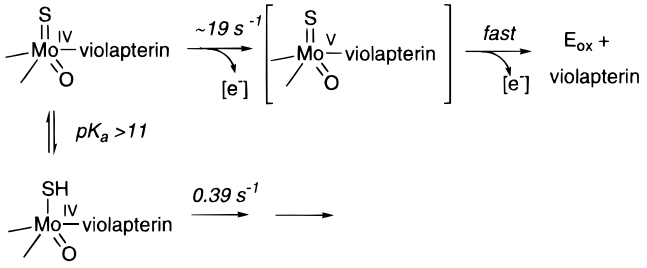

decay of the "very rapid" EPR signal generated upon reaction of enzyme with 2-hydroxy-6-methylpurine is found to be an acid-catalyzed process, governed by a group having a pK_a ≤ 5.5. In this case, protonation of the purine nucleus of molybdenum-bound product is proposed to drive product dissociation (Scheme 11), which is known to be the rate-limiting step of overall catalysis.[202] Each of the three steps examined (formation of E_{red}−P, oxidation to the "very rapid" species, and decay of the latter intermediate) also have been found to exhibit solvent kinetic isotope effects on the order of 1.7−2.4, consistent with the

Scheme 11

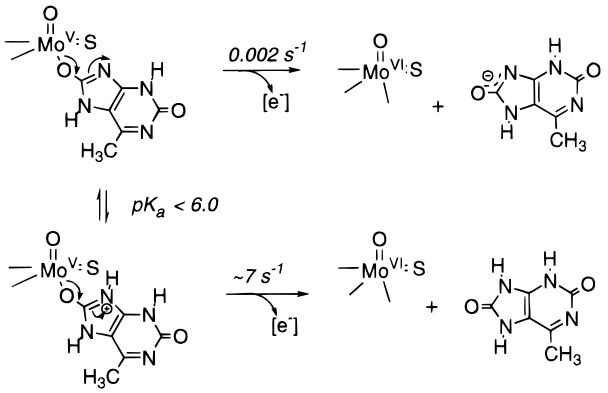

movement of solvent-exchangeable protons in the course of traversing the transition states associated with each of these processes.[202] It has long been known that the reduction potentials of even the simplest Mo=O complexes are strongly coupled to ionizations in the molybdenum coordination sphere,[66,78] and the pH dependence of the several steps of the reaction mechanism examined here demonstrates that there is a kinetic as well as thermodynamic manifestation of this phenomenon. In addition, two of the mechanistically relevant ionizations have strictly to do with the purine nucleus of substrate/product, and it appears likely that differences in pK_a from one substrate to the next play an important role in determining the overall effectiveness of a given heterocycle as a hydroxylatable substrate as well as the relative amount of each intermediate (particularly the Mo(V) species giving rise to the "very rapid" EPR signal) that accumulates in the course of the reaction.

The above pH dependence studies complement earlier work by Mondal and Mitra in which the temperature-dependence of the steady-state and rapid kinetics of the reaction of enzyme with xanthine were examined to obtain a more comprehensive picture of the thermodynamics of the overall reaction.[225] In these studies, the "chemical" step responsible for formation of the reduced enzyme−product complex was found to be unusual in possessing negative values for both the enthalpy and entropy of activation (−5.7 kcal/mol and −70 cal mol^{-1} deg^{-1}, respectively, yielding a free energy of activation of 15.1 kcal/mol). The implication of this result is that the transition state for this step of the reaction mechanism was quite highly ordered. In addition, using a combined relationship involving both steady-state ($k_{cat}/K_m^{xanthine}$) and rapid-reaction (k_{lim} and $K_d^{xanthine}$) parameters, it proved possible to calculate the rate constants for substrate binding to and dissociation from the oxidized enzyme: at pH 7.1, 25 °C these were 2.3 × 10^6 M^{-1} s^{-1} and 28 s^{-1}, respectively. Finally, in the process of rationalizing the nonlinear temperature dependence of the limiting rate constant for the reductive half-reaction it proved possible to resolve the individual rate constants for formation of the reduced enzyme−product complex and subsequent dissociation of product from reduced enzyme: again at pH 7.1, 25 °C the values obtained were 55 and 7.4 s^{-1}, respectively. (These values are not necessarily in conflict with the results of D'Ardenne and Edmondson,[182] who found from a comparison of kinetic and intrinsic isotope effects that the C_8−H bond-breaking step must be at least 75-fold faster than product release, as these latter workers performed their experiments at pH 8.5 rather than 7.1.) Interestingly, the temperature dependence of these two steps were such that above 37 °C the chemical step rather than product release became rate limiting: at 50 °C the rate constants obtained were 24 and 208 s^{-1}, respectively. These results imply that at sufficiently high temperature the kinetic isotope effect on the limiting rate constant for the reductive half-reaction should approach the value of ∼7.4 determined for the intrinsic isotope effect for the bond-breaking step of the reaction.[182]

In other work, the mechanistic role of the "rapid" family of Mo(V) EPR signals has been clarified. Although the "rapid type 1" signal, which typically predominates under catalytic conditions with xanthine, was for some time considered to arise from an intermediate in the catalytic sequence lying downstream from that giving rise to the "very rapid" EPR signal,[181] it is evident that this is not the case as the "rapid" signals are not observed in the course of single-turnover experiments.[183,197] The "rapid" signals arise only under those experimental conditions in which substrate (or, in some cases, product) encounters partially reduced enzyme in the course of the reaction, and indeed substantial amounts of both "rapid type 1" and "rapid type 2" signals can be generated extremely rapidly (within 5 ms) simply by mixing an appropriate substrate with enzyme that has been partially reduced with a reagent such as sodium dithionite.[175] Particularly with the slow substrate 2-hydroxy-6-methylpurine, formation of the "rapid type 2" signal observed with this substrate occurs much too rapidly to have been generated catalytically by breakdown of the "very rapid" species. It is now generally considered that the signal-giving species is simply a complex of substrate with enzyme that possesses molybdenum in the V valence state, as was in fact concluded in the initial studies of the signal.[174] As such, the species must lie off the main catalytic sequence (which must begin with Mo(VI)), but can be thought of as a paramagnetic analog of the true Michaelis complex and is therefore of considerable mechanistic interest. In this regard it is significant that addition of xanthine to partially reduced xanthine oxidase results in only relatively minor perturbations of the "rapid type 1" signal seen upon partial reduction of the enzyme with sodium dithionite,[172] indicating that the effect on the molybdenum coordination sphere of substrate binding is minimal and suggesting that substrate does not coordinate to the molybdenum directly. Indeed, several candidate substrate-binding sites have been identified in the crystal structure of the *D. gigas* aldehyde oxidoreductase[6] and none of these is at an appropriate distance and orientation for direct coordination of substrate to the metal. It is likely that the two "rapid" species differ principally in the orientation of substrate with respect to the molybdenum center, and it appears that the species giving rise to the "type 1" signal possesses the more catalytically relevant orientation. The basis for this

conclusion is that warming of an EPR sample possessing both "type 1" and "type 2" signals to 240 K (a temperature at which the sample remains frozen) allows the species giving rise to the "type 1" signal, but not that giving the "type 2", to progress through the catalytic sequence.[226]

If the "rapid" signals indeed represent paramagnetic analogs of the Michaelis complex, then they provide a unique opportunity to examine the starting point of catalysis. It has been shown that the more strongly coupled proton observed in the "rapid type 1" signal is derived from the C-8 position of substrate from a previous catalytic cycle, but bound to the enzyme in the signal-giving species. This proton exchanges rapidly with solvent,[222,223] and on the basis of the strength of its coupling is considered to be the $Mo^{V}-SH$ proton.[224] Although ionization of this group gives Mo=S as is found in the species giving rise to the "very rapid" EPR signal, it has been recognized for some time that the "rapid" and "very rapid" species do not constitute a conjugate acid/base pair;[227] in the context of the structures for the "very rapid" species considered here, this is clearly due to the absence of a Mo−OR interaction in the "rapid" species. As in the case of the "very rapid" signal, the "rapid type 1" signal has been examined using both ^{33}S [210] and ^{17}O [228] isotopic labeling of the enzyme active site. By contrast with the "very rapid" EPR signal, which exhibits strong and anisotropic coupling to ^{33}S, ^{33}S coupling in the "rapid type 1" signal generated with the substrate 1-methylxanthine is found to be relatively weak and isotropic, consistent with a $Mo-^{33}SH$ group present in the species giving rise to the "rapid" signal.[210] With ^{17}O, a single strongly and anisotropically coupled ^{17}O is observed in the "rapid type 1" signals generated with formamide or purine ($a_{av} \approx 14$ G) that was initially interpreted as arising from Mo=O.[228] As indicated above, however, more recent model compound work indicates that terminal oxo groups tend to be only weakly and rather isotropically coupled to the unpaired electron spin.[184,213] These model compound studies demonstrate that the strongly coupled oxygen in the "rapid type 1" EPR signal is unlikely to be Mo=O, but instead is presumably the $Mo-OH_2$ demonstrated to be present in the *D. gigas* aldehyde oxidoreductase.[6] The significance of this assignment has to do with the nature of the catalytically labile oxygen in oxidized enzyme that is destined to become strongly coupled in the "very rapid" signal. The outstanding mechanistic issue is whether this donor site is the Mo=O or $Mo-OH_2$ of the oxidized enzyme, and the key question is whether the strongly coupled $Mo-^{17}OH$ in the "rapid" signal is lost on a catalytic time scale. Although it is frequently assumed in discussions of the reaction mechanism of xanthine oxidase that the strongly coupled oxygen site in the "rapid" species represents the catalytically labile oxygen, this has not yet been unequivocally demonstrated. Were this the case, then clearly a reaction mechanism such as that shown in Scheme 5 or 7 in which a (strongly coupled) metal-activated water undergoes nucleophilic attack on the C-8 position of substrate in the course of the hydroxylation reaction would be reasonable—otherwise a mechanism based on an electrophilic Mo=O would be preferred. The question is whether exchange of label takes place on a catalytic time scale under catalytic conditions. Simple loss of label under multiple turnover conditions cannot be regarded as definitive as it has been shown that simple reduction of the enzyme under noncatalytic conditions is sufficient to accelerate exchange of the catalytically labile oxygen with solvent.[177] It thus remains for future experiments to establish the mechanistically critical point as to whether the catalytically labile oxygen is the Mo=O or $Mo-OH_2$ of the enzyme active site.

C. Studies of Electron Transfer within Xanthine Oxidase

The molybdenum center of xanthine oxidase participates directly only in the reductive half-reaction of the catalytic cycle, *i.e.*, the oxidative hydroxylation of xanthine that introduces reducing equivalents into the enzyme. Reoxidation of the molybdenum center takes place via simple electron transfer to the other redox-active centers of the enzyme, ultimately to the FAD where electrons are removed from the enzyme by reaction with dioxgen.[165, 203−205] Intramolecular electron transfer within xanthine oxidase and related enzymes is thus an integral aspect of catalysis and has been extensively studied from both a thermodynamic and kinetic standpoint. The behavior of xanthine oxidase in the course of reductive titrations has been shown to be quantitatively described by a model in which reducing equivalents distribute themselves among the several redox-active centers of the enzyme according to their relative reduction potentials;[202] there is no evidence for interactions of the type found in cytochrome *c* oxidase, for example, where the oxidation state of one center influences the reduction potential of another.[229] In xanthine oxidase, the reduction profiles for the several redox-active centers of the enzyme in the course of titrations with sodium dithionite are accurately described using a single set of six independent relative reduction potentials. The set of relative reduction potentials obtained from simulations of the set of reduction profiles has been independently confirmed by direct potentiometry, following the signature EPR signals of the enzyme (distinct signals arise for each of the two reduced iron−sulfur centers, as well as Mo(V) and $FADH^{\bullet}$) as a function of the electrochemically poised system potential,[230] providing strong support for a simple equilibrium model.

A basic assumption in the model as applied to the kinetic behavior of the enzyme is that reducing equivalents attain their equilibrium distribution within the enzyme rapidly relative to the rates of electron entry at the molybdenum center or egress at FAD in the course of turnover. This assumption has been validated in rapid kinetic studies of enzyme in which the native FAD has been substituted with chemically modified derivatives covering a range in midpoint potential of ~200 mV.[231] It is possible to ascertain the relative time courses for iron−sulfur and FAD reduction in this homologous series of enzyme forms by comparing kinetic transients at wavelengths specific for Fe-S and FAD reduction in

the course of the reaction of enzyme with substrate. It is found that when the enzyme possesses a high-potential flavin (*e.g.*, 8-Cl or 2-thioFAD), reduction of FAD precedes that of the iron−sulfur centers; the reverse is true when the enzyme possesses a low-potential flavin derivative (6- or 8-hydroxyFAD, for example). The most likely explanation for the apparent order of reduction of the centers distal to the molybdenum depending on the relative reduction potentials of the flavin and Fe-S centers is that the time scale of equilibration of reducing equivalents within the enzyme is faster than that for reaction of enzyme with substrate.

Although electron transfer among the redox-active centers of xanthine oxidase has been shown to be quite rapid (see below), turnover nevertheless can be severely attenuated when the internal equilibrium distribution of reducing equivalents becomes unfavorable. By using the same series of enzyme forms possessing chemically modified flavins, it is found that V_{max} depends sigmoidally on the flavin midpoint potential, with enzyme possessing low-potential flavin derivatives exhibiting less than 10% of the catalytic power of enzyme possessing high-potential derivatives.[231] This has been shown to be due to the accumulation of reduced molybdenum and oxidized flavin in the steady state as a result of an unfavorable distribution of reducing equivalents in the partially reduced enzyme species generated in the course of catalysis. To the extent that the molybdenum center becomes reduced to either the V or IV state or the flavin site remains oxidized in the steady-state catalysis should be compromised, since neither center is in the appropriate oxidation state to participate in its respective half-reaction. It is found that the V_{max} data can be quantitatively accounted for by assuming a simple two-electron redox equilibrium between the flavin and molybdenum centers of the enzyme (Scheme 12).[231] For the reasons given above,

Scheme 12

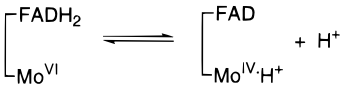

the electron distribution on the right-hand side of Scheme 10 is catalytically inert and its accumulation in the steady state results in loss of activity (even though the individual half-reactions proceed rapidly under optimal conditions: *i.e.*, 100% Mo(VI) for the reductive half-reaction and 100% $FADH_2$ for the oxidative half-reaction). This situation has been termed thermodynamic control[232] and may prove relevant to biological electron transport systems such as those found in the chloroplast and mitochondrion in addition to xanthine oxidase and closely related enzymes.

In other potentiometric studies, the pH dependence of the reduction potentials of xanthine oxidase have been examined using the room-temperature EPR signals of $FADH^{\bullet}$ and Mo^{V} and the circular dichroism changes associated with iron−sulfur reduction as experimental probes. It has been found that all the reduction potentials of xanthine oxidase are pH dependent to varying degrees (Table 3).[233−235] In the case of the flavin center, E_1 (the potential for the quinone/semiquinone couple) decreases approximately linearly by 170 mV over the pH range 7−10 (−319 mV at pH 8.3), consistent with the obligatory uptake of a proton to form the neutral semiquinone upon one-electron reduction of the flavin ($pK_a > 9$). On the other hand, E_2 (the potential for the semiquinone/hydroquinone couple) decreases by only 60 mV over the same pH range (−238 mV at pH 8.3), indicating that the flavin hydroquinone is predominantly $FADH^-$ at neutral pH ($pK_a < 6$).[233] The two half-potentials of the molybdenum center exhibit a somewhat greater pH dependence than do those of the flavin site; the Mo(VI/V) potential decreases by 190 mV in an approximately linear fashion over the pH range 6−10 (−360 mV at pH 8.3) and the Mo(V/IV) couple by 80 mV (−320 mV at pH 8.3).[233] As indicated above, this behavior is consistent with the known properties of molybdenum complexes, in which it is frequently found that prototropic equilibria are thermodynamically linked to changes in the molybdenum oxidation state.[66,78] As in the case of the FAD, addition of the first electron to the molybdenum center is more tightly coupled to proton uptake than is the second. The reduction potentials of the two iron−sulfur centers also exhibit some pH dependence, but the effect is substantially smaller than is observed with the flavin and molybdenum centers: both iron−sulfur potentials decrease in a linear fashion by ∼60 mV as the pH is increased from 6 to 10 (having values of −332 and −224 mV for Fe-S II and Fe-S I, respectively, at pH 8.3).[233]

Rate constants for electron transfer between specific pairs of redox-active centers within xanthine oxidase have been examined by flash photolysis, a pH-perturbation method, and pulse radiolysis. In the initial effort to examine intramolecular electron transfer, photolytically generated deazalumiflavin radical was used to rapidly introduce reducing equivalents into the enzyme.[236,237] This initial protein reduction event, which occurs principally at the flavin center with a second-order rate constant of 3×10^7 M^{-1} s^{-1}, is followed by spectral changes attributed to specific intramolecular electron transfer between the iron−sulfur centers and FAD with rate constants in the range of 10−80 s^{-1}. It was initially concluded that electron transfer was partially rate limiting in catalysis,[236] but this interpretation has since been modified.[237] In particular, the prominent kinetic process, taking place at ∼10 s^{-1} observed in the earlier work, is presently thought to be a kinetic artifact, and a new value of ∼100 s^{-1} has been assigned for the equilibration of a reducing equivalent between the flavin and one of the iron−sulfur centers (that designated Fe-S II); it has been concluded that electron transfer between Fe-S II and the molybdenum center takes place on a similar time scale.[237] The nature of the slow kinetic artifact observed in the flash photolysis work with xanthine oxidase, which amounts to a substantial portion of the observed absorbance change (as much as 50%, depending on the wavelength of observation), is at present not well understood.

A different approach to determining the rate of electron transfer within xanthine oxidase has utilized a pH-jump perturbation technique, it having been

Table 3. Reduction Potentials of Xanthine Oxidase and Related Enzymes

	Mo^{VI}/Mo^{V}	Mo^{V}/Mo^{IV}	Fe-S_I	Fe-S_{II}	FAD/FADH$^{\bullet}$	FADH$^{\bullet}$/$FADH_2$
xanthine oxidase[a]	−345	−315	−310	−217	−301	−237
xanthine oxidase[b]	−373	−377	−310	−255	−332	−234
chicken liver xanthine dehydrogenase[c]	−357	−337	−280	−275	−294	−330
milk xanthine dehydrogenase[d]	ND	ND	−310	−235	−270	−410
rabbit liver aldehyde oxidase[e]	−359	−351	−207	−310	−258	−212
	Mo^{VI}/Mo^{V}	Mo^{V}/Mo^{IV}	heme		FAD/FAD$^{-\bullet}$	FAD$^{-\bullet}$/$FADH_2$
chicken liver sulfite oxidase[f]	38	−239	68		NA	NA
spinach nitrate reductase[g]	2	−6	−123		−380	−180
Chlorella vulgaris nitrate reductase[h]	15	−25	−164		−372	−172

[a] At pH 7.7 (0.1 M potassium *N*,*B*-bis(2-hydroxyethyl)glycine, 25 °C): Porras, A. G.; Palmer, G. *J. Biol. Chem.* **1982**, *257*, 11617. [b] At pH 7.7 (50 mM bicine, 1 mM EDTA, 25 °C): Barber, M. J.; Siegel, L. M. *Biochemistry* **1982**, *21*, 1638. [c] At pH 7.8 (50 mM phosphate, 173 K and 25 K): Barber, M. J.; Coughlan, M. P.; Kanda, M.; Rajagopalan, K. V. *Arch. Biochem. Biophys.* **1980**, *201*, 468. [d] At pH 7.5 (0.1 M pyrophosphate, 0.3 mM EDTA, 25 °C): Hunt, J.; Massey, V.; Dunham, W. R.; Sands, R. H. *J. Biol. Chem.* **1993**, *268*, 18685. [e] At pH 7.8 (50 mM phosphate, 0.1 mM EDTA, 25 °C): Barber, M. J.; Coughlan, M. P.; Rajagopalan, K. V.; Siegel, L. M. *Biochemistry* **1982**, *21*, 3561. [f] At pH 7 (0.02 M "universal buffer" (equimolar Tris, Bis-Tris and Bis-Tris propane), 0.1 M KCl, 25 °C): Spence, J. T.; Kipke, C. A.; Enemark, J. H.; Sunde, R. A. *Inorg. Chem.* **1991**, *30*, 3011. [g] At pH 7 (50 mM MOPS, 25 °C): Kay, C. J.; Barber, M. J.; Notton, B. A.; Solomonson, L. P. *Biochem. J.* **1989**, *263*, 285. [h] At pH 7 (50 mM MOPS, 25 °C): Kay, C. J.; Barber, M. J.; Solomonson, L. P. *Biochemistry* **1988**, *27*, 6142.

demonstrated that the distribution of reducing equivalents within partially reduced xanthine oxidase is pH dependent.[233,234] The pH-driven redistribution of reducing equivalents within the enzyme, observed upon mixing partially reduced enzyme in dilute buffer with more concentrated buffer at another pH, is well-behaved kinetically, with the observed rate constant increasing linearly from 155 s^{-1} at pH 6 to 330 s^{-1} at pH 10.[238] The observed spectral change is consistent with electron transfer between Fe-S I and the FAD. A comparison of the static and kinetic difference spectra associated with the pH-jump reaction, however, indicates that there is a substantial spectral change taking place in the dead time of the stopped-flow apparatus (~2 ms) that is consistent with electron equilibration between Fe-S I and the molybdenum center. The observed rate constant for the kinetically observable process in the pH jump experiment, representing the slower kinetic phase, is at least 10-fold faster than k_{cat} at any given pH, thus demonstrating that the equilibration of reducing equivalents within xanthine oxidase is indeed rapid relative to overall catalysis and is not rate limiting.

The kinetics of intramolecular electron transfer within xanthine oxidase have also been examined using the technique of pulse radiolysis.[239,240] Like flash photolysis, the pulse radiolysis technique involves very rapidly generating a strong reductant that reacts rapidly with enzyme so that subsequent intramolecular electron transfer events taking place more slowly can be followed. Strongly reducing or oxidizing species can be generated radiolytically whose chemical reactivity is appropriate for the study of redox-active proteins, and undesirable reactions with the primary radiolytically generated radicals (such as the ionization of aromatic amino acid residues) can thereby be minimized.[241] In work with xanthine oxidase, radiolytically generated *N*-methylnicotinamide radical has been used most extensively, and is found to selectively reduce the molybdenum center of the enzyme with a diffusion-controlled rate constant of 9×10^8 M^{-1} s^{-1}. At pH 6.0, initial reduction of the molybdenum center is followed by two quite distinct kinetic phases, with rate constants of 8500 and 125 s^{-1}; both of these rate constants are independent of enzyme concentration and have been taken to represent intramolecular processes. The rate constant and spectral change associated with the slower kinetic phase agree well with the pH-jump results, and the process has been attributed to electron equilibration between Fe-S I and FAD.[239] On the basis of its associated spectral change, the faster of the two intramolecular kinetic phases, with a rate constant of 8500 s^{-1}, has been attributed to electron transfer from the initially reduced molybdenum center to one of the iron−sulfur centers of the enzyme.[282] Given the strong magnetic interaction that has been documented between Fe-S I and the molybdenum center,[162] it is likely that this is the iron−sulfur center involved in oxidation of the molybdenum. The reduction potentials for the donor and acceptor are known, and it can be assumed that the faster internal electron-transfer event takes place over a distance comparable to that separating the molybdenum center and nearer iron−sulfur cluster in the *D. gigas* aldehyde oxidoreductase (14.5 Å).[6] By using these values, the observed rate constant of 8500 s^{-1} yields reasonable values for β from Marcus theory in the range of 1.0−1.4 when estimates for the reorganizational energies in the range 1.0−1.5 eV are used.

When radiolytically generated deazariboflavin radical rather than methylnicotinamide radical is used as reductant, it is the flavin and iron−sulfur centers that become reduced initially, rather than the molybdenum,[240] consistent with the above flash photolysis studies.[237] At both pH 6 and 8.5, the initial reduction of enzyme is followed by spectral changes with rate constants of 120 and 218 s^{-1} at pH 6 and 8.5, respectively. The associated spectral changes are consistent with electron transfer between Fe-S and FAD, and the rate constants are in good agreement with the radiolytic studies using methylnicotinamide radical as reductant and also with the earlier pH jump studies. Surprisingly, slow kinetic processes such as observed in the flash photolysis work are not seen in the work with radiolytically generated deazariboflavin radical.

On the basis of this work, electron transfer within xanthine oxidase can be summarized as shown in Scheme 13:

Scheme 13

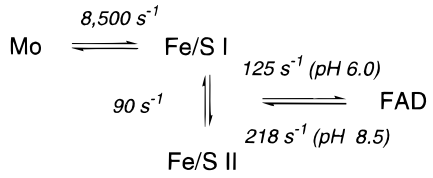

The observation of transient reduction of the iron−sulfur centers in the course of electron migration from the molybdenum to the FAD has been interpreted as evidence for mediation of electron transfer between the Mo and FAD sites of the enzyme by the iron−sulfur centers.[240] This interpretation is consistent with the crystallographic results with the *D. gigas* aldehyde oxidoreductase, which strongly suggest that electrons depart the molybdenum center for the iron−sulfur center that is in contact with the pterin cofactor of the molybdenum center (regardless of where the FAD center proves to be in xanthine oxidase).

Proton association/dissociation events have been found to play an important role in electron transfer involving the flavin center of xanthine oxidase.[242] Electron equilibration between the FAD and Fe-S I, as determined using the pH-jump protocol described above, exhibits a substantial solvent kinetic isotope effect of 7 regardless of the direction of the pH jump. The observed kinetic transients are always single exponential, with k_{obs} (the sum of the rate constants for discrete forward and reverse electron transfer between the two centers) directly proportional to the mole fraction D_2O in the reaction mix for the pH jump in each direction. This demonstrates that the effect arises from a single solvent-derived proton that, given the known pH dependence of the flavin reduction potentials, is undoubtedly the N_5-H proton of the neutral flavin semiquinone. Calculation of the microscopic rate constants for the forward and reverse steps in the equilibration in both H_2O to D_2O demonstrate that the solvent kinetic isotope effect for electron transfer from the flavin neutral semiquinone to oxidized Fe-S I is substantially larger than that for electron transfer in the opposite direction. The magnitude of the solvent isotope effect observed for the microscopic rate constant associated with $FADH^{\bullet} \rightarrow$ Fe-S I electron transfer is comparable to that seen in primary C−H bond cleavage reactions where bond breaking is rate limiting and demonstrates that the N_5−H bond of the neutral flavin semiquinone is being broken as the electron-transfer reaction traverses the transition state. That the transition state for electron transfer involves this motion of a solvent-exchangeable proton must be due to a significant destabilization of the anionic flavin semiquinone by the immediate protein environment of the FAD. Were this not the case discrete deprotonation to give the semiquinone anion would be expected prior to electron transfer. Indeed, only the neutral semiquinone of xanthine oxidase is observed under the experimental conditions used in these studies.[158] (The alternative situation in which electron transfer occurs prior to deprotonation is unlikely given the known instability of the protonated $FADH^+$ oxidized flavin.[243,244]) From an examination of the microscopic rate constants calculated for the reequilibration reaction at high and at low pH, where the driving force of the reaction is significantly different, it is evident that the preponderance of the kinetic effect observed upon changing the thermodynamic driving force for electron transfer is on the rate constant for electron transfer from flavin to Fe-S rather than the reverse. This too has been interpreted as a manifestation of the involvement of prototropic equilibria in these electron-transfer events, due to the effective coupling of nuclear motion to the electron-transfer event.[242] Given the strong evidence for coupling of prototropic events on the reduction potential of the molybdenum center and the several steps of the reductive half-reaction that have been investigated, it is quite likely that effects comparable to those described for electron transfer involving the FAD center of xanthine oxidase will be found for its molybdenum center as well.

D. Xanthine Dehydrogenase

Xanthine dehydrogenase as isolated from the liver of a variety of vertebrate species is quite similar to xanthine oxidase in its physical and spectroscopic properties. The distinction between oxidase and dehydrogenase forms is made on the basis substrate specificity in the oxidative half-reaction of the catalytic cycle: the oxidase is incapable of utilizing NAD^+ (although it is effectively reduced by NADH), while the dehydrogenase form is able to utilize both NAD^+ and O_2 as oxidant.[245−248] While xanthine dehydrogenase from chicken is stable as such, the mammalian dehydrogenases can be converted to an oxidase form by oxidation of protein thiols. In the case of the dehydrogenase from rat[249,250] or milk,[247,251] this process is fully reversible; the dehydrogenase from rat[91] can also be irreversibly converted to an oxidase form by limited proteolysis, which results in nicking at two positions. Three fragments are obtained on limited proteolysis of either the rat enzyme[91] (20, 40, and 85 kDa) which can be dissociated under denaturing conditions, but otherwise remain tightly associated with one another. Similarly, the chicken enzyme can be proteolytically cleaved into fragments of 20, 37, and 84 kDa, although in this case the enzyme is not converted to an oxidase.[252] A comparison of the N-terminal sequences of the isolated peptides with the deduced sequence for the intact protein from the DNA sequence places the peptides from the rat dehydrogenase in the order 20 kDa - 40 kDa - 85 kDa from N-terminus to C-terminus in the intact enzyme, and it is clear that these correspond to protease-resistant structural domains for the iron−sulfur-, FAD-, and molybdenum-binding regions of the proteins, respectively.[91] This is consistent with the results of studies of a family of *Drosophila* mutants from which it is clear that those activities associated with NAD^+ binding and the flavin site map to the intermediate domain of xanthine dehydrogenase (absent in the *D. gigas* aldehyde oxidoreductase).[253] The nick sites in the two xanthine dehydrogenases occur in comparable positions. It is

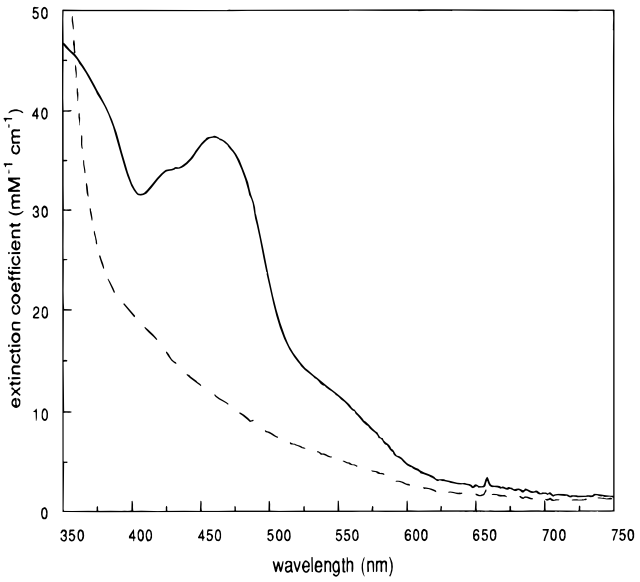

Figure 6. Absorption spectra of oxidized (solid line) and reduced (dashed line) xanthine dehydrogenase from chicken liver.

interesting that just as most of the dehydrogenases can be converted to oxidase forms, so xanthine oxidase from cow's milk can be isolated in a dehydrogenase form when care is taken to maintain complete reduction of protein thiols throughout the purification.[246,254] It is clear that differences in the two forms are restricted largely to the absence of an NAD^+ binding site in the oxidase (although obviously this may involve significant conformational differences between the two forms, at least in the flavin domain). In all likelihood, it is the dehydrogenase form that is the more physiologically significant.

The absorption features of the flavin and iron−sulfur centers dominate the UV/vis spectra of the dehydrogenase as they do in the oxidase. Figure 6 shows the absorption spectrum of oxidized and reduced chicken liver dehydrogenase, and it can be seen that there are small but distinct differences between the chicken dehydrogenase and milk oxidase, particularly in the 430−470 nm region (compare with Figure 3). These differences are apparently related to the source of enzyme rather than intrinsic differences between dehydrogenase and oxidase forms, however, since the absorption spectrum of the milk dehydrogenase is essentially indistinguishable from that of the corresponding oxidase form.[246,247]

As discussed in section II.B, the immediate coordination environment of the molybdenum in the dehydrogenase, as determined by X-ray absorption spectroscopy, is indistinguishable from that of the oxidase.[64] The xanthine dehydrogenase from turkey also exhibits a variety of EPR signals that are entirely homologous to those described above for the milk oxidase.[160] Thus "rapid" Mo(V) signals are observed with the dehydrogenase that are both qualitatively and quantitatively very similar to the corresponding signals from the milk oxidase (see Table 2). The iron−sulfur centers also exhibit EPR signals that are quite similar to those of the oxidase, including the fast spin−lattice relaxation manifested by the iron−sulfur signal designated Fe-S II. One significant difference is that the dehydrogenase forms that have thus far been examined do not exhibit nearly as much of the "very rapid" EPR signal in the course of the reaction of enzyme with xanthine[160] or even 2-hydroxy-6-methylpurine (K. Ratnam and R. Hille, unpublished) as does the oxidase. In addition, the various preparations of the dehydrogenase in the literature typically yield enzyme that possesses one or more forms of molybdenum in an air-stable Mo(V) valence state.[160] These signals are apparently artifacts that result from the use of organic solvents in the enzyme purification, particularly in the preparation of acetone powders from fresh liver. These signals are analogous to the "inhibited" signals exhibited by the oxidase and are absent from samples of the dehydrogenase that have been prepared using milder techniques.[254] Also, while the absorbance and CD changes associated with the molybdenum center of the chicken dehydrogenase are on the whole quite reminiscent of the corresponding changes observed with the milk oxidase, the pH dependence of the absorption change suggests that the dehydrogenase possesses a somewhat higher pK_a for the ionizable group responsible for the effect than does the oxidase.[166]

Although xanthine dehydrogenase is thought to operate via the same basic mechanism for the reductive half-reaction of its catalytic cycle as does xanthine oxidase, there are significant differences in the overall kinetic behavior of the two enzymes. The milk oxidase reacts with excess xanthine in a single apparent kinetic phase to give fully reduced enzyme, despite the fact that this necessarily involves the reaction of three successive equivalents of substrate.[202] The observed rate constant exhibits hyperbolic dependence on the concentration of xanthine, with a $K_d^{xanthine}$ of 13 μM and k_{red} of 17.5 s^{-1} at pH 8.5.[202] The dehydrogenase from either chicken[255] or milk[257] exhibits considerably greater kinetic complexity in its reaction with xanthine. The reaction of milk dehydrogenase with substrate exhibits three distinct kinetic phases: two faster phases with rate constants of 15 and 13 s^{-1}, respectively, and a slow phase with an observed rate constant in the range 0.5−1.5 s^{-1}. The spectral changes associated with the two faster phases indicate that they correspond to the formation of two- and four-electron reduced enzyme; both phases are independent of substrate concentration, indicating that the dissociation constant for xanthine is very low. The slow phase has been interpreted as the formation of a catalytically nonproductive complex of xanthine with enzyme possessing Mo(V) subsequent to the reaction of the first two equivalents of substrate.[256] The reaction of chicken liver dehydrogenase with excess substrate also exhibits three kinetic phases and, like the milk dehydrogenase, does not proceed further than four-electron reduced enzyme at catalytically significant rates.[255] The fastest of the observed kinetic phases with the chicken dehydrogenase has been interpreted as the formation of a Mo^{IV}−urate complex upon reaction of enzyme with the first equivalent of xanthine. This phase exhibits hyperbolic dependence on [xanthine], with a K_d and limiting rate constant of 280 μM and 180 s^{-1}, respectively (at pH 7.8 and 4 °C). The interme-

Scheme 14

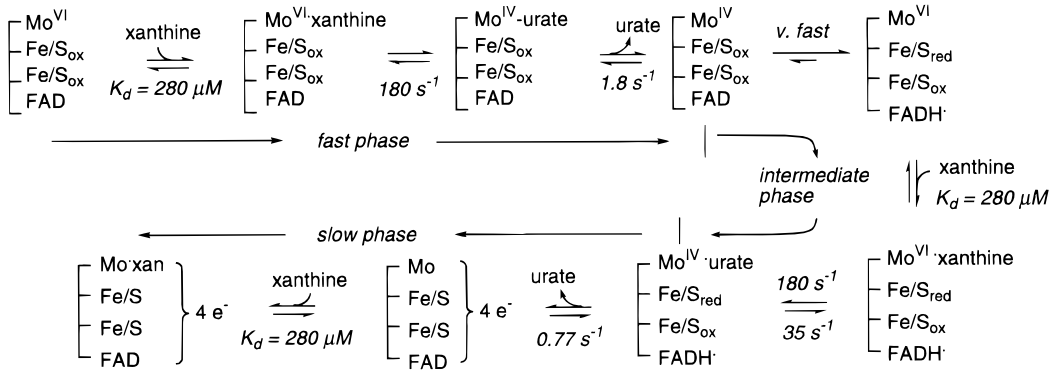

diate phase exhibits a rate constant of 1.8 s^{-1} that is independent of [xanthine] and is thought to arise from the dissociation of the first urate molecule followed by redistribution of reducing equivalents within the enzyme (and presumably also reaction of the second equivalent of xanthine with enzyme resulting in formation of a second Mo^{IV}−urate complex, a process that does not contribute significantly to the observed absorbance change). Finally, a slow phase is seen that is represented by an absorption decrease at all wavelengths. The observed rate constant for this last process is 0.77 s^{-1}, and its wavelength dependence is consistent with dissociation of the second equivalent of urate from the molybdenum center and further redistribution of reducing equivalents within enzyme that is now reduced by four equivalents. The reductive half-reaction for the chicken liver dehydrogenase[255] is summarized in Scheme 14.

The above kinetic differences between dehydrogenase and oxidase, particularly with regard to the extent to which enzyme becomes reduced on a catalytic time scale, undoubtedly have to do with the substantially lower reduction potential of the flavin center in the dehydrogenase relative to the oxidase (see below) and reflect a manifestation of the thermodynamic properties of the system on its kinetic behavior, as discussed above in the context of xanthine oxidase species possessing FAD derivatives of low midpoint potential. However, even in single-turnover experiments (where these considerations are of negligible consequence) the milk dehydrogenase and oxidase forms exhibit distinct kinetic behavior. The dehydrogenase form is reduced in a biphasic fashion, with rate constants of 15 and 13 s^{-1} (at pH 7.5), and on the basis of their associated spectral changes the two phases have been attributed to the formation and decay of a Mo^{V}−product intermediate, although this species was not characterized by EPR.[256] By way of comparison, the corresponding values for the reaction of the milk oxidase with substoichiometric xanthine are 20 and 2.5 s^{-1} (at pH 8.5, 5 °C).[197]

As indicated above, the fundamental difference between the dehydrogenase and oxidase is the presence of an NAD^+ binding site in the former. In addition to the distinction that only the dehydrogenase is able to use NAD^+ as oxidizing substrate, this is manifested spectrophotometrically by the ability of 3-aminopyridine adenine dinucleotide to perturb the absorption spectrum of the dehydrogenase but not the oxidase.[246,251] The NAD^+-binding site of the chicken dehydrogenase has been probed using 5′-[*p*-(fluorosulfonyl)benzoyl]adenosine (5′-FSBA), an affinity labeling analog of NAD^+ that reacts with tyrosine residues.[257,258] Reaction of the enzyme with this reagent results in covalent modification of a single tyrosine residue and loss of xanthine-NAD^+ activity, although the enzyme remains reducible by xanthine.[257] Interestingly, the xanthine-O_2 reactivity is unaffected by the covalent modification. Accompanying covalent modification is a spectral change quite similar to that elicited by binding of NAD^+ to the enzyme, strongly suggesting that the reactive tyrosine residue plays a specific role in binding NAD^+. The modified protein has been proteolytically digested and a comparison of the sequence for the modified peptide[258] with the deduced amino acid sequence for chicken xanthine dehydrogenase[252] indicates that it is Tyr 419 of the protein that is covalently modified. On the basis of sequence comparison with other members of the hydroxylase family[252,86] and in the context of the structure of the *D. gigas* aldehyde oxidoreductase[6] this residue lies well within the putative FAD-binding domain of the dehydrogenase (Figure 7), and notably is not conserved in the aldehyde oxidases (which lack dehydrogenase activity).

Comparisons of the dehydrogenases from milk,[251] chicken,[259] and rat[260] have been made with enzymes possessing chemically modified flavin derivatives such as 8-mercapto- and 6-hydroxy-FAD that possess ionizable groups and can exist in different spectroscopically distinct tautomeric forms. With these flavin derivatives as active site probes, it has been shown that in the oxidase form of either the rat or milk enzyme the 8-mercapto derivative exists principally as the anionic benzoquinonoid tautomer ($\lambda_{max} \approx 570$ nm) and the 6-hydroxy derivative in the anionic form ($\lambda_{max} \approx 430$ nm). With the dehydrogenase forms of these enzymes, both the 8-mercapto and 6-hydroxy derivatives exist predominantly as the neutral species ($\lambda_{max} \approx 456$ nm with a small shoulder at 570 nm for the 8-mercapto derivative, and $\lambda_{max} \approx$ 420 nm in the case of the 6-hydroxy derivative). These results suggest the presence of a strong negative charge in the immediate vicinity of the flavin N_1/C_2=O region of the dehydrogenase (and/or a positive

charge in the vicinity of the flavin of the oxidase), resulting in decrease in pK_a of approximately 4 units on going from the dehydrogenase to the oxidase.

In addition to these spectroscopic differences between FAD sites of the oxidase and dehydrogenase, there are substantial differences in the flavin reduction potentials of the two forms. The most significant difference is the greater thermodynamic stabilization of the flavin semiquinone in the dehydrogenase relative to the oxidase,[261,262] due principally to a substantial decrease in the reduction potential for the $FADH^{\bullet}/FADH_2$ couple in the dehydrogenase relative to the oxidase (by 180 mV in the case of the milk enzyme[262]). The net result is that little flavin hydroquinone accumulates when the dehydrogenase possesses fewer than five reducing equivalents. In reductive titrations of the milk dehydrogenase at pH 7.5, approximately 90% of the enzyme flavin accumulates at maximum as the blue neutral form of the flavin semiquinone, substantial enough that above 640 nm there is an absorption increase intermediate in the titration as semiquinone accumulates.[262] With the avian dehydrogenases, the accumulation of semiquinone appears to be not quite so pronounced at neutral pH.[261,263] In the case of the chicken enzyme, however, the extent of semiquinone accumulation in the course of reductive titrations is extremely pH dependent, decreasing as the pH is increased from 6 to 8.5, but increasing significantly (to near-quantitative) at pH 10.[263] This anomalous accumulation of neutral flavin semiquinone at high pH is lost upon reaction of the dehydrogenase with iodoacetate, and the ionization of a protein thiol has been suggested to be responsible for the effect.[263] The dehydrogenase form of the milk enzyme also manifests this paradoxical stabilization of the neutral form of the flavin semiquinone at high pH (K. Ratnam and R. Hille, unpublished).

The lower reduction potential for the semiquinone/hydroquinone couple in the dehydrogenase form also results in a decrease in the flavin midpoint potential (to −360 mV at pH 7.5) to a value comparable to that of the NAD^+/NADH couple ($\Delta E^{\circ\prime} = -320$ mV). The higher flavin midpoint potential in the oxidase undoubtedly contributes to its catalytic inertness toward NAD^+. With oxygen as substrate, the inability of the dehydrogenase to effectively form substantial amounts of flavin hydroquinone implies that the principal reactive flavin species must be the semiquinone. This provides an explanation, at least qualitatively, for the slower rates of reaction with O_2 and the second-order character of the reaction, as well as the increased yield of superoxide relative to that observed in the reaction with the oxidase, since it has been shown that oxygen reacts preferentially with the fully reduced hydroquinone of the oxidase.[204,205] Of course, only the flavin hydroquinone in the dehydrogenase can react with NAD^+, but in this case secondary perturbations of the flavin potentials on binding NAD^+ would serve to facilitate the overall reaction (a phenomenon that is commonly encountered with the nicotinamide cofactor,[258] but is without precedent for dioxygen). Differences in the distribution of reducing equivalents within the partially reduced dehydrogenase and oxidase forms resulting from the different flavin potentials also account for the observed differences in the kinetic behavior of the two forms in the reductive half-reaction. The argument is analogous to that accounting for the complex kinetic behavior exhibited by xanthine oxidase possessing low-potential flavins: once the dehydrogenase is reduced to the level of four equivalents, the distribution of reducing equivalents favors reduction of both iron−sulfur centers along with formation of $FADH^{\bullet}$ and Mo^{V}. The molybdenum center is thus already partially reduced and thus unable to oxidize a third equivalent of xanthine.

The kinetics of electron transfer within chicken xanthine dehydrogenase has been examined both by flash photolysis[237] and pulse radiolysis.[264] As in the case of the oxidase, electron transfer is found to be considerably faster than k_{cat} and is not in itself rate limiting to catalysis. By using photolytically generated deazaflavin radical at pH 7.8, a second-order rate constant for initial reduction of the chicken dehydrogenase of 6×10^7 M^{-1} s^{-1} is found, which is comparable to the value of 3×10^7 M^{-1} s^{-1} seen with the oxidase.[237] Initial reduction of the dehydrogenase, however, appears to take place at the molybdenum center, whereas that for the oxidase occurs at the flavin. With the dehydrogenase, the kinetic transient subsequent to the initial protein reduction event is triphasic, with rate constants of 1600, 110, and 8 s^{-1}. The spectral changes associated with the two faster of these processes are consistent with electron transfer from Mo^{V} to FAD (to give the neutral flavin semiquinone) and electron transfer from the flavin semiquinone to an iron−sulfur center, respectively. It is to be noted that direct electron transfer between the molybdenum and flavin is surprising in light of the likely proximity of the molybdenum center and one of the iron−sulfur clusters (again assuming structural homology between xanthine dehydrogenase and the *D. gigas* aldehyde oxidoreductase). The slowest kinetic phase has been attributed to a small fraction of structurally altered protein. These results compare with the photolytic results obtained with the milk oxidase discussed above, in which the kinetics subsequent to initial reduction of enzyme were biphasic with rate constants of 100 and 10 s^{-1} (with the slower rate constant again thought to represent a slow kinetic artifact).

The pulse radiolysis studies of xanthine dehydrogenase have utilized radiolytically generated salicylate anion and the radicals of NAD and *N*-methylnicotinamide as proximal reductants of the milk enzyme.[264] With the last species, an apparent second-order rate constant for initial reduction of the enzyme of 6.5×10^7 M^{-1} s^{-1} is observed; the spectral change indicates that this involves reduction of one of the iron−sulfur centers of the enzyme. This faster kinetic phase is followed by a slower process (k_{obs} on the order of 400 s^{-1}) whose associated spectral change clearly indicates accumulation of the neutral flavin semiquinone at the expense of reduced iron−sulfur, as expected on the basis of the reduction potentials of the dehydrogenase. The rate constant for this slower phase is somewhat faster than the rate constant of 230 s^{-1} observed in pH jump experiments

with the oxidase form of the milk enzyme under the same conditions (pH 7.4),[238] but may be regarded as generally consistent with the results obtained with the oxidase. The rate constant for initial reduction of the dehydrogenase by the methylnicotinamide radical, on the other hand, is significantly slower than the corresponding rate (at pH 6.0) of the 9×10^8 M^{-1} s^{-1} seen with the oxidase,[240] and it is possible that separate processes for initial reduction at the molybdenum center and subsequent rapid electron transfer to an iron−sulfur center are left unresolved in the work with the dehydrogenase. At the highest enzyme concentration used in this study, the largest pseudo-first-order rate constant for reduction of the enzyme (at an enzyme concentration of 80 μM), is just over 5000 s^{-1},[264] insufficiently fast to completely resolve a discrete electron-transfer event from molybdenum to iron−sulfur were it taking place at the 8500 s^{-1} seen with the oxidase.[240] A significant difference in the two studies is that the initial radiolytic studies with the oxidase utilized the inactive, desulfo form of the enzyme (the enzyme was found to slowly hydroxylate the methylnicotinamide under the experimental conditions used, accumulating reducing equivalents in the course of anaerobic sample preparation and thereby slowing the rate of reaction with the radiolytically generated radical). Although it is possible that the desulfo enzyme could be intrinsically more reactive toward the radiolytically generated radical than the functional form of the enzyme used in the radiolytic study with the dehydrogenase, it would be surprising if this were the case. Instead, it appears more likely that the structural differences between the dehydrogenase and oxidase are sufficient to significantly attenuate the rate of reaction of the molybdenum center with the radical, thereby complicating resolution of molybdenum-mediated reduction of the iron−sulfur centers of xanthine dehydrogenase by the radiolytically generated radical. With salicylate radical anion as proximal reductant of the enzyme, the situation is even worse, as the apparent second-order rate constant for the initial reduction of the dehydrogenase is even slower, only 2.9×10^7 M^{-1} s^{-1}, some 3-fold slower than reduction by the methylnicotinamide radical.[264]

E. Mammalian Aldehyde Oxidases

Like xanthine dehydrogenase, aldehyde oxidase from eukaryotic sources is extremely similar to xanthine oxidase, as evidenced by the overall sequence similarity. Although both xanthine oxidase and aldehyde oxidase have broad and extensively overlapping substrate specificity, it is clear that their differences are not due to variations among species: in particular, in humans[90,107] and cows[111,113] the two proteins have been shown to be encoded by genes which, while exhibiting very significant sequence homology, are nevertheless distinct. Furthermore, the human aldehyde oxidase[107] bears greater sequence homology to bovine[111] aldehyde oxidase than it does to human xanthine dehydrogenase.[90] A comparison of the inferred amino acid sequences for three aldehyde oxidases (including the aldehyde oxidoreductase from *D. gigas*) and eight xanthine dehydrogenases is given in Figure 7.

A unique aspect of aldehyde oxidase relative to the xanthine-utilizing enzymes is its inability to convert to a dehydrogenase form able to utilize NAD^+ as oxidizing substrate.[110] A comparison of the amino acid sequences of xanthine dehydrogenase with the aldehyde oxidases indicates that among the areas exhibiting relatively low sequence homology is the region in the vicinity of the tyrosine residue implicated in binding NAD^+ Tyr 419 in the chicken sequence,[257] which is not conserved in either the human or bovine aldehyde oxidase. The consensus sequence among all animal dehydrogenases in this region is FFxGYR(R/K) (see Figure 7), while the corresponding sequence in the aldehyde oxidases is FLxKCPxAD.[111,113] It is evident that the NAD^+ binding site is not conserved in the aldehyde oxidases, and it is unlikely that it will be possible to find conditions under which the enzyme can be converted to a form able to utilize NAD^+ as an oxidizing substrate. Also, it is evident from an examination of Figure 7 that there numerous other regions throughout the length of the sequences in which the two aldehyde oxidases differ from the consensus sequence for the xanthine-utilizing enzymes, including the region in the vicinity of residues 351−369 in the human aldehyde oxidase sequence that has been previously identified.[110] It is clear that the aldehyde oxidases are quite distinct enzymes from the xanthine dehydrogenases.

Aldehyde oxidase has been most extensively studied in purified form from rabbit liver.[265] Its activity is distinguished from that of xanthine oxidase on the basis of its specificity for reducing substrate: aldehyde oxidase is able to effectively hydroxylate a wide range of aldehydes and also *N*-methylnicotinamide (the product of the reaction being the 6-pyridone),[266] but is relatively unreactive toward xanthine.[267] Xanthine oxidase, on the other hand, hydroxylates *N*-methylnicotinamide only very slowly. Aldehyde oxidase is readily distinguished from xanthine dehydrogenase by its inability to utilize NAD^+ as oxidizing substrate. In addition, it is interesting that aldehyde oxidase, in contrast to other members of the hydroxylase class, is able to catalyze the reduction of sulfoxides, notably several sulfa drugs,[268] in a reaction reminiscent of that catalyzed by DMSO reductase (see below). Like xanthine oxidase, aldehyde oxidase is rendered nonfunctional upon reaction with cyanide, which reacts with the Mo=S group of the molybdenum center to yield 1 equiv of thiocyanate.[269] Overall, aldehyde oxidase exhibits well-behaved kinetic properties. Like xanthine oxidase, the reaction of aldehyde oxidase with reducing substrate proceeds in a monophasic fashion and results in full reduction of the functional enzyme, with a limiting rate constant and $K_d^{N-\text{methylnicotinamide}}$ of 13 s^{-1} and 400 μM respectively, at pH 7.8, 25 °C.[270] The oxidative half-reaction with oxygen also proceeds as a single exponential process, albeit with linear dependence on dioxygen concentration ($k_{obs} = 5.3 \times 10^5$ M^{-1} s^{-1}). Neither oxidative nor reductive half-reaction displays any of the kinetic complexity exhibited by xanthine dehydrogenase.[269] The activity of aldehyde oxidase

drops off more precipitously at low pH than that of xanthine oxidase.[110,270] Assuming a common reaction mechanism for the two enzymes, this implies that the pK_a of the enzyme group which must be deprotonated for catalysis to proceed has a higher pK_a in aldehyde oxidase than in xanthine oxidase. It is of note that aldehyde oxidase has recently been identified as identical to a previously described retinal oxidase,[271] and it is possible that this is the physiological substrate for the enzyme.

The UV/vis absorption spectrum and the spectral change observed on reduction of either the native or deflavo form of aldehyde oxidase from rabbit liver is essentially indistinguishable from that shown in Figure 3 for milk xanthine oxidase.[272,273] As with xanthine dehydrogenase from liver sources, earlier preparations of aldehyde oxidase yielded small amounts (~5% of the enzyme molybdenum) of a "resting" Mo(V) EPR signal that apparently arises from enzyme that has been inactivated by treatment with organic solvent. It is possible to obtain enzyme in a form that is devoid of this signal.[110,273,276] The "rapid type 2" Mo(V) EPR signal is readily seen with aldehyde oxidase and is quite similar to that seen with xanthine oxidase ($g_{1,2,3}$ = 1.9895, 1.9701, 1.9624; a_{av} = 14 and 8.3 G for the two strongly coupled protons).[110,276] The second proton is coupled less strongly in the "type 2" signal in aldehyde oxidase than is seen with xanthine oxidase, however, and the signal-giving species seen in aldehyde oxidase is considered to be intermediate in some conformational sense to the species giving the "type 1" and "type 2" signals in xanthine oxidase. The implication is that the second proton of both signal-giving species is bound at the same site in the two signal-giving species, with the difference between them involving differences in coordination geometry and/or orientation of substrate with respect to the molybdenum center.[110] It is also interesting that whereas xanthine oxidase yields a "type 1" signal with purine and hydroxylates at the 6 position to give hypoxanthine, aldehyde oxidase gives a "type 2" signal with this substrate and preferentially hydroxylates at the 8 position.[267] This suggests that substrate is indeed oriented differently in the species, giving rise to the two "rapid" signals, and that xanthine and aldehyde oxidases preferentially bind substrate in different orientations. Mo(V) signals corresponding closely to the "arsenite-inhibited" and "slow" signals seen with xanthine oxidase are also observed with aldehyde oxidase.[110] Neither the "very rapid" or "rapid type 1" Mo(V) signals have been unambiguously documented with aldehyde oxidase using *N*-methylnicotinamide as substrate, however, although a "rapid type 1" signal is observed when 2-methylquinonine is used.[273,277]

The reduction potentials of aldehyde oxidase have been reported[274] and are given in Table 3. While the reduction potentials for the Mo(VI/V) and Mo(V/IV) couples of the functional enzyme are quite comparable to those seen with xanthine oxidase and xanthine dehydrogenase, the iron−sulfur and FAD potentials are rather different. The potentials for Fe-S I and II of aldehyde oxidase at pH 7.8 are −207 and −310 mV, respectively, comparable to the potentials seen with xanthine oxidase[233] at the same pH but with the assignments for the higher and lower potential centers reversed. As in xanthine oxidase, the molybdenum center and Fe-S I exhibit strong dipolar coupling to one another. In the case of the flavin site of aldehyde oxidase, while the reduction potential for the $FADH^{\bullet}/FADH_2$ couple is comparable to that of xanthine oxidase, the $FAD/FADH^{\bullet}$ couple is some 50 mV higher in aldehyde oxidase. As a result, the flavin semiquinone accumulates to an appreciably greater extent in the course of reductive titrations with aldehyde oxidase than with xanthine oxidase[274] (~18% of the total enzyme flavin, compared with approximately 5%). Although the above demonstrate that the molybdenum centers of xanthine oxidase and aldehyde oxidase are fundamentally very similar, there are some interesting differences. Aldehyde oxidase reacts several orders of magnitude more rapidly with cyanide to give the desulfo form of the enzyme than does xanthine oxidase, and inhibition of aldehyde oxidase by either *p*-(chloromercuri)benzoate or arsenite is reversible and competitive with respect to reducing substrate (both are essentially irreversible inhibitors of xanthine oxidase, exhibiting uncompetitive inhibition with respect to xanthine).[265,270,275,278] This suggests that the active site of aldehyde oxidase is substantially more accessible to solvent than is true of xanthine oxidase, particularly in the vicinity of the Mo=S group.

It is interesting to note that an aldehyde oxidase very similar to that found in mammalian systems has recently been purified to homogeneity from maize seedlings and characterized.[279] The protein is found to possess molybdenum and flavin in a 300 kDa homodimer; it is distinct from the mammalian form in not being able to hydroxylate *N*-methylnicotinamide and is not inhibited by menadione. Unlike the mammalian systems, indole-3-acetaldehyde is an effective substrate for the plant enzyme, and this in all likelihood represents the physiological reaction for the enzyme. This is consistent with the localization of the enzyme to the apical region of the seedling coleoptiles where the hormone indole-3-acetate is known to be synthesized.

IV. Sulfite Oxidase and the Assimilatory Nitrate Reductases

The second major family of mononuclear molybdenum enzymes consists of sulfite oxidase and the assimilatory nitrate reductases, enzymes that possess a MoO_2 unit in the active site and in all likelihood a single pterin cofactor coordinated via its dithiolene side chain. While these enzymes have been shown to be strongly inhibited by cyanide, it is only the reduced form of the enzyme that is sensitive and the inhibition is fully reversible.[278] Members of this family catalyze net oxygen atom transfer to or from a heteroatom lone electron pair rather than hydroxylation of a carbon center.

A. Sulfite Oxidase

Sulfite oxidase catalyzes the oxidation of sulfite to sulfate, with cytochrome *c* as physiological oxidizing

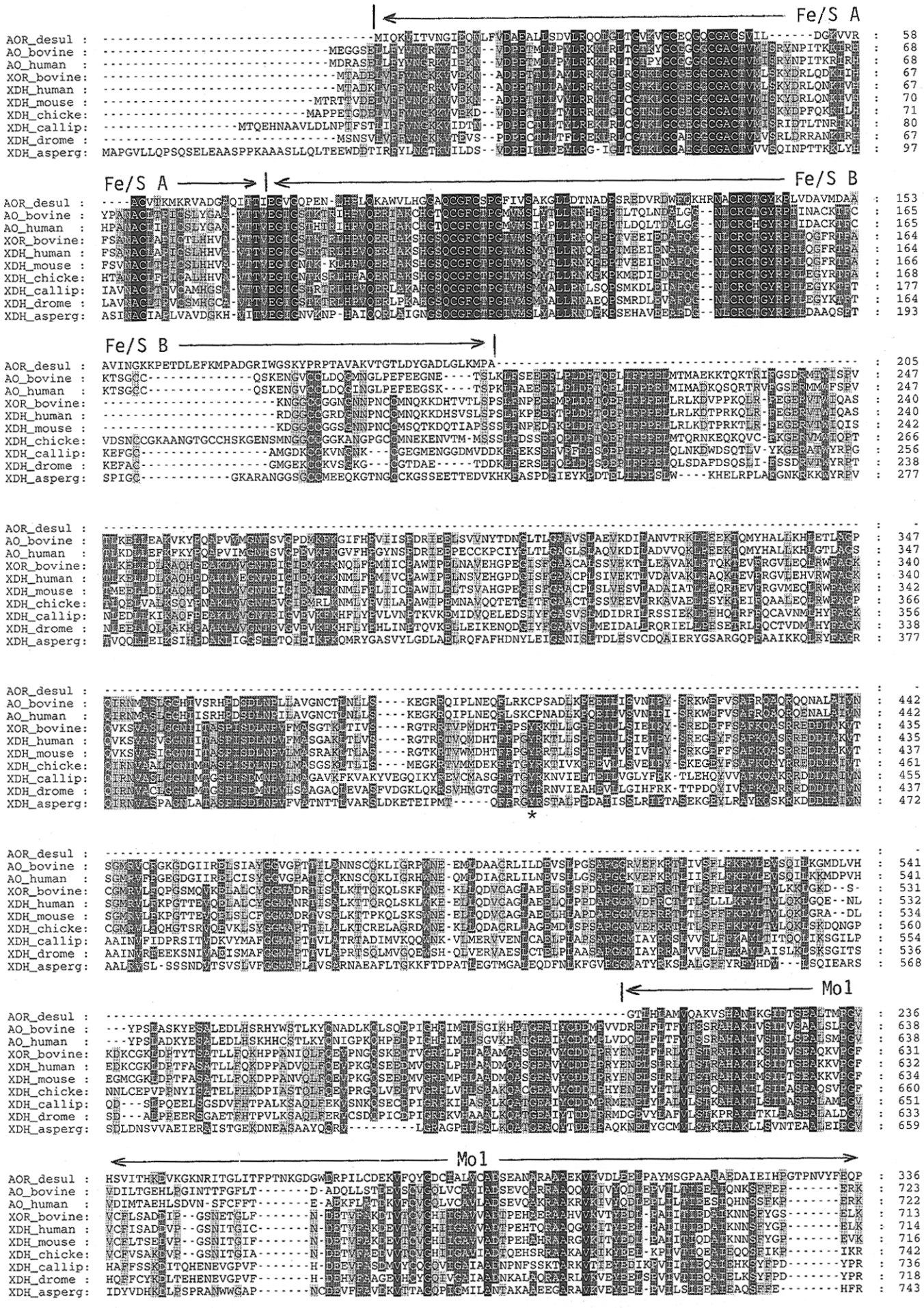

Figure 7. Sequence comparisons for and the aldehyde oxidoreductase from *Desulfovibrio gigas* (Thoenes *et al.*[156]), bovine (Li Calzi *et al.*[111]) and human (Wright *et al.*[107]) aldehyde oxidases and xanthine dehydrogenases from cow (Berglund *et al.*[113]), human (Ichida *et al.*[90])

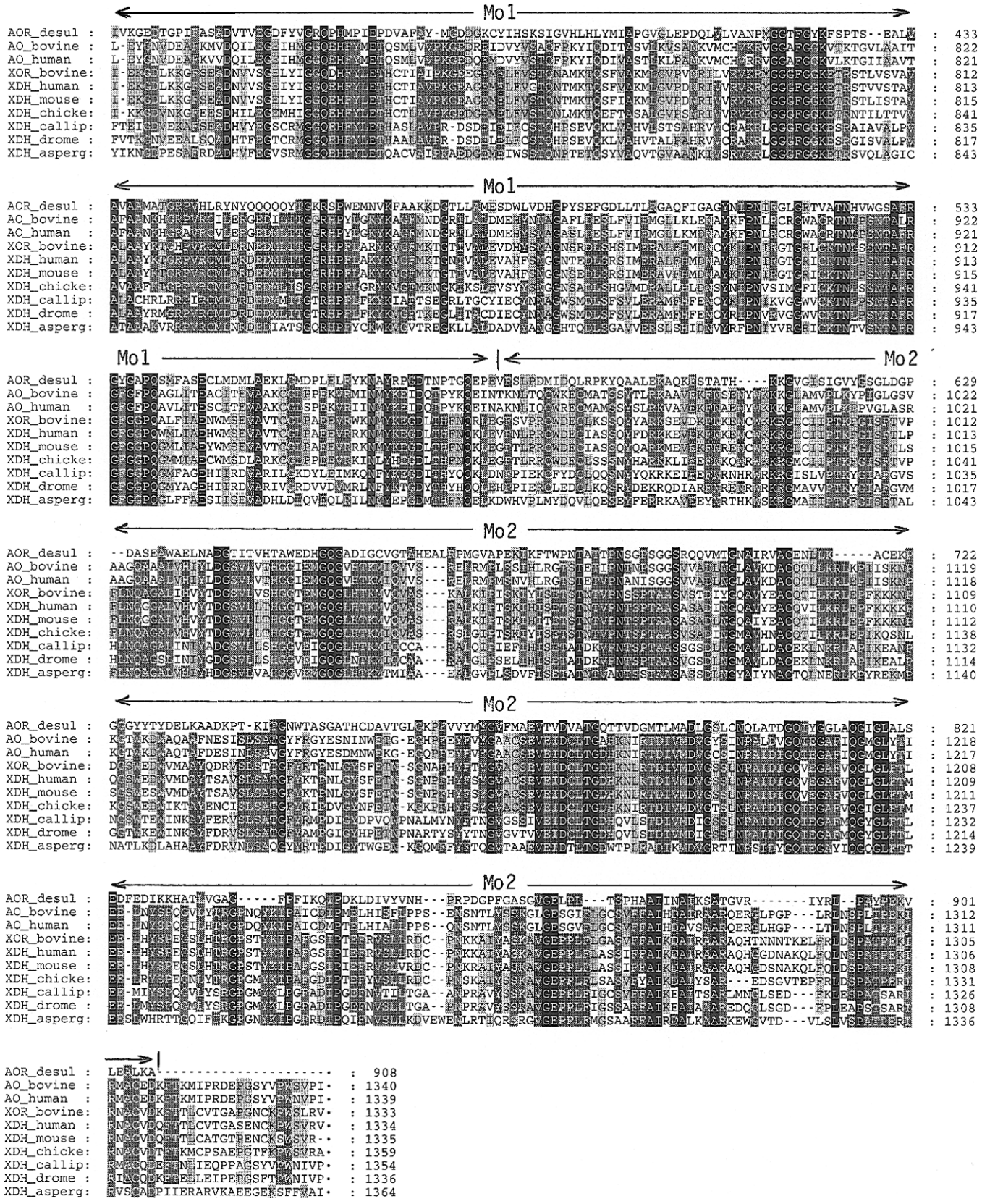

(Figure 7, continued) rat (Amaya *et al.*[91]), mouse (Terao *et al.*, *Biochem. J.* **1992**, *283*, 863), chicken (Sato *et al.*[251]),*Calliphora vicina* (Houde *et al. Gene* **1989**, *85*, 391), *Drosophila melanogaster* (Lee *et al., Genetics* **1987**, *116*, 55; Keith *et al., Genetics*, **1987**, *116*, 67), and *Aspergillus nidulans* (Glatigny and Scazzoccio[108]). The alignments were made with the program MACAW using regions of homology previously identified by Li Calzi *et al.*,[111] Sato *et al.*,[251] and Glatigny and Schazzocchio.[108] Sequences used were the current versions deposited in GenBank as of Feb 29, 1996. Regions of sequence identity are indicated by degrees of shading, depending on the extent of conservation at a given position among all members of the family. Regions where the bovine and human aldehyde oxidases exhibit distinct sequences from the corresponding vertebrate xanthine dehydrogenases are evident throughout the iron−sulfur, flavin-, and molybdenum-binding portions of the proteins. The tyrosine residue modified by reaction with 5′-FSBA (and implicated in the NAD^+ binding site of the dehydrogenases, as discussed in the text) is indicated with an asterisk. The regions corresponding to the discrete iron−sulfur and molybdenum domains of the aldehyde oxidoreductase from *D. gigas* are indicated, with the intervening region corresponding to the flavin

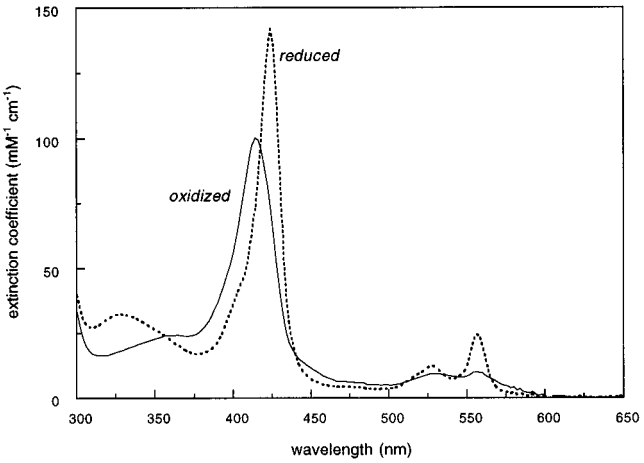

Figure 8. Absorption spectra of oxidized (solid line) and reduced (dashed line) sulfite oxidase from chicken liver.

substrate, according to the overall reaction stoichiometry shown in Scheme 15.[4] The molybdenum

Scheme 15

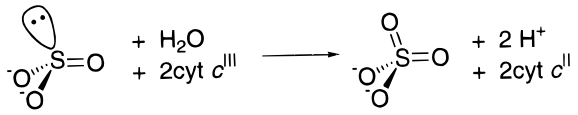

center of sulfite oxidase is reduced from the VI to the IV valence state in the reductive half-reaction of the catalytic cycle (*i.e.*, the reaction of enzyme with sulfite), and the reducing equivalents are then transferred individually to the heme center, where they are passed to cytochrome *c* in the oxidative half-reaction.

The UV/vis absorption spectrum of oxidized and reduced sulfite oxidase from chicken liver is shown in Figure 8, where it is seen that both spectra are dominated by the features of the heme group. Although the spectral features of the proteolytically cleaved molybdenum domain have been characterized,[129] the absorption spectrum and the spectral change observed upon reduction are weak and unfortunately have not proven to be useful probes of the active site of the intact enzyme.

As indicated in section II.B, structural studies of sulfite oxidase have been limited to X-ray absorption spectroscopy in an effort to elucidate the coordination environment of the molybdenum in the oxidized and reduced enzyme.[64,75−77] Two Mo=O groups, with a short Mo−O distance of 1.71 Å, are found in the oxidized enzyme, along with two or three thiolates at a distance of 2.42 Å; the two Mo=O groups are presumably *cis* to one another.[64] The coordination environment has been shown to be quite sensitive to the molybdenum oxidation state and solution pH, as indicated in Figure 9.[64,77] Reduction of the enzyme at both high and low pH causes one of the two oxo groups to become protonated, consistent with the expected linkage of prototropic equilibria to the oxidation state of the molybdenum.[66,78] Work with enzyme that has been is partially reduced to a level maximizing the accumulation of Mo^{V} indicates that protonation of the Mo=O is associated with the Mo(VI/V) rather than the Mo(V/IV) couple.[77] A comparison of the XAS data at high and low pH indicates

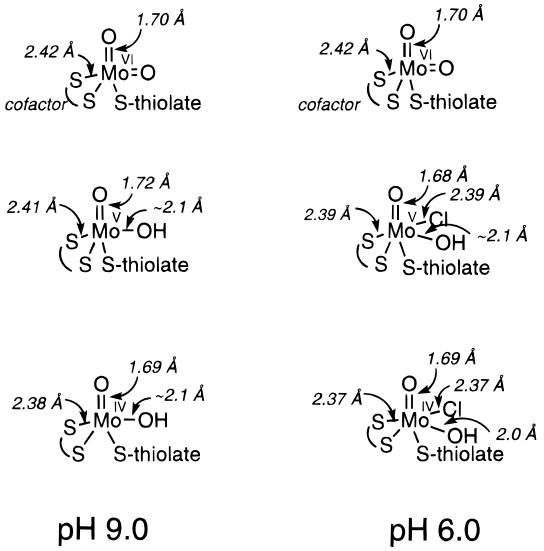

Figure 9. A summary of XAS results obtained with oxidized and reduced sulfite oxidase at both high and low pH. Bond distances are from George *et al.*[77]

that the Mo^{V} and Mo^{IV} oxidation states (but not Mo^{VI}) possess an additional sulfur or chloride ligand in the molybdenum coordination sphere at low pH. In all, the data are most consistent with the molybdenum center of oxidized sulfite oxidase consisting of a single pterin cofactor coordinated to a MoO_2 unit. As indicated in section II.B, additional likely ligands to the molybdenum are the cysteine residue that is conserved among sulfite oxidase and the assimilatory nitrate reductases, and possibly an oxygen derived from solvent (either water or hydroxide). Given the number of thiolate ligands found by XAS (2 or 3), it is unlikely that the active site of sulfite oxidase possesses 2 equiv of the pterin cofactor coordinated to the molybdenum, as has been found in the case of DMSO reductase (see below).

Electron paramagnetic resonance studies of sulfite oxidase have also proven useful in probing the chemical nature of the molybdenum center. As with the molybdenum center of xanthine oxidase, a variety of Mo(V) signals are seen with sulfite oxidase, reflecting the sensitivity of the molybdenum center to its environment.[280,281] The three principal EPR signals that are observed have been designated “high-pH”, “low-pH”, and “phosphate-complexed” on the basis of the experimental conditions under which they are generated (Figure 10).[280] Consistent with the above XAS results suggesting protonation of one of the Mo=O groups of oxidized enzyme becomes protonated upon partial reduction, the “low pH” spectrum possesses a strongly coupled, solvent-exchangeable proton (with $a_{1,2,3} = 8.5, 8.0, 13$ G) that is absent in the former. Although proton coupling is not readily apparent in the “high-pH” signal, the observation of “forbidden” $\Delta M_I = \pm 1$ proton−spin flip transitions in the “high-pH” signal suggests the presence of an otherwise undetected proton in the signal-giving species[282]). When the “high-pH and “low-pH” EPR signals of sulfite oxidase are generated in ^{17}O-labeled water, both develop strong coupling to oxygen ($a_{av} =$ 11 and 8 G, respectively).[283] The *g* values for the two signals are also distinct,[280] the “high pH” signal has $g_{1,2,3} = 1.987, 1.964, 1.953$ and the “low-pH” signal

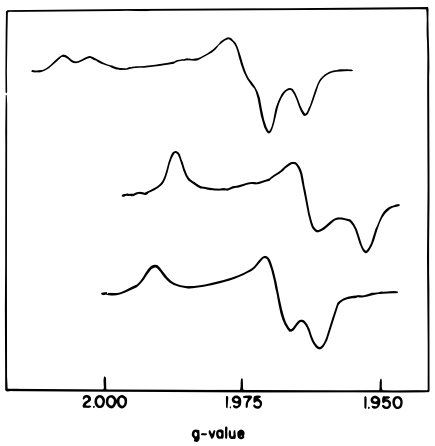

Figure 10. EPR signals attributable to the Mo(V) center of sulfite oxidase: (from top to bottom) "low pH", "high pH", and "phosphate-complexed" enzyme. After Lamy *et al.*,[281] with permission.

has $g_{1,2,3} = 2.004, 1.972, 1.966$, indicating a significant change in the molybdenum coordination sphere as the pH is increased. Although the two signals appear to represent a conjugate acid/base pair, with an associated pK_a of 7 in the absence of chloride, this pK_a is increased to 9 in the presence of 100 mM chloride. It has been suggested that the principal difference between the two species is the presence of an anion binding site at low pH that is absent (or of significantly lower affinity) at high pH.[281,284] Supporting this conclusion is the observation that substitution of fluoride for chloride results additional splitting of the "low-pH" signal due to the $I = {}^1/_2$ nucleus of ^{19}F ($a_{1,2,3} = 5.2, 3.1, 7.5$ G).[281] On the basis of the effect of chloride on the pK_a associated with the interconversion of the "low-" and "high-pH" forms of the Mo^V EPR signal, it has been concluded that the additional scatterer observed in the XAS of sulfite oxidase at low pH is more likely to be chloride.[77] Two alternate structural changes have been considered for the low pH/high pH interconversion of sulfite oxidase: (1) displacement of hydroxide by chloride directly in the molybdenum coordination sphere, or (2) protonation of an unidentified ligand followed by its displacement by chloride. It has not proven possible on the basis of the presently available XAS data to distinguish between these two alternatives.

The "phosphate-complexed" signal of sulfite oxidase has $g_{1,2,3} = 1.992, 1.969, 1.961$ and, like the "high-pH" signal, no detectable proton splitting; the phosphorus atom is only very weakly coupled to the unpaired electron spin, with a ^{31}P hyperfine splitting of less than 1 G.[285] At low pH, sulfite is also found to give a "complexed" EPR signal that may represent a Mo(V) analog of the Michaelis complex.[284] Interestingly, the phosphate-complexed EPR signal exhibits strong, anisotropic coupling ($a_{1,2,3} = 1.0, 13.0, 12.5$ G) only when the sample is prepared using ^{17}O-labeled phosphate.[286] The implication is that phosphate coordinates directly to the molybdenum via at least one of its oxygen atoms and, perhaps, is coordinated to molybdenum in a bidentate fashion. Enemark and co-workers have recently examined the phosphate complexed EPR signal by multifrequency ESEEM and find strong evidence in support of direct coordination of phosphate to molybdenum in the Mo(V) complex (J. Enemark, personal communication). Simulation of the data obtained over the microwave frequency range 8.9−15.3 GHz indicates that the phosphate adopts a distribution of orientations with respect to the metal (possibly both mono- and bidentate), but with a mean Mo−P distance of 3.2−3.3 Å that is well within the range expected for phosphate directly coordinated to the molybdenum.

Understanding of the chemical mechanism of the mononuclear molybdenum enzymes, particularly those of enzymes of the sulfite oxidase family, has been greatly facilitated by studies of the chemistry of inorganic complexes that are useful mechanistic models for the enzymes.[287−294] These complexes are of the form L_nMoO_2, where L is a bulky ligand that effectively prevents the thermodynamically very favorable dimerization of the mononuclear complexes to give μ-oxo bridged Mo_2 clusters. The first of the three most germane systems is $MoO_2(LNS_2)$ (L = 2,6-bis(2,2-diphenyl-2-mercaptoethyl)pyridine),[287−289] having the structure shown in Scheme 16. The oxidized

Scheme 16

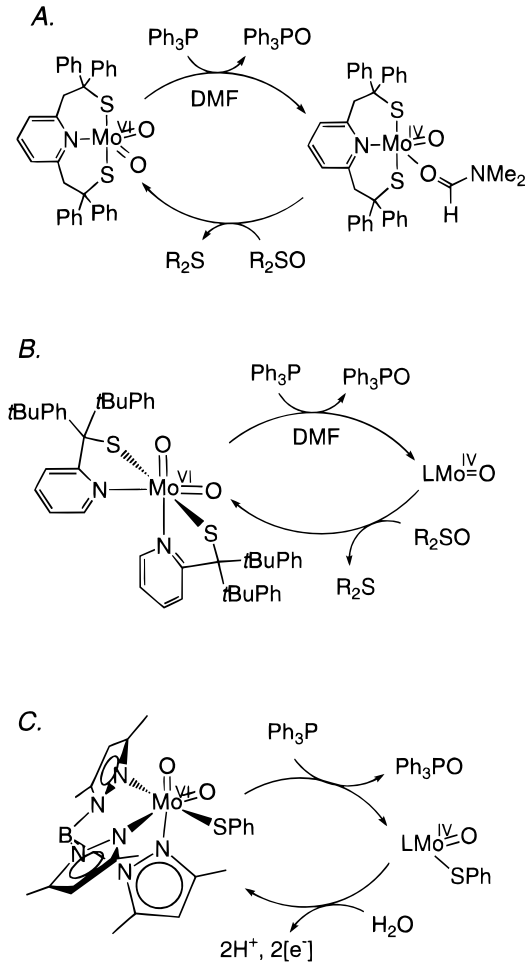

Mo(VI) *cis* dioxo compound has a distorted trigonal-bipyramidal coordination geometry, with Mo−O distances of 1.69 Å and an O−Mo−O bond angle of 110°.[287] In dimethylformamide, the compound oxidizes Ph_3P stoichiometrically to give the reduced $MoO(LNS_2)$(DMF) and Ph_3PO, and the reduced monooxo complex thus obtained can be returned to the oxidized parent compound by reaction with dimethyl sulfoxide (giving dimethyl sulfide).[288,289] Despite the

known stability of the Mo=O bond ($\Delta H \approx -45$ kcal/mol[178]), the reactivity of the $Mo^{VI}O_2$ compound demonstrates that the bond is relatively labile in solution, permitting effective oxygen atom transfer under the appropriate conditions. A variety of oxo donors and acceptors have been examined, and the suitability of a given pair as substrates for catalytic turnover by the complex has been justified thermodynamically (sulfoxides, nitrate, and *N*-oxides are good oxo group donors, for example, and phosphines and sulfite are good oxo group acceptors).[178,295] Catalytic turnover in this model system is rate limited by oxygen atom transfer from the $Mo^{VI}O_2$ complex to the oxo acceptor, and on the basis of the large negative entropy of activation for this reaction (−28 eu) an associative mechanism for this step has been proposed.[179] The chemistry involves nucleophilic attack of the phosphine lone pair on a π^* orbital of one of the Mo=O bonds with concomitant reduction of the molybdenum, followed by displacement of product, as shown in Scheme 17. This mechanism is predicated on the

Scheme 17

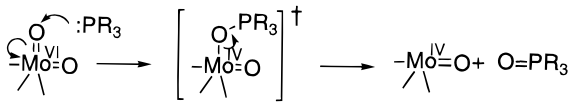

assumption that coordination of the oxygen to molybdenum renders it electrophilic, and indeed there is abundant evidence in the inorganic literature that metal−oxo groups are susceptible to nucleophilic attack, but not capable of it.[3,178] In biological systems, the closest precedent is the chemical reactivity of the presumed heme oxyferryl intermediate in the reaction of cytochrome P450.[296]

Another compound found to effectively catalyze oxygen atom transfer is MoO_2(*t*BuLNS)$_2$ (*t*BuLNS = 4-*tert*-butylphenyl 2-pyridylmethanethiolate) which presumably due to its greater steric crowding does not form a complex with DMF when reduced to the $Mo^{IV}O$ species (Scheme 16B).[290] A comprehensive kinetic analysis of the reaction of the MoO_2(*t*BuLNS)$_2$/MoO(*t*BuLNS)$_2$ couple with a range of oxo donors and acceptors has been undertaken.[294] Quite negative entropies of activation ($\Delta S^{\ddagger}$ −21 to −33 eu) in the reaction of the $L_2Mo^{IV}O$ species with sulfur or nitrogen oxides as oxo donors are observed, consistent with an associative transition state for the oxidative limb of the catalytic cycle (Scheme 18).[294] No sys-

Scheme 18

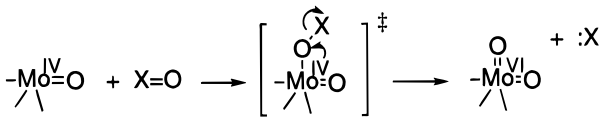

tematic correlation between the XO bond energy and the activation enthalpy for the reaction is observed, presumably due to a dominant contribution to $\Delta H^{\ddagger}$ of the substantial reorganizational energy associated with return to the $Mo^{VI}O_2$ parent (there being significant changes in the N−Mo−N and S−Mo−S bond angles upon addition or loss of the second oxo group). Overall, it appears that both limbs of the reaction cycle for the model systems shown in Scheme 16 pass through transition states whose structures may approximate Michaelis complexes seen with substrate/product in the case of the enzyme-catalyzed reactions.

A last model based on the tripyrazolyl borate ligand (Scheme 16C) has the same MoO_2 structural element as the two systems described above and, like them, is able to catalyze the transfer of an oxygen atom from a suitable donor to an acceptor.[291] This system reacts with phosphines (as oxo acceptors) and sulfoxides (as oxo donors) in a manner entirely analogous to the two previous model systems. This model is especially significant from the standpoint of the enzyme-catalyzed reaction since the reduced LMoOX form of this system reacts with H_2O (in the presence of a suitable oxidant) to return to the oxidized $LMoO_2X$ parent compound.[292] The oxo group lost in the reaction of the oxidized $LMoO_2X$ complex with Ph_3P is thus regenerated from water, as is the case in the reaction mechanism of sulfite oxidase. The chemistry of these and related complexes and their relevance to the mononuclear molybdenum enzymes has been extensively reviewed.[3,178,297]

With this chemistry in mind, a mechanism for sulfite oxidase has been suggested that involves nucleophilic attack of a sulfite lone pair on one of the Mo=O oxygens of oxidized enzyme,[4] as shown in Scheme 19. This reaction mechanism does not

Scheme 19

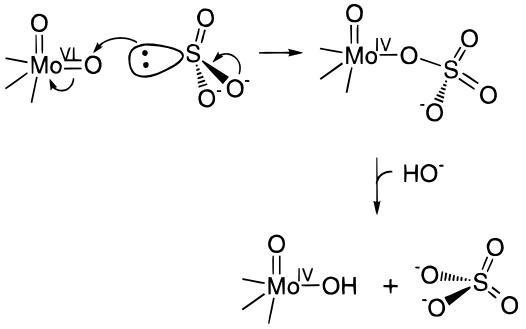

require direct coordination of substrate to the molybdenum, but if substrate does coordinate it must do so *cis* to one of the Mo=O groups. Should this be the case, a bidentate intermediate formed subsequent to nucleophilic attack on the Mo=O is expected, as has been proposed for the species giving rise to the "phosphate-complexed" Mo(V) EPR signal exhibited by sulfite oxidase,[281] and the observation of a comparable adduct with sulfite itself.[284] Completion of the catalytic cycle would presumably take place via displacement of sulfate from the molybdenum coordination sphere by hydroxide from solvent, followed by sequential electron transfer from the molybdenum center to the heme of the enzyme and concomitant deprotonation to return to the $Mo^{VI}O_2$ starting complex.

The reaction mechanism shown in Scheme 19 implies that the principal aspect of catalysis is attack on a Mo=O by a substrate lone pair. That this is in fact the case is strongly suggested from the results of a comparison of the kinetic behavior of sulfite and dimethyl sulfite as substrates for sulfite oxidase.[298] An examination of the substrate concentration dependence of the observed rate constant for enzyme

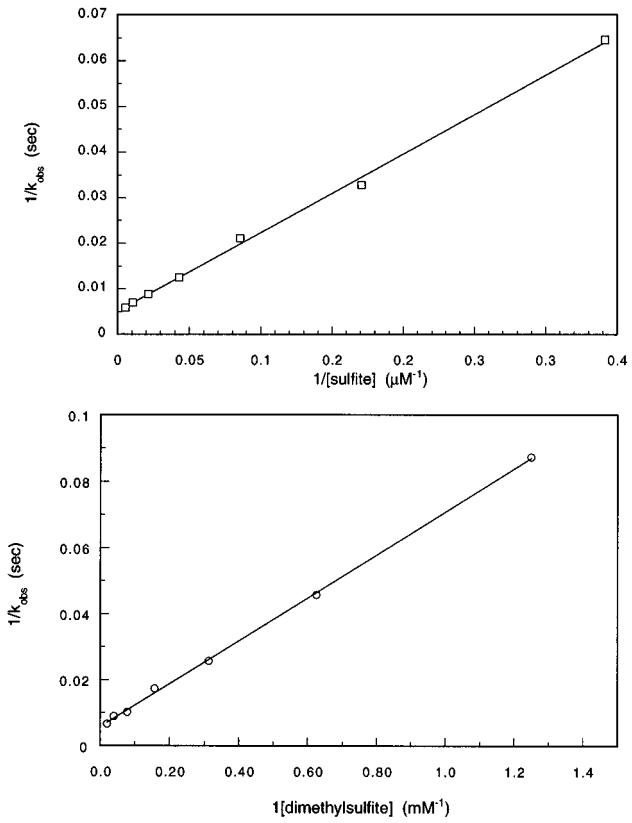

Figure 11. The reductive half-reaction of sulfite oxidase with sulfite (panel A) and dimethyl sulfite (panel B). The reaction conditions were 0.02 M Tris-acetate, pH 8.0, 25 °C. K_d and k_{lim} for sulfite are 33 μM and 194 s^{-1}, respectively. K_d and k_{lim} for dimethyl sulfite are 11 mM and 170 s^{-1}. After Brody and Hille,[297] with permission.

reduction (Figure 11) indicates that methylation of the sulfite oxyanions to give $(MeO)_2S{=}O$ results in a significant increase in the dissociation constant K_d for the reaction (from 33 μM for sulfite to 11 mM for dimethyl sulfite), but the limiting rate constant for enzyme reduction is essentially unaffected (194 and 170 s^{-1}, respectively). Thus while substrate oxyanion groups are clearly effective in stabilizing the $E_{ox}{\cdot}S$ complex, in all likelihood by direct coordination to molybdenum as previously proposed,[281] the breakdown of the Michaelis complex proceeds with undiminished rate even in their absence, as expected for a reaction mechanism of the type shown in Scheme 19. It is worth noting that even with the oxyanion groups blocked, sulfite oxidase still exhibits saturating kinetics in the reductive half-reaction with dimethyl sulfite, indicating that a Michaelis complex still forms with this substrate (presumably involving nonelectrostatic interactions with amino acid residues of the active site that also interact with sulfite). The upshot of this work is that the fundamental requirement for reactivity of sulfite oxidase appears to be the availability a suitable lone-pair on substrate that is able to undertake nucleophilic attack on a Mo=O group of the active site. It is reasonable to assume that only one of the two Mo=O groups present in the active site represents the catalytically labile oxygen (dictated by steric restrictions in the active site of the enzyme), with the other possibly functioning as a "spectator oxo" group as discussed above.[189,190]

The reduction potentials of sulfite oxidase have been examined by both potentiometry[299] and microcoulometry.[300] At pH 9.0 (and in the absence of coordinating ions such as phosphate or chloride), the enzyme potentials are Mo(VI/V), −57 mV; Mo(V/IV), −233 mV; and heme, 51 mV, indicating a very substantial thermodynamic stabilization of the Mo(V) oxidation state; at pH 6 in the presence of 0.1 N KCl, the corresponding values are 131, −86, and 90 mV.[299] Both molybdenum half-potentials increase significantly as the pH decreases from 9 to 6, the Mo(VI/V) couple by 190 mV and the Mo(V/IV) couple by 150 mV, again reflecting the involvement of prototropic equilibria in the oxidation−reduction chemistry of the molybdenum center.[299] On the other hand, the heme potential decreases only 40 mV over the same pH range.

As with xanthine oxidase and related enzymes, catalytic turnover of sulfite oxidase necessarily involves intramolecular electron transfer, from the molybdenum to the heme in the case of sulfite oxidase, and this has been investigated by flash photolysis.[79,301,302] In the more recent work,[79,302] using deazariboflavin radical as reductant, the heme is found to be reduced in the bimolecular reaction with photolytically generated radical, and subsequent oxidation−reduction equilibration with the molybdenum center to occur at ∼1600 s^{-1} at pH 6.0. The observed electron transfer rate is found to be quite pH dependent, increasing to 2400 s^{-1} at pH 7 before decreasing dramatically to 60 s^{-1} at pH 9.0.[79] In addition, it has been found that anions dramatically slow the reaction: in 23 mM sulfate the observed rate constant for electron transfer decreases to 35 s^{-1} at neutral pH. Inhibitory constants for sulfate, chloride, and phosphate of 0.8, 4, and 1.2 mM, respectively, have been estimated from the concentration dependence of the effect on both the electron-transfer kinetics and steady-state behavior of the enzyme.[79,302] Slow processes (k_{obs} 150−310 s^{-1}) associated with heme reduction that were reported in the original work apparently are not reproducible, and it appears that electron transfer in sulfite oxidase is in no way rate limiting to overall catalysis.

Recently a series of covalently linked molybdenum^{V}/heme^{III} complexes have been prepared as simple models for cofactor interaction in sulfite oxidase.[303,304] The molybdenum portion of the complexes is based on the tripyrazolyl borate complex shown in Scheme 16C, covalently linked to a series of tetraarylporphyrin iron(III) compounds via a catechol side chain of the latter that serves to coordinate the molybdenum directly (structure 2). Interestingly, despite the covalent linkage between the two metal centers, only weak magnetic coupling is observed between the ferric heme and Mo^{V} over distances ranging from 7.9 to 9.4 Å in these complexes. The mechanism of coupling is quite sensitive to the metal−metal distance: at shorter distances the coupling is due to a weak exchange interaction of no more than 0.06 cm^{-1}, while at longer distances this exchange interaction becomes negligible and is superseded by a weak, anisotropic dipolar coupling between the Mo(V) and low-spin Fe(III) heme.[304] In these complexes, the Mo(VI/V) and heme redox couples behave independently

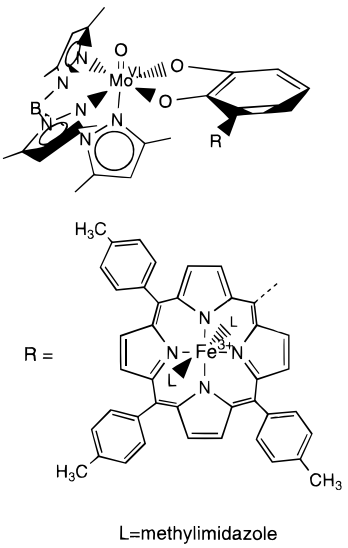

of one another, but the reduction potential for the Mo(V/IV) couple is found to be influenced by both the charge and electronic state of the heme, as well as by substitutions on the linking catechol ring. It is anticipated that further investigations of systems such as this will greatly advance our understanding of the electron transfer and related properties of sulfite oxidase.

B. The Assimilatory Nitrate Reductases

The assimilatory nitrate reductases are enzymes isolated from fungi, algae, and higher plants that are responsible for the first step in the uptake and utilization of nitrate by these organisms. These enzymes possess a *b*-type cytochrome and FAD in addition to the molybdenum center, and the absorption spectra of both oxidized and reduced enzyme are dominated by the spectral contribution of the enzyme's heme group and, to a lesser extent, the FAD (Figure 12). Although there is a great deal known about the molecular biology of the assimilatory nitrate reductases,[305] there has been surprisingly little mechanistic work done with the enzyme. The overall reaction catalyzed, which is generally the rate-limiting step in nitrogen assimilation in these organisms, is shown in Scheme 20. The reaction is

Scheme 20

thought to be essentially the reverse of that seen with sulfite oxidase due to the relative stabilities of the N═O and S═O bonds: nitrate is an effective oxo donor while sulfite is a more effective oxo acceptor.[178,295] With regard to the reducing substrate, nitrate reductases from higher plants are specific for NADH while the enzyme from fungal sources is specific for NADPH. The algal enzymes are typically specific for NADH, although some nonspecific enzymes able to utilize either NADH or NADPH have been described.[122] As discussed in section II.B, the enzyme is a homodimer with a subunit mass of ~110 kDa. Each subunit (from the spinach protein) consists of a large N-terminal portion (~59 kDa) that possesses the molybdenum center, a small central

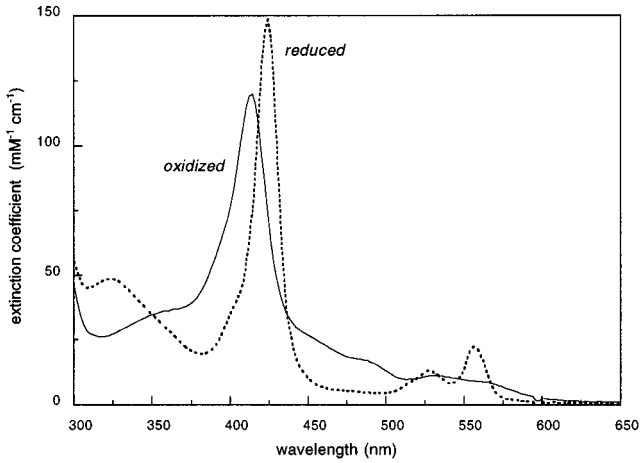

Figure 12. The absorption spectra of oxidized (solid line) and reduced (dashed line) recombinant squash nitrate reductase flavoheme domains. The spectra are indistinguishable from native plant nitrate reductase.

domain possessing a *b*-type cytochrome (14 kDa), and a C-terminal domain containing FAD and the NAD(P)$^+$ binding site (24 kDa).[131] The flavin domain isolated after limited proteolysis of the *Chlorella* enzyme is somewhat larger at ~30 kDa.[306] As in the case of sulfite oxidase, the isolated domains retain the partial activity of their constituent cofactors, the molybdenum domain being an effective methylene blue:nitrate reductase, and the flavin domain an effective NADH:ferricyanide and NADH:cytochrome *b* reductase.[131,306] As indicated above, the molybdenum- and heme-containing domains possess significant homology to the corresponding portions of sulfite oxidase and cytochrome b_5, (although in sulfite oxidase the heme domain is N-terminal to the molybdenum) and the flavin-binding portion to members of the ferredoxin:NADP$^+$ reductase family of flavoproteins. As indicated in Figure 13, while the molybdenum domains of the assimilatory nitrate reductases and sulfite oxidase exhibit very substantial homology to one another,[80,81] homology with the molybdenum-binding regions of the molybdenum hydroxylases is largely restricted to the region corresponding to the first of the two molybdenum domains of the *D. gigas* aldehyde oxidoreductase. In the molybdenum-binding regions of the nitrate reductases, there are seven regions where 7−16 residues present in the hydroxylases have been deleted, with the result that the molybdenum-binding fragment of the nitrate reductases are some 80 amino acid residues shorter than is found in the hydroxylases.[86]

That the several cofactor domains constitute autonomous structural elements within the intact nitrate reductase molecule has been demonstrated by cloning and expression of the separate domains of nitrate reductase that bind heme,[133,307] flavin,[134] and the two domains together as a single polypeptide.[135] The flavin domain, referred to as the cytochrome *b* reductase (CbR) portion of nitrate reductase, has recently been crystallized and its X-ray structure reported at a resolution of 2.5 Å.[308] The protein is found to consist of an N-terminal FAD-binding domain and a C-terminal NADH-binding domain, connected by a linker region that takes the form of a three-stranded antiparallel β sheet. The peptide fold

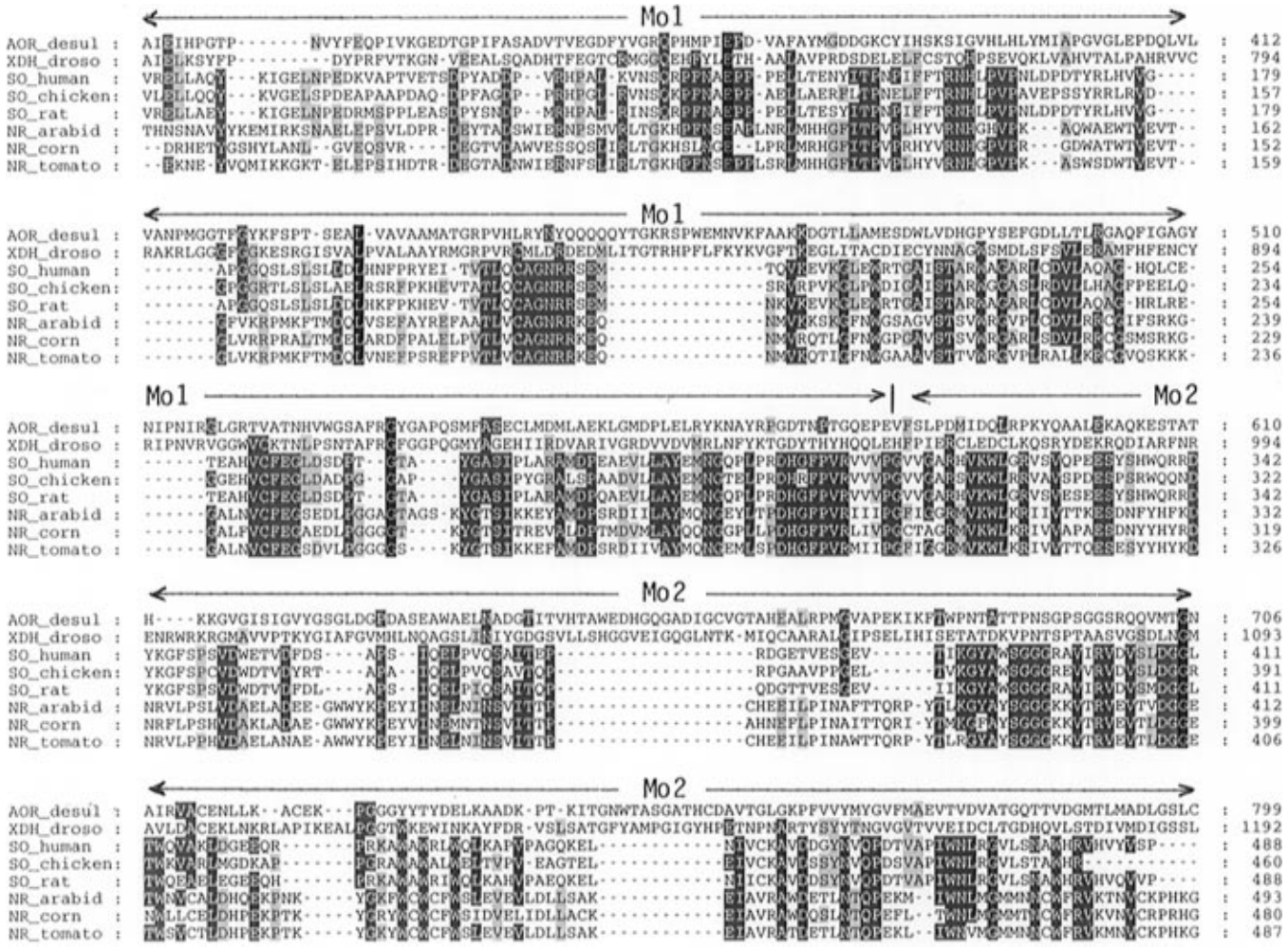

Figure 13. Sequence alignments for the molybdenum-binding portions of aldehyde oxidoreductase from *Desulfovibrio gigas* (Thoenes *et al.*[156]), *D. malanogaster* xanthine dehydrogenase (Lee *et al.*, *Genetics* **1987**, *116*, 55; Keith *et al.*, *Genetics* **1987**, *116*, 67), human (Garrett *et al.*[121]), chicken (Neame and Barber[80]), and rat (Garrett and Rajagopalan, *J. Biol. Chem.* **1994**, *269*, 272), sulfite oxidases and nitrate reductases from *Arabadopsis thaliana* (Crawford *et al.*[123]), corn (Hyde and Campbell[134]), and tomato (Daniel-Vedele *et al.*, *Gene* **1989**, *85*, 371). The alignments were made with the program MACAW using previously identified regions of homology.[80,86,123] Sequences used were the current versions deposited in GenBank as of Feb 29, 1996. Regions of sequence identity are indicated by degrees of shading, depending on the extent of conservation at a given position among all members of the family. The regions corresponding to the two molybdenum-binding domains of the aldehyde oxidoreductase from *D. gigas* are indicated.

of the flavin-binding domain of the nitrate reductase CbR is an antiparallel β barrel with the strands tracing a "Greek key" motif. The fold of the NADH-binding domain consists of a six-strand parallel β sheet flanked on each side by an α helix, and represents a slight variation on the typical folding pattern of nucleotide-binding proteins.[309] Although the overall folding patterns of the two domains of the CbR are quite similar to those observed in the corresponding domains of ferredoxin:$NADP^+$ reductase[125] and phthalate dioxygenase reductase[310] (proteins with which CbR shares 15% and 17% sequence identity, respectively) they differ in orientation by a rotation of ~15° compared to that found in the other two proteins.

The structure of the CbR in complex with ADP has also been determined, permitting the binding site of NADH to be defined in large part.[311] In addition, a model of the complex of the flavin-binding portion of nitrate reductase with chicken cytochrome b_5 has been constructed that presumably reproduces the basic elements of the flavin- and heme-domain interactions in nitrate reductase.[311] The optimal orientation, consistent with the covalent linkage of the two units in the intact nitrate reductase, implicates a highly conserved histidine residue (His 48 in the CbR fragment of nitrate reductase) in mediating electron transfer from the flavin to the heme within nitrate reductase (Figure 14). This residue hydrogen bonds to the exposed heme propionate of cytochrome b_5 in the model of the complex and is located in the immediate vicinity of the C_8-methyl group of the FAD. Although the corresponding histidine in the nitrate reductase from *Aspergillus nidulans* (His 654) has been mutated (to alanine) with negligible effect on nitrate reductase activity in crude extracts,[82] electron transfer from the flavin to the heme is unlikely to be rate-limiting in turnover, and this observation does not preclude a significant role for the histidine in mediating electron transfer between the two centers. The relative orientation of flavin and heme in the complex[311] is generally similar to that seen in flavocytochrome b_2,[312] with the two redox-active centers approximately coplanar.

A comparison has been made of the spectroscopic and kinetic properties of the CbR fragment of nitrate reductase and a mutant in which cysteine 242 is replaced with a serine residue (C242S). This cysteine

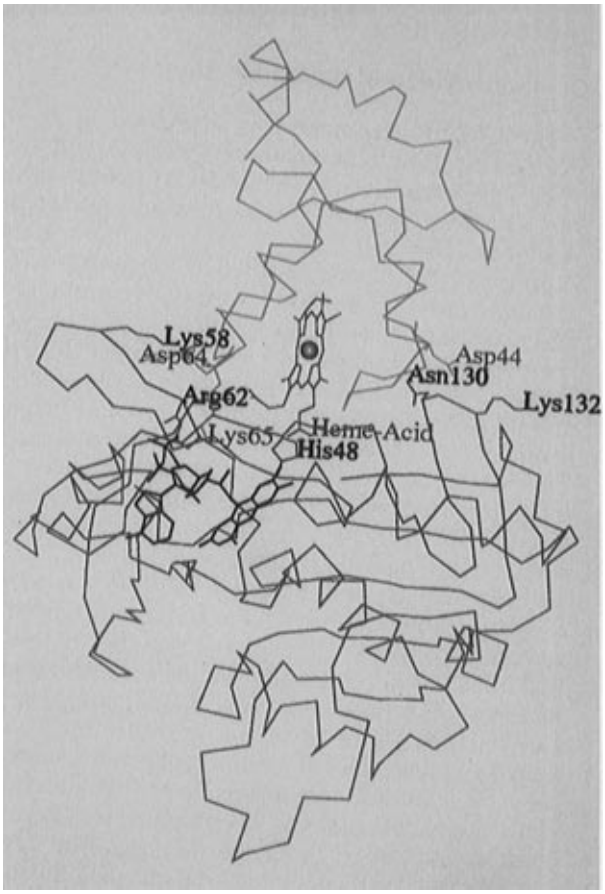

Figure 14. Model of the complex of cytochrome b_5 (red) and the flavin domain (CbR) (green) of corn nitrate reductase. Reproduced from Lu *et al.*,[310] with permission.

has been implicated previously as playing an important role in the reductive half-reaction of the catalytic cycle, on the basis of it being highly conserved among nitrate reductases.[313] Although the UV/vis and CD spectral properties are largely unchanged upon mutation, as are the reduction potentials for the flavin, the rate for reduction by NADH of the C242S mutant is some 7-fold slower than that for the wild-type protein (68 s^{-1} as compared with 478 s^{-1}) and the K_d is larger by a factor of 2 (6 μM *vs* 3 μM). These results indicate that Cys 242 residue plays a role principally in facilitating electron transfer from NADH to the flavin rather than in binding of NADH to the enzyme, and while not essential for the reaction, it nevertheless influences k_{red}/K_d (corresponding to the second-order rate constant for reaction of enzyme with reduced NADH in the low concentration regime) by a factor of greater than 10.[314] More recent work with the cytochrome *c* reductase fragment of nitrate reductase (CcR, consisting of the heme- as well as flavin-containing domain) suggests that electron transfer from the flavin to the cytochrome does not take place until NAD^+ has dissociated from the active site (K. Ratnam, N. Shiraishi, W. H. Campbell, and R. Hille, unpublished). It is possible that the reason Cys 242 is so highly conserved among nitrate reductases has to do with its role in facilitating product release (which appears to be the rate-limiting step in catalysis) rather than initial reduction of the FAD.

The assimilatory nitrate reductase from *Chlorella vulgaris* has been examined by X-ray absorption spectroscopy,[315] and its molybdenum center is found

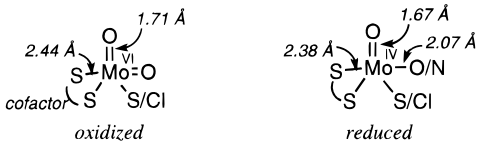

Figure 15. Summary of XAS results with the assimilatory nitrate reductase from *Chlorella vulgaris*. The bond distances given are from Cramer *et al.*[314]

to exhibit a striking resemblance to that of sulfite oxidase (Figure 15). The EXAFS pattern of the oxidized enzyme is dominated by two Mo=O groups at a distance of 1.71 Å, with two or three Mo thiolates at a distance of 2.44 Å. Reduction of the enzyme by either NADH or sodium dithionite results in loss of one of the Mo=O groups and appearance of a new Mo−O at a distance of 2.07 Å (presumably a Mo−OH formed upon protonation of a Mo=O concomitant with reduction of the molybdenum); the remaining Mo=O distance decreases to 1.67 Å (consistent with it playing the role of a spectator oxo group) and the Mo thiolates to 2.38 Å. The number of thiolate sulfur ligands to molybdenum increases upon reduction of the metal, but as in the case of sulfite oxidase the inability of the technique to distinguish between sulfur and chlorine makes it impossible to determine whether this is due to resolution of an additional sulfur indigenous to the molybdenum coordination sphere or binding of chloride to the reduced enzyme (as is thought to occur in the case of sulfite oxidase).

The EPR properties of the molybdenum center of nitrate reductase from *Chlorella vulgaris*[316,317] and *Candida nitratophila*,[318] as well as spinach,[319] have been reported and while there is a substantial degree of similarity between these enzymes and sulfite oxidase, there are also significant differences as well. There is evidence for "high-pH" and "low-pH" signals from all three nitrate reductases, analogous to the signals seen with sulfite oxidase, with the "low-pH" signals exhibiting coupling to a single solvent-exchangeable proton. However, phosphate does not perturb the EPR signal of the *Chlorella* nitrate reductase in a manner analogous to that seen with sulfite oxidase.[317] Also, in the case of the *Chlorella* nitrate reductase the strong proton coupling observed in the "low-pH" signal (a_{av} = 13.5 G) is abolished upon addition of chloride or nitrite with no effect on the observed *g* values ($g_{1,2,3}$ = 1.996, 1.969, 1.967, reminiscent of the corresponding *g* values for the "low-pH" signal from sulfite oxidase).

Finally, the reduction potentials for the several redox-active centers in nitrate reductase from both *Chlorella*[320−322] and spinach[323] have been reported. By using room-temperature visible absorbance, circular dichroism and EPR changes to follow reduction of each of the centers in the course of potentiometric titrations, the reduction potentials given in Table 3 have been determined.[320] It is seen that the midpoint potential of the FAD, the reduction potential for the cytochrome and the midpoint potential for the molybdenum center at pH 7.0 increase in the order −272, −162, and −7 mV, respectively, indicating that the physiological direction of electron flow is thermodynamically favorable at neutral pH. These potentiometric results are in reasonable agreement with microcoulometric determinations,[322] and as with sulfite oxidase, it is apparent that nitrate reductase

operates in a considerably higher redox regime than do the molybdenum hydroxylases. The reduction potential obtained for the proteolytically derived flavin[320] domain from the *Chlorella* nitrate reductase is in reasonable agreement with the value seen in the intact enzyme, but that for the recombinant heme domain is significantly higher (+16 mV *vs* −160 mV at pH 7.0) than is observed in the holoenzyme.[307] This suggests that the heme potential is perturbed by interdomain interactions within the intact protein.

The reduction potentials obtained at pH 7.0 with spinach nitrate reductase are quite similar to the values seen with the enzyme from *Chlorella* with the exception of the cytochrome, which is found to have a 40 mV higher potential in the plant protein as compared with the algal form.[323] Discrepancies with the results of earlier reductive titrations in which the molybdenum center was followed by its EPR spectrum at liquid nitrogen temperatures[315] appear to be attributable to a temperature-dependent distribution of reducing equivalents within partially reduced nitrate reductase[320] that is entirely analogous to the effect documented with xanthine oxidase.[227] The reduction potential for the *b*-type cytochrome of *Chlorella* nitrate reductase is essentially independent of pH, as is the FAD/FAD$^{\bullet-}$ half-potential, consistent with the flavin semiquinone being in the anionic form. The FAD$^{\bullet-}$/FADH^{-} half-potential and the potential of both molybdenum couples, on the other hand, exhibit approximately a 60 mV drop per pH unit over the range 6.0 to 9.0, indicating that uptake of a proton upon reduction is associated with each of these three couples and in particular that full reduction of the molybdenum center involves the uptake of two protons rather than just one. By contrast to the flavin center where very little flavin semiquinone accumulates at maximum (owing to a significantly higher reduction potential for the semiquinone/hydroquinone couple compared to that for the quinone/semiquinone couple) approximately 50% of the enzyme molybdenum accumulates at maximum as Mo(V). This indicates that the first half-potential is somewhat higher than the second over the entire pH range investigated.[321]

The activity of assimilatory nitrate reductases is under tight physiological control, and includes regulation at the transcriptional, translational and post-translational levels. Although a detailed discussion of these regulatory mechanisms is beyond the scope of the present account (the reader is referred to the book edited by Wray and Kinghorn[305] for a detailed review of the literature), it is interesting to note that the site of phosphorylation in spinach nitrate reductase has recently been identified as Ser 543.[324] This residue lies in the interdomain region spanning the molybdenum and heme domains, and its phosphorylation by a nitrate reductase-specific kinase is responsible for the short-term down-regulation of nitrate reductase activity in course of the diurnal cycle (presumably so as to avoid accumulation of nitrite in the absence of an adequate supply of photosynthetically generated reducing equivalents). This inhibition of activity is indirect, in that it is binding of a nitrate reductase inhibitor protein to the phosphorylated enzyme that brings about inhibition. It is possible that the mechanism of inhibition involves a disruption of electron transfer from the flavin to the molybdenum center by altering the domain interactions within the enzyme, rather than shutting down the chemistry of the molybdenum or flavin center *per se*.

V. The DMSO Reductase Family

The DMSO reductase family consists of a number of molybdenum enzymes, all from bacterial and archaeal sources, exhibiting substantial sequence homology that justifies their grouping into a single family. Some of these enzymes are particularly interesting in that, unlike all of the enzymes discussed to this point, they possess a molybdenum center as their sole redox-active center, and this exhibits fairly strong absorption in the visible/near infrared region. This absorption provides an extremely useful experimental probe that makes the molybdenum center amenable to a variety of spectroscopic and kinetic techniques, promising rapid progress in our understanding of their mechanism of action.

A. Periplasmic DMSO Reductase and Biotin-*S*-oxide Reductase

DMSO reductase as isolated from *Rhodobacter* species is an 82 kDa monomeric, soluble protein found in the periplasmic space of the organism that catalyzes the reductive deoxygenation of dimethyl sulfoxide to dimethyl sulfide as shown in Scheme 21.

Scheme 21

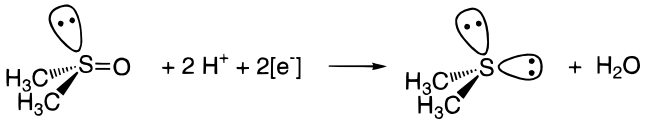

The enzyme is able to utilize a variety of dialkyl and alkylaryl sulfoxides as oxidizing substrate.[325] The gene encoding the *R. sphaeroides* enzyme has been cloned and sequenced,[72−74] and as indicated in section II.B exhibits negligible homology to members of the two previous families of molybdenum enzymes. As illustrated in Figure 16, however, the inferred amino acid sequence does exhibit strong sequence homology (up to 40% sequence identity) with other members of this family of molybdenum enzymes. This homology is particularly strong in six regions previously identified by Yamamoto *et al.*,[72] as indicated in the figure.

The enzyme is expressed in *Rhodobacter sphaeroides*[136,326] and *Rhodobacter capsulatus*[137] when grown under photoheterotrophic conditions, particularly when a highly reduced carbon source is used. The two proteins have been purified from both organisms and that from *R. sphaeroides* found to possess the guanine dinucleotide form of the pterin cofactor.[19] Most recently, both proteins have been crystallized, and the crystal structure for the *R. sphaeroides* protein has been reported.[7] As indicated in section II.B, the molybdenum center of this enzyme is found to consist of the metal coordinated to a pair of pterin cofactors, with additional Mo=O and serine ligands to the molybdenum in an overall distorted trigonal prismatic coordination geometry. This structure is

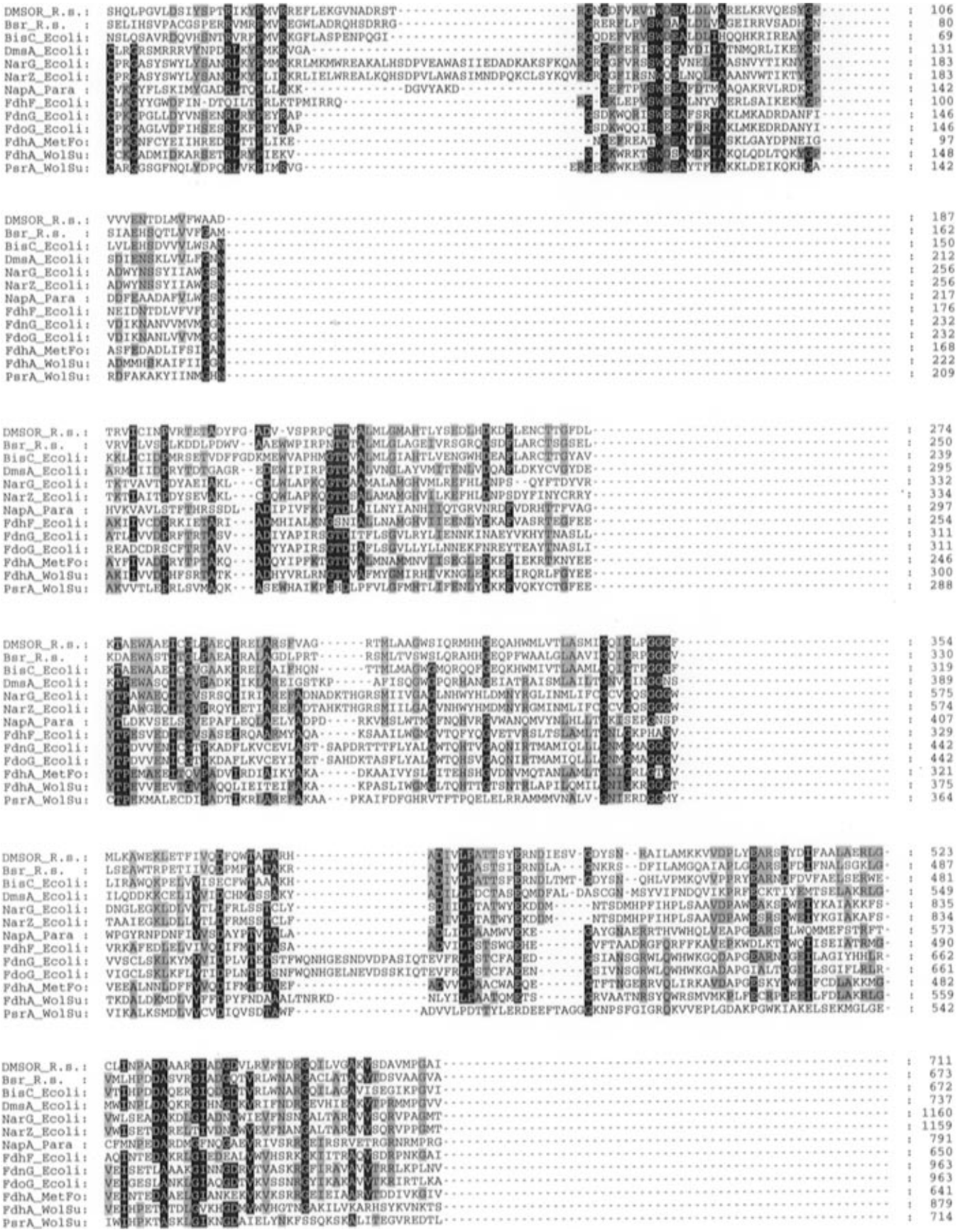

Figure 16. Sequence alignments for several molybdenum enzymes of the DMSO reductase family. The sequences are for (from top to bottom) DMSO reductase from *Rhodobacter sphaeroides* (Yamamoto *et al.*[72]), biotin sulfoxide reductase from *R. sphaeroides* (Pollock and Barber[337]), biotin sulfoxide reductase from *Escherichia coli* (Pierson and Campbell[336]), DMSO reductase (A subunit) from *E. coli* (Bilous *et al.*[348]), nitrate reductase A (G subunit) from *E. coli*, nitrate reductase Z (Z subunit) *from E. coli* (Blasco *et al.*[357]), nitrate reductase O (A subunit) from *E. coli* (Berks *et al.*[393]), formate dehydrogenase F from *E. coli* (Zinoni *et al.*[401]), formate dehydrogenase N (G subunit) from *E. coli* (Blasco *et al.*[141]), formate dehydrogenase O (G subunit) from *E. coli* (Blattner *et al.*[406]), formate dehydrogenase (A subunit) from *Methanobacterium formicicum* (Shuber *et al.*[409]), formate dehydrogenase (A subunit) from *Wollinella succinogenes* (Bokranz *et al.*[410]), and polysulfide

consistent with recent XAS studies of the protein indicating a single Mo=O, approximately four thiolate ligands and a single Mo−O/N in the oxidized enzyme.[67] Overall, the immediate environment of the molybdenum center is reminiscent of the active site of the tungsten-containing aldehyde:ferredoxin oxidoreductase for *Pyrococcus furiosus*,[14] although the two enzymes share only minimal sequence homology (apparently limited to the immediate binding sites for the pterin cofactors).[19] Quite surprisingly, upon reduction of DMSO reductase, the crystal data indicate the Mo=O group is lost, possibly by protonation to give a second Mo−O,[67] and the molybdenum bond to one of the sulfur ligands from one of the dithiolene ligands is significantly lengthened, to 3.7 Å. The mechanistic implication of this structural work is that DMSO reductase cycles between a monooxo Mo(VI) and *des*oxo Mo(IV) species in the course of its catalytic sequence, with the loss of one of the Mo−S bonds upon reduction possibly creating a vacant ligand coordination position at which the substrate DMSO may bind in the active site.[7]

The overall polypeptide fold of the *R. sphaeroides* DMSO reductase is organized into four domains, only one of which (the fourth) is formed by a contiguous portion of the polypeptide chain;[7] the overall dimensions of the protein are 75 × 55 × 65 Å. Domain I consists of a pair of three-stranded antiparallel β sheets and three α helices (two oriented parallel to the sheets, one perpendicular. Domain II consists of a central six-stranded β sheet surrounded by nine α helices and is flanked by a pair of β strands that constitute part of the wall to the large surface depression that provides solvent access to the active site. Domain III is located opposite the molybdenum center from Domain II, and also consists of a core β sheet (5-stranded in this case) surround by 12 α helices. The overall topology of this domain constitutes a variation on the classical nucleotide-binding domain. Together, domains II and III provide most of the protein contacts (principally hydrogen-bonding interactions) with the guanosine diphosphate portion of the two pterin cofactors of the active site (there are also a few contacts with the pterin portion of the cofactor), with each domain largely associated with one or the other cofactor molecule. Together, these two domains create a surface depression that provides solvent access to the active site. Y114 of domain II hydrogen-bonds to the Mo=O of the active site, and S147 of domain III is the serine residue that coordinates the metal directly. Domain III makes somewhat less contact overall with its cofactor than does domain II, and it is the domain III cofactor that partially dissociates from the molybdenum upon reduction of the enzyme. (There is also a substantial change in conformation of this pterin upon reduction of the enzyme that has been interpreted as reflecting a tautomerization within the dithiolene moiety subsequent to protonation of the now dissociated thiolate ligand.) Finally, domain IV consists of a six-stranded β barrel, and lies between domains II and III opposite the active site from the solvent access channel. Domain IV provides protein contacts to the diphosphate groups of both cofactors, as well as their pterin nuclei, but does not directly contact the immediate coordination environment of the molybdenum center.

Unlike the molybdenum centers of the other two families considered above, that of DMSO reductase has been shown to exhibit a characteristic absorption spectrum[137,326] as shown in Figure 17. The relatively strong absorption exhibited by the molybdenum center of DMSO reductase was in fact the first clue that the center was fundamentally distinct from that found in other molybdenum-containing enzymes. Taking advantage of this spectral probe of the active site, DMSO reductase has been investigated using both resonance Raman[327,328] and magnetic circular dichroism[329,330] spectroscopy. Exciting at 676.4 nm, in the lowest-energy transition in the absorption spectrum, a vibrational mode at 1575 cm^{-1} is observed in the resonance Raman spectrum of the oxidized enzyme that was initially attributed to the C=C stretch of the dithiolene side chain.[327] This mode shifts to 1568 cm^{-1} upon reduction of the enzyme, consistent with it arising from the redox-active molybdenum center and suggesting a partial delocalization of electron density onto the dithiolene upon reduction of the molybdenum. More recently, a comparison of the high-frequency Raman shift region of the enzyme and the comparable region of 6-methylpterin, biopterin, and 6-methyl-7,8-dihydropterin suggests that the pterin of the enzyme is in the 5,8-dihydro oxidation state, with the dithiolene C=C conjugated to the C_7=C_8 double bond.[328] The coupled stretching modes of these two double bonds has been proposed to rise to the 1526 and 1576 cm^{-1} modes of oxidized enzyme, respectively. This revised assignment for the dithiolene stretch is more in line with the Raman spectra of the dithiolene compounds[331] shown in Scheme 22, in which the dithiolene stretching modes have been (tentatively) assigned to bands in the 1506−1535 cm^{-1} region.

It is clear from these studies that pterin ring modes are resonance-enhanced upon excitation in the near-infrared, that this electronic transition must therefore be of a charge-transfer nature, and that the pterin ring itself contributes to this interaction (but via coupling with dithiolene vibrational modes rather than by direct coordination to the molybdenum) in order to account for the observed resonance enhancement. In the low-frequency Raman shift region of the enzyme, a ^{34}S-sensitive mode at 350 cm^{-1} in the natural-abundance sample (shifting to 343 cm^{-1} upon isotopic substitution) is assigned to the Mo−S dithiolene stretch, and the observation of other modes exhibiting smaller shifts is again taken to be a reflection of extensive coupling of the Mo−S modes with other vibrational modes intrinsic to the chro-

(Figure 16, continued) reductase (A subunit) *from W. succinogenes* (Krafft *et al.*[422]). The alignments were made with the program MACAW using regions of homology previously identified by Berks *et al.*,[393] Yamamoto *et al.*,[72] Weiner *et al.*,[140] and Wootton *et al.*[86] Sequences used were the current versions deposited in GenBank as of Feb 29, 1996, with the exception of NarG, where the modified sequence presented by Wootton *et al.*[86] was used. Regions of sequence identity are indicated by degrees of shading, depending on the extent of conservation at a given position among all members of the family. The position corresponding to the serine, cysteine, or selenocysteine residue that coordinates to the molybdenum is present in a region of very low homology and is not shown.

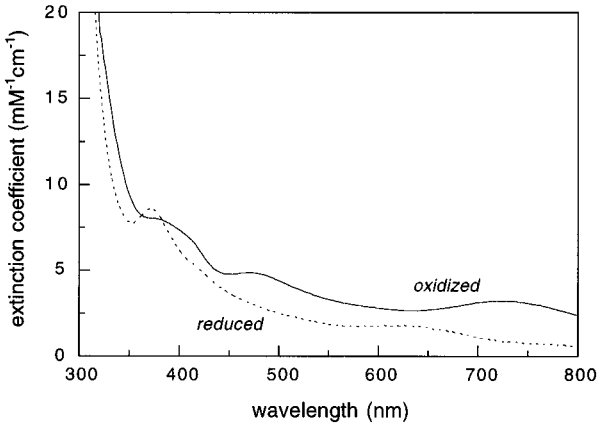

Figure 17. The absorption spectra of oxidized (solid line) and reduced (dashed line) DMSO reductase from *Rhodobacter sphaeroides*. After Bastian *et al.*,[325] with permission.

Scheme 22

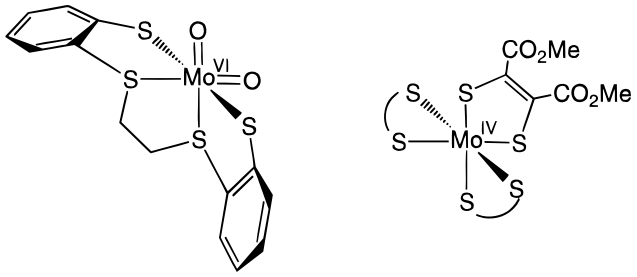

mophore. As in the case of the resonance Raman study of xanthine oxidase,[195] however, no modes attributable to the Mo=O could be identified in the resonance Raman spectrum of oxidized DMSO reductase, presumably because they are so weakly resonance enhanced.

The low-temperature magnetic circular dichroism spectra of partially reduced native DMSO reductase[329] and a glycerol-inhibited form of the enzyme[330] have also been examined, the latter form having been found to stabilize the Mo(V) valence state. With the native enzyme, the MCD spectrum in the 550−700 nm region exhibits a pattern of alternately positive and negative features that have been assigned to dithiolene → Mo^{V} charge-transfer transitions.[329] A simple Mo-dithiolene model has been proposed in which the electronic transitions involve electron promotion from one of four dithiolene π or σ molecular orbitals to the singly occupied d orbital (thought to be d_{xy}) of the molybdenum. On the basis of the reasonable simulation of the spectrum with only the dithiolene ligand, it has been concluded that there are no other sulfur-containing ligands, specifically cysteine residues, to the metal (a conclusion substantiated by the crystal structure of the enzyme). The MCD results obtained with the glycerol-inhibited enzyme, in which a substantially greater amount of the molybdenum is found in the (V) valence state, have also been interpreted as indicating that the observed electronic transitions in the visible/near-IR region are due to ligand-to-metal charge-transfer bands (Figure 18).[330] The detailed model used to interpret the MCD of the glycerol-treated enzyme is substantively different from that proposed for the native enzyme, however, in that the electronic transitions are assigned to electron promotion from one of a set of three dithiolene p orbitals to either the

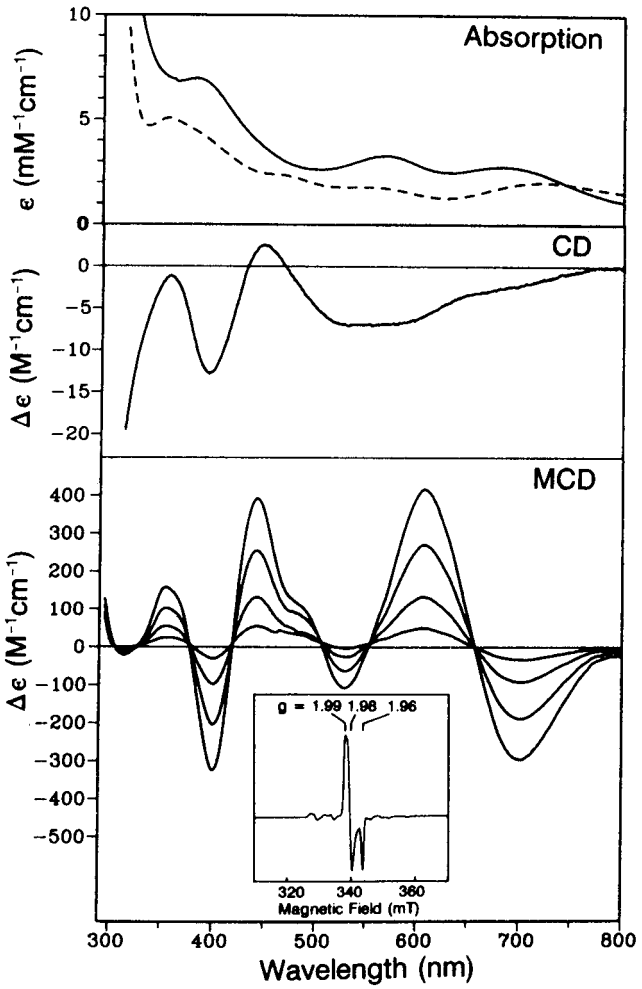

Figure 18. The magnetic circular dichroism spectrum of DMSO reductase from *Rhodobacter sphaeroides*: (from top to bottom) the absorption spectra of native (dashed line) and glycerol-inhibited (solid line) enzyme; the circular dichroism spectrum of the glycerol-inhibited enzyme at room temperature; and the low-temperature magnetic circular dichroism of the glycerol-inhibited enzyme. The MCD conditions were 4.5 T magnetic field and 1.61, 4.22, 9.6, and 27.2 K. The inset to the bottom panel shows the EPR signal exhibited by the glycerol-inhibited enzyme. Reproduced from Finnegan *et al.*,[329] with permission.

singly occupied d_{xy} orbital of molybdenum or its unoccupied d_{yz} orbital.

Both the above interpretations may require modification in light of a comprehensive spectroscopic study of $LMo^{V}O$ compounds (L being the tripyrazolyl borate ligand of Scheme 16).[332] It is pointed out in this work that the filled C=C dithiolene π orbital is expected to be of significantly lower energy than the sulfur p orbitals of the ligand and that the latter are therefore more likely to act as the π donors into molybdenum d orbitals in a charge-transfer interaction. Donation into the half-filled d_{xy} orbital is proposed to give rise to the transitions in the 9000−15000 cm^{-1} region of the electronic spectrum (625−1100 nm), and into the vacant metal d_{xz} and d_{yz} orbitals to transitions in the 17000−35000 cm^{-1} region (290−590 nm). In support of this conclusion, the overall similarity in spectral properties of saturated and unsaturated dithiol ligands has been pointed out and taken to indicate that the dithiolene C=C does not make a significant contribution to the spectral properties of the models, and by inference

the enzyme also.[332] It is noted in this work that charge-transfer donation from the ligand sulfurs into d orbitals that are antibonding with respect to the Mo=O bond are expected to weaken the Mo=O, thereby facilitating oxygen atom transfer. An explicit consideration of the Mo=O group leads to the conclusion that the energies of d_{xz} and d_{yz} are closely spaced and their relative energies sensitive to the ligands of the $x-y$ plane. It has been suggested that the inversion of sign observed in comparing the MCD of the models and data in the range 21000−30000 cm^{-1} (330−475 nm) is due to this phenomenon. It is further suggested that additional sulfur on the molybdenum coordination sphere could account for the intense band at 15000 cm^{-1} (667 nm) that is observed in the enzyme as compared with the model compounds, an interpretation borne out by the recent crystallography indicating the presence of two rather than a single dithiolene ligand to the molybdenum. It is expected that additional spectroscopic characterization of the molybdenum center of DMSO reductase will further clarify the electronic structure of the active site in a way that will complement the X-ray crystal data.

Although DMSO reductase undoubtedly functions physiologically as indicated in Scheme 21, the enzyme has recently been found to be effectively reduced by the water-soluble phosphine shown in Scheme 23, generating the corresponding phosphine

Scheme 23

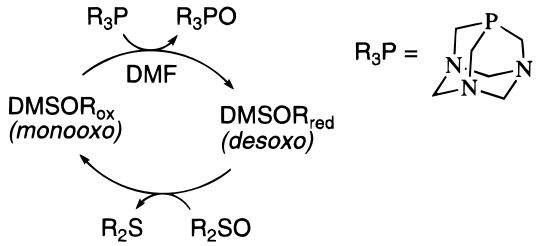

oxide.[333] When labeled by reoxidation of dithionite-reduced enzyme with ^{18}O-labeled dimethyl sulfoxide, the enzyme quantitatively transfers ^{18}O to phosphine, as evidenced by mass spectral characterization of the recovered phosphine oxide.[333] Thus, as has been demonstrated for xanthine oxidase, there is a catalytically labile oxygen site which with each turnover passes oxygen from the enzyme to an oxo acceptor only to be regenerated by subsequent reaction with an oxo donor. In light of the recent crystal structure for DMSO reductase, this catalytically labile oxygen can only be the single Mo=O of the oxidized enzyme. At one level the reaction mechanism of DMSO reductase is reminiscent of the model chemistry depicted in Scheme 16 in that the enzyme is involved in transfer from an oxo donor to an acceptor with the catalyst cycling between a $Mo^{VI}{=}O_n$ and $Mo^{IV}{=}O_{n-1}$ species. In the case of DMSO reductase, however, the enzyme must cycle between a monooxo Mo(VI) and a *des*oxo Mo(IV) species. Nevertheless, the ability of the enzyme to function as indicated in Scheme 23 suggests that the mechanisms proposed for the reductive and oxidative half-reactions of the models (Schemes 17 and 18, respectively) are likely to be directly relevant to the catalytic cycle of DMSO reductase.

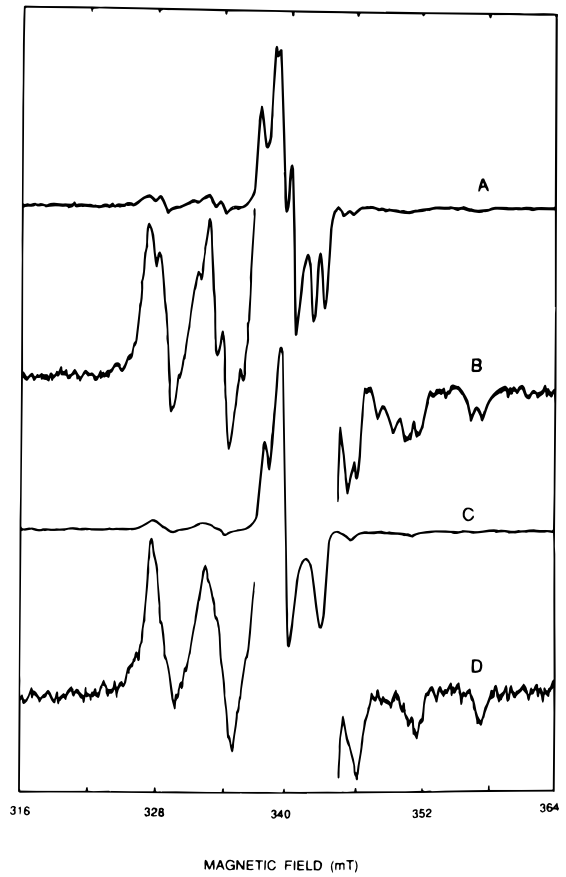

Figure 19. Mo(V) EPR signals exhibited by DMSO reductase from *Rhodobacter sphaeroides*: (from top to bottom) partially reduced native enzyme in Tricine buffer, pH 7.5; enlargement of same illustrating the hyperfine lines attributable to the natural abundance $^{95,97}Mo$; partially reduced native enzyme prepared in D_2O; enlargement of same, again illustrating the hyperfine lines attributable to the natural abundance $^{95,97}Mo$. The signal corresponds to $g_{1,2,3} = 1.988, 1.977, 1.961$, with $a_{av} = 10.5$ G. Reproduced from Bastian *et al.*,[325] with permission.

Although the catalytic sequence of DMSO reductase in the reaction described above does not involve the Mo(V) oxidation state, it is likely that the electron donor in the physiological reaction shown in Scheme 21 is a one-electron carrier (possibly thioredoxin), in which case the Mo(V) state would be formed transiently in the course of the return to the Mo(IV) state. As a result, the enzyme in all likelihood passes through a Mo(V) oxidation state in the course of regenerating the Mo(IV) state from the Mo(VI) subsequent to reaction with dimethyl sulfoxide. The EPR-active Mo(V) state of DMSO reductase is readily generated either by partial reduction with a reagent such as reduced benzyl viologen or air reoxidation of fully reduced enzyme with signal accumulation as great as 0.3 spins/Mo (Figure 19). The EPR of the Mo(V) enzyme has been investigated studies with the enzyme from *Rhodobacter sphaeroides*[326] and *R. capsulatus*.[334] The signal observed with the *R. sphaeroides* enzyme at pH 7 has $g_{1,2,3} = 1.988, 1.977, 1.961$, with a single strongly coupled, solvent-exchangeable proton ($a_{av} = 10.5$ G).[326] In addition there is evidence for a poorly defined high-pH form of the signal that lacks proton hyperfine. The well-defined g values associated with the low-pH form of DMSO reductase are in the range observed for the various Mo(V) EPR signals of sulfite oxidase and

nitrate reductase, and the results were initially taken to reflect a MoO_2 unit in oxidized DMSO reductase and a MoO(OH) unit in the reduced form, as with these other enzymes. In light of the recent crystal structure of DMSO reductase it is clear that the oxidized enzyme is a $Mo^{VI}O$ species. The obvious similarities in Mo(V) EPR properties between DMSO reductase and the members of the sulfite oxidase class of molybdenum enzymes suggest that the single oxo group of DMSO reductase persists in the Mo(V) valence state rather than becoming protonated, with the result that the EPR-active state is a Mo^{V}═O species in all cases. This conclusion must be tempered, however, by concern that one of the dithiolene ligands to the molybdenum may have dissociated from the metal in the course of sample preparation, possibly replaced by hydroxide from solvent (see below). Following the integrated EPR signal intensity at room temperature in the course of potentiometric titrations, the reduction potentials for the Mo(VI/V) and Mo(V/IV) couples of the *R. sphaeroides* DMSO reductase have been determined to be +144 mV and +160 mV, making the midpoint potential for the molybdenum center of the enzyme one of the highest for a biological Mo═O center.[326]

Work with DMSO reductase from *R. capsulatus* has confirmed that the enzyme is fundamentally the same as in *R. sphaeroides*, and extended the above EPR studies.[334] A family of discrete "high-*g*" forms of the signal observed initially with the *R. sphaeroides* protein have been described, including signals which differ in the time scale of their development in the course of the reaction of enzyme with dithionite as reductant ($g_{1,2,3}$ of 1.9935, 1.9829, 1.9683 and 1.9904, 1.9819, 1.9651, respectively, in bicine buffer, pH 8.2). The signal observed is also seen to vary modestly with buffer conditions in a manner reminiscent of sulfite oxidase and nitrate reductase.[334] In addition to these signals, all of which exhibit the previously observed strong coupling to a solvent-exchangeable proton, EPR signals are also observed in the as-isolated enzyme which lack obvious coupling to protons. Signals generated by reoxidation of enzyme that has been fully reduced in the presence of ethylene glycol also lack such coupling.[330] All these signals exhibit g_{av} in the range 1.977−1.983, and contrast sharply with two other "split" signals with g_{av} below 1.96 that are observed upon incubation of the enzyme with excess dithionite for short periods of time in bicine buffer. The first of these signals quite closely resembles the Mo(V) EPR signal exhibited by xanthine oxidase subsequent to inactivation with cyanide and has $g_{1,2,3} = 1.9702, 1.9678, 1.9560$. The second signal has $g_{1,2,3} = 1.9759, 1.9540, 1.9359$ and is conspicuously shifted to lower *g*. Such a decrease in *g* value is expected on substitution of sulfur with oxygen in the equatorial plane of the molybdenum coordination sphere, and it has been concluded that this is likely to be the fundamental structural difference between the species giving rise to the low-*g* and high-*g* families of EPR signals in DMSO reductase.[334] In light of the crystallographic information presently available, indicating that the molybdenum is coordinated to two cofactor dithiolenes and that upon reduction one sulfur ligand may be lost, it appears likely that the low-*g* signals may arise from enzyme in which one (or more) of the dithiolene sulfur ligands to the molybdenum have dissociated to be replaced by oxygen derived from solvent. It is not clear at present, however, whether this change in molybdenum coordination upon reduction is mechanistically relevant or is an artifact of sample preparation. As has been pointed out,[334] the diversity of EPR signals exhibited by DMSO reductase must at minimum reflect an unusual degree of conformational flexibility in the molybdenum coordination sphere of the enzyme.

Closely related to these DMSO reductases in reaction catalyzed are biotin-d-sulfoxide reductases from *Escherichia coli*[335,336] and *Rhodobacter sphaeroides*,[337] which catalyze the reduction of the *S*-oxide (presumably the product of spontaneous oxidation of the natural product) as shown in Scheme 24. A thioredoxin-like iron protein has been suggested as the physiological electron donor for the enzyme.[335] Both proteins are ~80 kDa and the genes encoding them (*bisC*) have been sequenced;[336,337] the inferred sequences are found to share considerable sequence homology with one another and with the DMSO reductase from *R. sphaeroides*[73] (see Figure 16). Quite recently, *E. coli* has been shown to possess not one but two genes encoding biotin-d-sulfoxide reductases.[338] In addition to the *bisC* gene encoding the predominant form of the enzyme, a *bisZ* gene has been identified that exhibits 65% sequence identity to *bisC*. Deletion of *bisZ* removes all residual biotin-d-sulfoxide reductase activity in *bisC*$^-$ strains of *E. coli*, and appears to be responsible for pseudoreversion in at least some temperature-sensitive mutants of *bisC*. The spectroscopic and mechanistic properties of these enzymes have yet to be investigated in any detail, however. Even less well characterized are separate methionine-*S*-oxide[339] and protein:methionine-*S*-oxide[340,341] reductases, which have not yet been demonstrated to be molybdenum-containing enzymes but may well prove to be given the similarity of the reaction catalyzed to the enzymes considered above.

Scheme 24

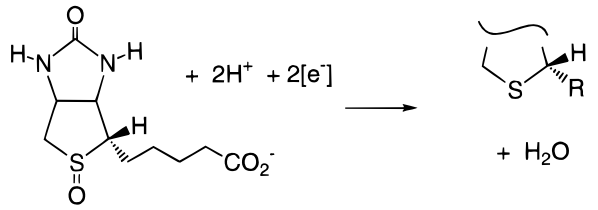

B. DMSO Reductase from *Escherichia coli*

By contrast to the soluble, periplasmic DMSO reductase of *Rhodobacter*, the DMSO reductase of *E. coli* is a terminal respiratory oxidase whose reduction of DMSO at the expense of menaquinol is coupled to generation of a transmembrane proton gradient across the inner membrane of the organism,[342] as indicated in Scheme 25. The *E. coli* enzyme consists of three polypeptides of 82.6, 23.6, and 22.7 kDa, the gene products of the *dmsABC* operon.[139,140] The enzyme is closely related to, but genetically distinct from. trimethylamine-*N*-oxide reductase and three separate dissimilatory nitrate reductases from the

Scheme 25

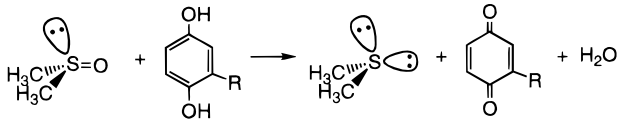

same organism (see below). The genes encoding the corresponding DMSO reductase from *Hemophilus influenzae* have recently been cloned and found to be comparably organized, with a high degree of homology to the *E. coli* system.[343] A DMSO reductase broadly similar to the *E. coli* enzyme has also been isolated from the anaerobic rumen bacterium *Wolinella succinogenes*.[344]

The molybdenum center of the *E. coli* DMSO reductase is found in the DmsA subunit, which exhibits considerable sequence homology (29% sequence identity) to the *Rhodobacter sphaeroides* DMSO reductase discussed above.[72] Like the periplasmic DMSO reductases from *Rhodobacter*,[20] the pterin cofactor found in the *E. coli* membrane-bound DMSO reductase is present as the guanine dinucleotide.[345] In addition to the molybdenum center, the N-terminal portion of DmsA possesses a cluster of cysteine residues that appear to represent a vestigial Fe-S cluster. This region exhibits considerable homology to the molybdenum-containing NapA subunit of one of the nitrate reductases of *E. coli*, which has been shown to possess a 4Fe-4S center (see below). On the basis of the most recent work, however, it appears that a 4Fe-4S cluster is not present in the wild-type DmsA subunit. Mutation of one of the cluster cysteines (Cys 38) to either a serine or alanine leads to assembly of a 3Fe-4S cluster having a high reduction potential (+170 mV for C38S and +140 mV for C38A).[346,347] It has so far proven impossible, however, to create a 4Fe-4S cluster in DmsA that would be comparable to the Fe-S center found in the molybdenum-containing subunit of the NapA nitrate reductase from *E. coli*. This N-terminal cluster of cysteine residues is absent altogether in the *Rhodobacter* DMSO reductases and the biotin-*S*-oxide reductases.

The DmsB subunit of the *E. coli* DMSO reductase possesses four distinct sequence motifs for binding 4Fe-4S iron−sulfur clusters,[348] and upon reduction yields EPR signals typical of bacterial ferredoxin-like clusters.[143,349] The DmsB subunit in fact exhibits very substantial sequence homology to several other multicluster Fe-S proteins, including the NarH and NarY subunits of the *E. coli* nitrate reductases A and Z (see below).[140] With the molybdenum-containing DmsA subunit, DmsB constitutes the membrane-extrinsic catalytic portion of the enzyme, extending into the cytoplasm from the inner membrane.[351,352] In this sense it is compartmentalized differently than the periplasmically localized soluble DMSO reductase from *Rhodobacter*. The DmsC subunit is an integral membrane protein that serves to anchor the catalytic dimer[351,352] and appears to possess the site of menaquinol oxidation. The topology of the DmsC subunit has been examined using gene fusion technology, and a model proposed that involves a set of eight transmembrane α helices with both N- and C-termini exposed to the periplasmic space, along with three prominent interhelix loops. Consistent with expectation, a predominance of the positively charged amino acid residues are found in the shorter cytoplasmic loops of the subunit.[353]

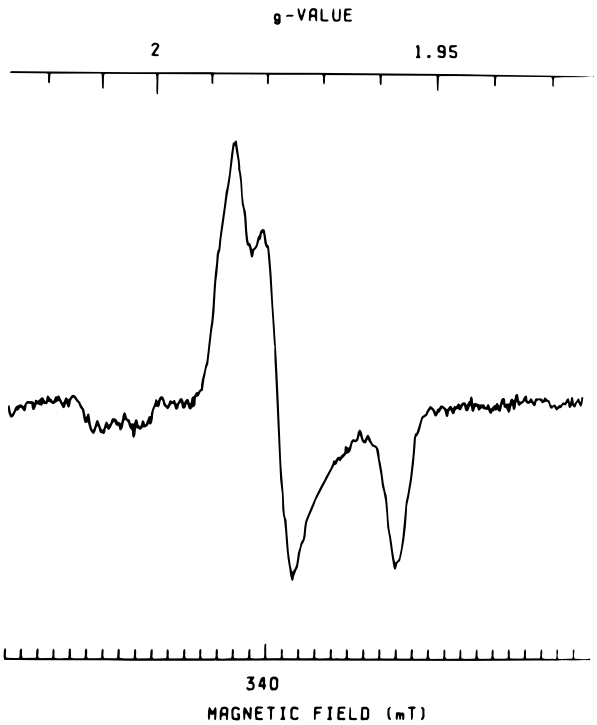

Figure 20. Mo(V) EPR signal of DMSO reductase from *Escherichia coli*. The signal was generated by electrochemically poising purified enzyme at −51 mV in 0.1 M MOPS buffer, pH 7.0, and corresponds to $g_{1,2,3}$ = 1.987, 1.976, 1.960. Reproduced from Cammack and Weiner,[143] with permission.

The molybdenum center of the purified respiratory DMSO reductase has been examined by EPR and is found to exhibit a rhombic, unsplit Mo(V) EPR signal with $g_{1,2,3}$ = 1.987, 1.976, 1.960, when the enzyme is poised potentiometrically at −51 mV (Figure 20);[143] this signal is reminiscent of the "high-*g* unsplit" signals seen with the periplasmic DMSO reductase from *Rhodobacter capsulatus*.[335] The midpoint potential for the molybdenum center, as determined by following by the formation and decay of the Mo(V) EPR signal as observed at 120 K, is preparation dependent, but in the range −50 to −80 mV at pH 7.0.[143] As with other molybdenum centers, the midpoint potential is found to be pH dependent, decreasing some 180 mV as the pH is increased from 5.5 to 9.0, consistent with the uptake of two protons with reduction of the molybdenum from the VI to the IV oxidation state.[143] In conjunction with the extensive sequence homology between the molybdenum subunit of the respiratory DMSO reductase and the periplasmic DMSO reductase (Figure 16), the EPR results indicate that the molybdenum centers of the two proteins are fundamentally very similar.

The iron−sulfur centers of the DmsB subunit have also been investigated by EPR.[143] The reduction potentials, for example, are found to be in the range −50 to −330 mV (−50, −120, −240, and −330 mV in the high specific activity "Sephacryl form" of the enzyme at pH 7.0, and also in the enzyme present in enriched membranes). As is true of the molybdenum center, the reduction potentials of the iron−sulfur centers are found to be both preparation and pH dependent.[143] Site-directed mutagenesis of one of the

conserved cysteines, Cys 102, has been undertaken and found to convert one of the 4Fe-4S clusters of DmsB (the third from the N-terminus of the protein) into a 3Fe-4S cluster analogous to that found in the closely related Fe-S subunit of the *E. coli* dissimilatory nitrate reductase.[349,350] Somewhat surprisingly, all four mutations made at Cys 102 result in loss of menaquinol:DMSO oxidoreductase activity (with no corresponding loss of benzylviologen:DMSO oxidoreductase activity), indicating that the Fe-S center that has been modified is required for effective electron transfer from the site of menaquinol oxidation in DmsC to the molybdenum center of DmsA for DMSO reduction. Using dysprosium^{III}EDTA as a magnetic probe on the solvent accessibility of the oxidized 3Fe-4S cluster of DmsB by virtue of its effect on the EPR line shape and relaxation properties, it has been estimated that the cluster lies deeply buried (~20 Å) in the DmsAB catalytic dimer.[352]

C. The Dissimilatory Nitrate Reductases

The eukaryotic assimilatory nitrate reductases (and their prokaryotic counterparts from organisms such as *Anacystis nidulans*[354]) described in section IV.B possess molybdenum centers related to that found in sulfite oxidase. The dissimilatory (or respiratory) nitrate reductases from a variety of bacterial and archaeal sources, on the other hand, are more closely related to the respiratory DMSO reductase of *E. coli* and, as discussed in section II.B, have active sites that are in all likelihood Mo(VI)O centers with two dithiolene cofactor ligands. These enzymes couple the reduction of nitrate to nitrite at the expense of menaquinol to generate a transmembrane proton gradient[355] (Scheme 26), and like the DMSO

Scheme 26

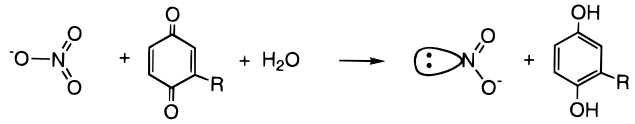

reductase from *E. coli* are comprised of three subunits: a membrane-extrinsic dimer that consists of separate molybdenum- and Fe-S-containing subunits, and an integral membrane anchor. As with the *E. coli* DMSO reductase, the catalytic dimer of nitrate reductase is cytoplasmic rather than periplasmic.[355] *E. coli* expresses three different nitrate reductases: the predominant nitrate reductase A form, inducible under anaerobic conditions, is encoded by the *narGHJI* operon,[141] a minor nitrate reductase Z form, expressed under aerobic growth,[356] is encoded by the *narZYWV* operon,[357] and a third periplasmic form encoded by the *napEDABC* operon (see below). The first two operons are very closely related genetically, with inferred sequence identity in the homologous gene products ranging from 69% to 87%, depending on the subunit. Both nitrate reductase A and Z exhibit significant sequence homology to the DmsABC subunits of the *E. coli* respiratory DMSO reductase discussed in the previous section (the NarG/Z, NarH/Y, and NarI/V subunits have M_r 145, 60, and 20 kDa, respectively, and correspond to the DmsA, DmsB, and DmsC subunits of the *E. coli* DMSO reductase). The two nitrate reductases are sufficiently similar that antibodies raised against one form partially cross-react with the other.[356] In addition to the genes *narGHI*/*narZYV* that encode the three structural subunits for the two nitrate reductases, each nitrate reductase operon possesses a fourth gene, *narJ*/*narW*,[357,358] encoding a protein that is not incorporated into the functional enzyme but which is strictly required for proper maturation of functional nitrate reductase.[359,360] This gene product, for which there is no counterpart in the *dms* operon, is probably not involved in cofactor assembly or insertion but instead facilitates assembly/stabilization of the NarGH (or NarZY) catalytic dimer, and/or its attachment to the NarI (or NarV) membrane anchor.[358−360] In the work described below, it is presumably the predominant nitrate reductase A form of the *E. coli* enzyme that is under investigation when no specific designation is made.

In contrast to the membrane-bound DMSO reductases discussed in the previous section, both dissimilatory nitrate reductases A and Z from *E. coli* possess a *b*-type cytochrome component in their transmembrane subunits.[361−364] In the case of nitrate reductase A, this membrane-bound cytochrome has been purified and spectrally characterized[364] and, as indicated in section II.B, recently found to possess tightly bound menaquinone in addition to the heme prosthetic group.[144] The heme group dominates the absorption spectrum of both oxidized and reduced nitrate reductase, with a Soret maximum for oxidized enzyme at 414 nm shifting to 427 nm upon reduction.[364] In the $\alpha\beta$ region of the spectrum, the oxidized enzyme exhibits a broad absorption maximum at ~530 nm that resolves into discrete α and β bands at 558 and 529 nm, respectively, upon reduction. The absolute absorption spectrum of the iron−sulfur clusters and the spectral change upon reduction are unresolved in the presence of the heme, but the isolated NarGH catalytic dimer has been shown to possess an absorption spectrum typical of Fe-S-containing proteins.[365,366] No EPR signal attributable to the ferric cytochrome *b* has been observed, although these are frequently quite weak. Surprisingly, simple reduction of the enzyme results in the generation of a $g \approx 2$ signal with the characteristic well-resolved three-line hyperfine of a pentacoordinate ferrous heme-NO species.[367] This signal undoubtedly arises from the *b*-type cytochrome of the membrane anchor subunit, with the nitric oxide presumably generated *in situ* upon addition of reducing equivalents to the enzyme in the presence of nitrate.

In addition to preparations of the intact nitrate reductase A,[365,368,369] it is possible to solubilize the NarGH catalytic dimer, consisting of the molybdenum- and Fe-S-containing subunits of nitrate reductase, either by detergent[363] or heat treatment[370,371] in a form that retains dye:nitrate oxidoreductase activity. The X-ray absorption data obtained with both the solubilized[315] and intact[372] *E. coli* nitrate reductase indicate the presence of only a single Mo=O group (at 1.66 to 1.73 Å), which is lost upon reduction. Consistent with the structure shown in Figure 1, the remainder of the molybdenum coordination sphere consists of three to four sulfur (or chloride) ligands at ~2.34 Å, and a longer Mo−O(N)

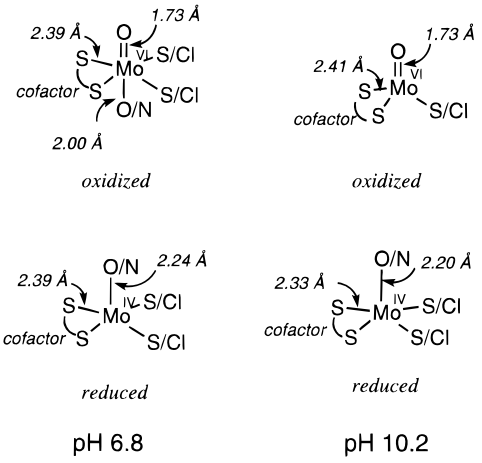

Figure 21. Summary of XAS results for the molybdenum center of nitrate reductase from *Escherichia coli* in both oxidized (top) and reduced (bottom) forms at pH 6.8 (left) and 10.2 (right). The structures shown and bond distances given represent a composite of data from Cramer *et al.*[314] and George *et al.*[372] (The latter work reported noninteger amounts of Mo=O in all but the pH 6.8 oxidized sample.)

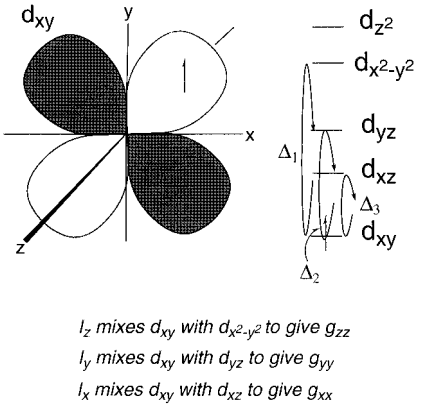

Figure 22. The ligand field of Mo(V), indicating the origin of *g* anisotropy arising from mixing of d orbitals due to spin−orbit coupling along the three principal axes of the system. Shift in *g* along each axis from the value for the free electron is inversely proportional to the energy separation Δ for the relevant pair of d orbitals.

ligand at ∼2.1 Å. The Mo−S distances in nitrate reductase are found to decrease upon reduction of the molybdenum center (by approximately 0.06 Å in the case of nitrate reductase), and the number of sulfur/chloride ligands increases by one.[372] Although both XAS studies have been hampered by the difficulty of obtaining fully oxidized Mo(VI) in the enzyme samples, overall the data are consistent with the crystallographic results obtained with the *Rhodobacter sphaeroides* DMSO reductase in which the molybdenum center of the enzyme exists as a monooxo-*bis*(dithiolene) complex in the oxidized state and a *des*oxo-*bis*(dithiolene) complex in the reduced state. It is possible that the Mo=O group of oxidized enzyme is replaced by an anion such as chloride upon reduction of the enzyme, as indicated in Figure 21. It is to be noted that Ser 147 of the *R. sphaeroides* DMSO reductase (which coordinates directly to the molybdenum) is conserved in NarG (Ser 228, see Figure 16) and is undoubtedly coordinated to the molybdenum, although not always detected by XAS.

The EPR properties of *E. coli* nitrate reductase have also been extensively investigated. With regard to the molybdenum center, well-defined "low-pH" and "high-pH" forms have been identified in the solubilized nitrate reductase, which represent a conjugate acid/base pair having a pK_a of 8.26 in the absence of chloride (interestingly, catalytic activity exhibits a comparable pH profile, with the enzyme rapidly losing activity above pH 8.5).[367] The "low-pH" Mo(V) EPR signal has $g_{1,2,3} = 1.9989, 1.9855, 1.9628$ with strong coupling to a single, solvent-exchangeable proton having $a_{av} \sim 10$ G; the "high-pH" signal has $g_{1,2,3} = 1.9870, 1.9805, 1.9612$,[367] and possesses a more weakly coupled proton with $a_{av} = 3$ G.[373] Complexes with nitrate ($g_{1,2,3} = 2.002, 1.986, 1.964$) and nitrite ($g_{1,2,3} = 1.999, 1.985, 1.964$) are also observed which presumably represent analogs of the catalytically relevant E_{red}−S and E_{ox}−P complexes (both complexes are actually found in two alternate forms that differ very slightly in *g* value and hyperfine splitting[373]). Well-defined EPR signals from other anion complexes of nitrate reductase have also been observed, most importantly those with chloride and fluoride; the latter signal exhibits the expected coupling to ^{19}F with $a_{av} = 7$ G, indicating that the bound anion is coordinated to the molybdenum.[373] When nitrate reductase is prepared in $H_2{}^{17}O$, there is no evidence for strong coupling to oxygen, as is observed with sulfite oxidase, consistent with the XAS results indicating the presence of Mo^V=O rather than Mo^V—OH in the signal-giving species.[372]

Although the earlier EPR results obtained with *E. coli* nitrate reductase were originally discussed in the context of a comparison with sulfite oxidase, it is clear with the advantage of hindsight that its EPR properties more closely resemble those of the more recently described *R. sphaeroides* DMSO reductase. The "low-pH" signal of the *E. coli* nitrate reductase, for example, is quite reminiscent of the "high-*g* split" signal of DMSO reductase,[335] although the signals are not identical. In general enzymes of the sulfite oxidase family give EPR spectra which, while rhombic, are more closely pronate with $g_2 \approx g_3$, while the EPR spectra of the DMSO reductase family (at least the "high-*g*" signals) tend to be either fully rhombic with g_2 intermediate between g_1 and g_3 (*e.g.*, the "high-*g*" split signal of DMSO reductase, and the "low-pH" signal of *E. coli* nitrate reductase) or more oblate with $g_1 \approx g_2$ (*e.g.*, the "high-*g*" unsplit signals of DMSO reductase or the "high-pH" signal of the *E. coli* nitrate reductase). Assuming that the symmetry of the molybdenum coordination sphere in these enzymes can be arrived at by distortion of an octahedral coordination geometry and that a Mo=O group defining the molecular z axis is present in all Mo(V) species, the ligand field diagram given in Figure 22 is obtained, with *g* anisotropy along the *x*, *y*, and *z* coordinates (corresponding to g_3, g_2, and g_1, respectively) due to mixing of the half-filled d_{xy} orbital with d_{xz}, d_{yz}, and $d_{x^2-y^2}$, respectively, driven by spin-orbit coupling. The implication is that in members of the sulfite oxidase family d_{yz} lies closer in energy to d_{xz}, while for members of the DMSO reductase family d_{yz} is either intermediate between d_{xz} and $d_{x^2-y^2}$, or closer to the latter.

The iron−sulfur centers of *E. coli* nitrate reductase have also been examined using a variety of spectro-

Scheme 27

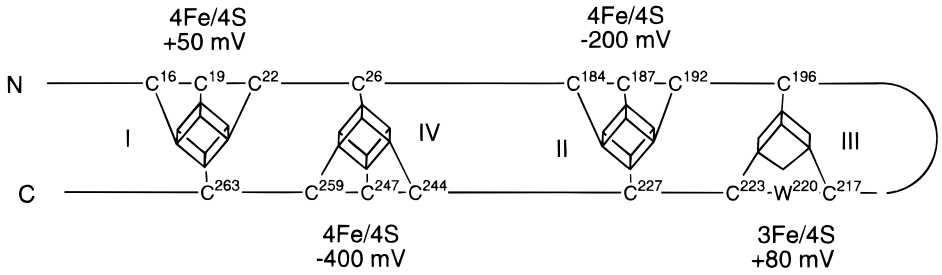

scopic techniques. The solubilized NarGH catalytic dimer exhibits an EPR signal in its oxidized form[367,374] that is reminiscent of the signals arising from the oxidized 3Fe-4S clusters of the seven-iron ferredoxins from *Azotobacter vinelandii*,[375] *Desulfovibrio gigas*,[376] and *Thermus thermophilus*.[377] By contrast to the quite featureless absorption spectrum of the solubilized nitrate reductase, the low-temperature MCD of the oxidized enzyme exhibits a series of strong, alternating positive and negative features in the region 300−600 nm whose features are strongly reminiscent of the spectral signature of a 3Fe-4S cluster, and the magnetization of the observed MCD spectrum indicates a ground-state $S = {}^1/_2$ system.[374] Thus, although the integrated signal intensity of the oxidized Fe-S signal of nitrate reductase is only half that expected, it is evident that the enzyme possesses a 3Fe-4S cluster. Comparison of the sequence of NarH with that of DmsB and related iron−sulfur proteins indicates that it is the third cluster from the N-terminus, which possesses a tryptophan in place of the second iron-coordinating cysteine in the cluster, that lacks the fourth iron.[140] The remaining three Fe-S clusters are of the 4Fe-4S variety and are EPR-active when reduced.[367,374,378] The form of the 4Fe-4S EPR signals observed with nitrate reductase is very sensitive to the level of reduction, and it has been suggested that the clusters are weakly magnetically coupled to one another.[374] At incomplete levels of reduction, quite distinct EPR signals having $g_{1,2,3}$ = 2.041, 1.945, 1.921 and 2.003, 1.888, 1.870 have been observed.[367]

The reduction potentials of the several redox-active centers in the *E. coli* nitrate reductase have also been examined.[379,380] Following the intensity of the "low pH" EPR signal as a function of the poised system potential, it is found that the molybdenum center possesses potentials for the Mo(VI/V) and Mo(V/IV) couples of +220 and +180 mV, respectively, giving a midpoint potential of +200 mV at pH 7.14, and +190 and +80 at pH 8.3 (E_{mid} = 135 mV).[379] The data suggest the coupling of two protons to the uptake of two electrons by the molybdenum center in this pH range. The molybdenum potentials are even higher than is observed in sulfite oxidase and nitrate reductase, and are consistent with the role of the center in catalyzing the terminal reaction of respiratory electron transfer. The 3Fe-4S cluster and one of the 4Fe-4S clusters have quite high reduction potentials, +80 and +50 mV, respectively,[379,380] while the two remaining 4Fe-4S clusters have much lower potentials of −200 and −400 mV,[380] more typical of bacterial ferredoxin centers. Site-directed mutagenesis studies in which the cysteine residues responsible for iron coordination in the NarH protein have been systematically mutated indicate that the second 4Fe-4S cluster of the protein is the one with a potential of −200 mV,[381] and the first is the 4Fe-4S cluster with the +50 mV potential,[382] permitting the iron−sulfur clusters of NarH to be assigned as indicated in Scheme 27.[383] Mutation of either Cys 16, 19,[382] or 263[383] in the N-terminal cluster I results in loss of the high-potential cluster, and mutation of Cys 26 results in loss of the low-potential cluster IV,[385] constituting the principal support for the designation that the fourth cysteine of the first and fourth clusters participate in binding of different centers than the first three cysteines of each cluster. A comparable arrangement is proposed for clusters II and III, with the overall conclusion being that the four Fe-S centers are arranged in pairs: I/IV and II/III consistent with the observed pattern of magnetic interactions between the centers in the reduced enzyme.[383] It appears that the II/III pair constitute the more important clusters from a structural standpoint. Protein with individual mutations in clusters I or IV properly folds and incorporates the other three iron−sulfur clusters, whereas mutations in clusters II or III tend to yield enzyme devoid of all the iron−sulfur clusters.[382] *E. coli* strains carrying mutations in cluster I or IV remain able to grow anaerobically on nitrate as the respiratory acceptor of reducing equivalents, although at a somewhat reduced level compared to wild-type, and both benzyl viologen:nitrate and formate:nitrate oxidoreductase activities in crude cell extracts are reduced to about 15% of wild-type.[382] Mutations in cluster I, but not IV, selectively abolish the ability of the protein to catalyze menaquinone-mediated reduction of nitrate, despite the cytochromes *b* being reduced, strongly suggesting that cluster I is an obligatory component of electron transport from the cytochromes to the molybdenum center.[383] (Although it has been demonstrated in this work that the amount of gene expression as determined by immunoblotting is comparable for each of the mutants investigated, the fact that NarGHI and NarZYV cross-react immunologically make it unclear at present as to whether nitrate reductase A is able to function at a reduced level in the absence of cluster I in NarH, or whether nitrate reductase A activity is lost completely and the organism circumvents lethality by recruiting a partially effective nitrate reductase Z under anaerobic growth conditions on nitrate.) A comparison of the A and Z forms of nitrate reductase from *E. coli* indicate that the two high-potential Fe-S clusters of nitrate reductase Z have reduction potentials some 100 mV lower than is observed with nitrate reductase A.[381] It has been pointed out that for both forms of the *E. coli* nitrate reductase, only the two high-potential Fe-S centers are thermodynamically poised to mediate electron transfer from the quinone pool (−80 mV) to

the molybdenum center (+200 mV) and on to nitrate (+420 mV).[381] The role of the low-potential iron−sulfur centers in nitrate reductase is at present unknown.

As with other members of this family, there has been little mechanistic work on the *E. coli* nitrate reductase, although its steady-state kinetic behavior has been examined. Using ubiquinol as electron donor, the intact enzyme is found to operate via a ping-pong mechanism and exhibit the following kinetic parameters: $k_{cat} = 7.2\ s^{-1}$, $K_m^{ubiquinol} = 78\ \mu M$, $K_m^{nitrate} = 2\ \mu M$, and a $k_{cat}/K_m^{nitrate} = 5 \times 10^6\ M^{-1}\ s^{-1}$.[369] The kinetic behavior is consistent with a two-site system in which ubiquinol and nitrate bind to different sites of the enzyme, as expected on the basis of the known structure of the enzyme. Using only the soluble NarGH catalytic dimer of nitrate reductase in the reduction of nitrate by reduced viologen dyes (which appear to reduce the molybdenum center directly rather than via the iron−sulfur clusters) it is found that k_{cat} is much reduced, with a value of $0.26\ s^{-1}$, and a $K_m^{nitrate}$ of over 200 μM.[384] It is likely that physiological turnover is rate limited by the reaction with nitrate, while turnover with artificial dyes is rate limited by the reduction of the enzyme by the nonphysiological dyes.

As with the DMSO reductases, periplasmic forms of dissimilatory nitrate reductase have been isolated from species such as *Paracoccus denitrificans*[385] (previously designated *Thiosphaera pantotropha*[386]), *Alcaligenes eutropha*,[387] *Rhodobacter sphaeroides*,[388,389] and *R. capsulatus*[390,391] (this last enzyme being distinct from the periplasmic DMSO reductase from that species[137]). The *P. denitrificans* enzyme is encoded by the *napEDABC* gene cluster and consists of a 93 kDa molybdenum- and 4Fe-4S-containing NapA subunit,[385,392] a 16 kDa double cytochrome c_{552} NapB subunit[385] and a 27 kDa four-heme cytochrome *c* that appears to span the inner bacterial membrane. The *P. denitrificans* NapA shows 71% sequence identity to the *A. eutropha* NapA, and 66% identity with a comparable periplasmic nitrate reductase recently shown to be encoded by *E. coli* (by the *aeg*-46.5 gene locus).[394,395] The NapABC nitrate reductase from *R. sphaeroides* exhibits comparable sequence identity to *the A. eutrophus* protein, and has been shown to possess an organization entirely analogous to that of the *P. denitrificans* NapABC nitrate reductase.[389] NapA from all these sources exhibits significant sequence homology to the *E. coli* NarG and *R. sphaeroides* DMSO reductase but have a cysteine residue (Cys 181 in the case of *P. denitrificans*) at the position of the serine residue found in these enzymes.[393] The N-terminus of NapA from *P. denitrificans* possesses a four-cysteine motif that provides the coordination sites for a 4Fe-4S center and, on the basis of sequence homology, may also be present in the *E. coli* formate dehydrogenases. In the case of NapA the assignment of the 4Fe-4S EPR signal that arises upon reduction of the NapAB catalytic dimer to NapA ($g_{1,2,3} = 2.03, 1.94, 1.89$)[392] is straightforward as the NapB is a cytochrome, rather than Fe-S-containing enzyme. Interestingly, one of the cysteines in the cluster is replaced by a histidine in the NarG and NarZ subunits, and it is not clear at present whether this site represents a 3Fe-4S cluster (or a histidine-substituted analog) in these dissimilatory nitrate reductases, or whether this substitution destroys the cluster altogether. As indicated above, it appears that the homologous cysteine residues in the DmsA subunit of the *E. coli* DMSO reductase do not constitute an Fe-S center analogous to that found in NapA. The reduction potential of the NapA Fe-S cluster is −160 mV at pH 7.4,[392] indicating that it is thermodynamically unlikely to become reduced by the quinone pool (at ∼−80 mV) but has instead been suggested to serve as a conduit for electron transfer between the cytochromes of NapB and the molybdenum center of NapA.[392] NapB possesses two *c*-type cytochrome binding motifs, and has 45% sequence identity with the NapB from *A. eutrophus* and 41% identity with the NapB gene product from the *E. coli aeg*-46.5 locus.[392] The two cytochromes of the *P. denitrificans* enzyme are distinguishable on the basis of their reduction potentials, with values of +77 and −18 mV at pH 7.0.[385] The NapC membrane anchor subunit from *P. denitrificans* and related systems may exist in complex with the NapE gene product, which on the basis of hydropathy analysis is expected to be an integral membrane protein. It has been suggested that the complex represents a quinol oxidase that provides the physiological reducing equivalents to the soluble NapAB catalytic dimer.[393]

Like the *R. capsulatus* DMSO reductase and the *E. coli* nitrate reductase A, the periplasmic nitrate reductase from *Paracoccus denitrificans* exhibits a variety of EPR signals attributable to its molybdenum center when partially reduced with sodium dithionite.[396] These include "high-*g* split" forms observed in the absence ($g_{1,2,3} = 1.9990, 1.9905, 1.9810$) or presence ($g_{1,2,3} = 1.9988, 1.9892, 1.9820$) of nitrate, both of which exhibit moderate coupling to a solvent-exchangeable proton (a_{av} = 5.6 and 5.1 G, respectively). A "pseudo-rapid" form with considerable similarity to the signal exhibited by xanthine oxidase and related enzymes ($g_{1,2,3} = 1.9957, 1.9688, 1.9607$) is observed (at low pH in the presence of chloride) that exhibits coupling to two solvent-exchangeable protons (a_{av} = 14 G for the strongly coupled proton). Finally, an unusual Mo(V) EPR signal, designated "very high-*g*" split, is also seen upon prolonged incubation with dithionite in the presence of cyanide. This signal possesses $g_{1,2,3} = 2.0229, 2.0000, 1.9940$ and moderate coupling to a single nonexchangeable proton (a_{av} = 7.9 G). Nitrate is unable to oxidize the reduced Fe-S clusters of the enzyme in the form giving rise to this EPR signal, and it presumably arises from an inhibitory complex of cyanide at the molybdenum center. It has recently been demonstrated that the "high-*g* split" Mo(V) EPR signal is detectable in intact cells of *Paracoccus denitrificans*[397] and is in all likelihood the most mechanistically relevant of the signals that have been detected.

D. The Formate Dehydrogenases and Polysulfide Reductase

As with the nitrate reductases, there are several different classes of formate dehydrogenases. The pyridine nucleotide-dependent enzyme from aerobes is typically a soluble enzyme devoid of molybdenum

and other redox-active cofactors (although the NAD^+-linked formate dehydrogenase from *Methylosinus trichosporum* possesses not only molybdenum but also a flavin cofactor and several iron−sulfur centers,[398] and the protein from *Clostridium thermoaceticum* is a tungsten−Fe-S enzyme[399]); the enzyme from anaerobic bacteria, on the other hand, is membrane bound and typically found to possess molybdenum, while the enzyme from archaeal sources may contain either a molybdenum or tungsten center.[400] In this section, discussion is restricted to the latter molybdenum-containing enzymes.

Among the enzymes considered in the present review, the reaction catalyzed by formate dehydrogenase is unusual in that, at least formally, it does not involve oxygen atom transfer but rather represents the cleavage of a C−H bond with concomitant formation of a C=O bond from C−OH, as indicated in Scheme 28. Given the reaction catalyzed, it is

Scheme 28

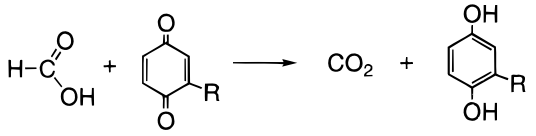

evident that the enzyme need not act via an oxygen atom-transfer mechanism, and given that some formate dehydrogenases appear to possess a Mo=S rather than Mo=O[146] in their active sites (as discussed in section II.B), it may be that the reaction proceeds directly via hydride transfer to yield CO_2 directly (Scheme 29A). It is also possible, however, that the

Scheme 29

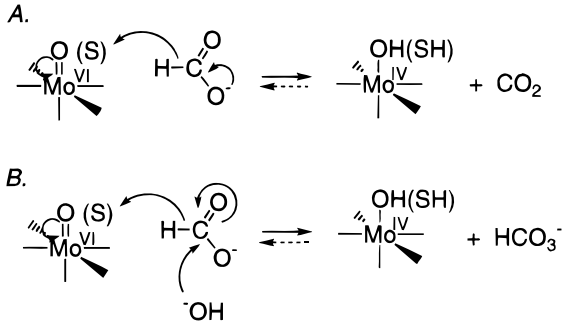

reaction proceeds in a manner analogous to that of the hydroxylase family of molybdenum enzymes, in which formate is oxidatively hydroxylated to carbonic acid, followed by dehydration to give water and CO_2 (Scheme 29B). In such a mechanism, however, the origin of the oxygen atom incorporated into carbonic acid is problematic, at least in the cases of the enzymes containing Mo=S.

The considerable similarity in amino acid sequence between formate dehydrogenases and other enzymes of the DMSO reductase family (Figure 16) strongly suggests that these enzymes possess the *bis*(dithiolene) coordination to the metal that is the defining feature of this class of molybdenum enzymes. The proximal oxygen atom donor cannot be a Mo=O if the enzyme possesses a sulfur (or selenium) at its apical position, but it is conceivable that the reaction catalyzed is sufficiently facile that a solvent molecule present in the active site need not be activated by coordination to the active site molybdenum.

The genome of *Escherichia coli* encodes no fewer than three discrete formate dehydrogenases. Formate dehydrogenase H, encoded by the *fdhF* gene,[401] is part of the formate−hydrogen lyase complex that is expressed under anaerobic conditions in the absence of an exogenous electron acceptor. Under anaerobic growth conditions in the presence of nitrate, *E. coli* also expresses an inducible formate dehydrogenase N that is encoded by the *fdnGHI* operon[402,403] and linked not only in expression but also in function to nitrate reductase A: the two enzymes constitute a formate:nitrate oxidoreductase system that represents the principal respiratory pathway in cells growing under anaerobic conditions on nitrate. Electron transfer between the two enzymes is mediated by the intramembrane quinone pool.[400,404] In addition to this inducible formate dehydrogenase N, a constitutively expressed formate dehydrogenase Z, the product of the *fdoGHI* operon, has recently been characterized that appears to act in conjunction with nitrate reductase Z in facilitating the transition from aerobic to anaerobic growth.[405,406] Formate dehydrogenase Z is found to bear the same strong genetic relationship to the N form that nitrate reductase Z bears to nitrate reductase A.[406] In all three formate dehydrogenases, the catalytic subunit is exposed to the periplasmic space and the reaction catalyzed is coupled to generation of a transmembrane proton gradient and ATP biosynthesis.

The 80 kDa FdhF formate dehydrogenase H[401] exhibits considerable sequence homology to the somewhat larger (110 kDa) FdnG/FdoG subunits of formate dehydrogenase N and Z of *E. coli*,[407] and the formate dehydrogenases of *Methanobacterium formicicum* and *Wolinella succinogenes*.[403] The *E. coli* formate dehydrogenases also share somewhat less homology to the DmsA subunit of the DMSO reductase and the NarG/Z subunits of the dissimilatory nitrate reductases of *E. coli*[140] (Figure 16). In particular, six segments of homology have been identified,[140,141] one of which appears to represent a consensus sequence that has been suggested to be a pterin-binding domain common to all these enzymes.[140] The homology between the FdhF, FdnG, and FdoG proteins includes a cysteine-rich region that may constitute a 4Fe-4S cluster as found in the *Paracoccus denitrificans* periplasmic nitrate reductase;[392,393] indeed the purified FdhF peptide is found to contain 3−4 g/atom Fe per mol. All three formate dehydrogenases possess a selenocysteine residue (residue 140 of FdhF, 196 of FdnG and FdoG),[401,403,406] encoded by a UGA "stop" codon positioned in a putative stem−loop region of the mRNA,[403,408] that is found in the position homologous to Ser 147 of the *R. sphaeroides* DMSO reductase. This selenocysteine been shown in the case of formate dehydrogenase H to coordinate directly to the molybdenum: when the Mo(V) EPR signals of natural abundance enzyme and that seen with enzyme isolated from cells grown on ^{77}Se are compared, strong anisotropic coupling is observed in the ^{77}Se sample.[149] It is interesting to note that the homologous position in the formate dehydrogenases from *Methanobacterium formicicum*[409] and *Wolinella succinogenes*[410] is occupied by

a normal cysteine residue,[86,403] but that substitution of cysteine for selenocysteine in the *E. coli* formate dehydrogenase H, at least, not only perturbs the EPR signal of the Mo(V) center, but also results in a 300-fold decrease in catalytic activity (see below).[149] Conditions for the stabilization of formate dehydrogenase H have recently been reported along with preliminary crystallographic analysis of both oxidized and reduced forms of the enzyme,[411] and it is anticipated that a structure will be forthcoming in the very near future.

Formate dehydrogenases N and Z have constitutions quite similar to their nitrate reductase counterparts. In addition to the 110 kDa FdnG/FdoG subunit that possess the molybdenum center (and in all likelihood an N-terminal 4Fe-4S cluster), these proteins possess a 32 kDa FdnH/FdoH subunit containing four Fe-S clusters and a 20 kDa membrane-anchoring FdnI/FdoI subunit that contains a *b*-type cytochrome. Each of these subunits exhibits significant sequence homology to its nitrate reductase NarGHI/NarZYV counterpart.[403,406]

What mechanistic work as has been done with formate dehydrogenase has been done for the most part with the H form (the FdhF protein). A variety of anions, particularly nitrate and chloride, are found to inhibit the enzyme, as does azide (the significant advantage of this last inhibitor is that it prevents inactivation of the enzyme by molecular oxygen).[148] The pH optimum of formate dehydrogenase H is 7.5 (using benzyl viologen as electron acceptor), but the pH optimum for enzyme stability is ~6.0 and it rapidly loses activity above pH 7.5. At the optimum pH of 7.5, steady-state analysis of formate dehydrogenase H using benzyl viologen as reducing substrate yields parallel lines as expected for a ping-pong mechanism, with $k_{cat} = 2800\ s^{-1}$, $K_m^{formate} = 26$ mM, and $k_{cat}/K_m = 1.1 \times 10^5\ M^{-1}\ s^{-1}$ [413] (by way of comparison, formate dehydrogenase N gives $k_{cat} = 560\ s^{-1}$, $K_m^{formate} = 120\ \mu M$, and $k_{cat}/K_m = 4.7 \times 10^7\ M^{-1}\ s^{-1}$ [368]). There is a negligible primary isotope effect on k_{cat} with formate dehydrogenase H, consistent with the notion that the chemistry of the reductive half-reaction with formate is not rate limiting.[413] By contrast, the primary isotope effect on k_{cat}/K_m is ~4.3, consistent with C−H bond cleavage taking place in the course of the first committed step of the reductive half-reaction. Formate dehydrogenase H catalyzes the exchange of ^{14}C-labeled formate with atmospheric CO_2 in the absence of a supply of external reducing equivalents, indicating that the reductive half-reaction is freely reversible under the assay conditions.[413] This result contrasts with that seen with formate dehydrogenase N, in which no exchange is observed, indicating a functionally irreversible reductive half-reaction.[368] Compared to the calculated K_d for formate of 100 mM, it is found that azide is a quite tight-binding inhibitor of formate dehydrogenase H ($K_i = 80\ \mu M$), and it has been suggested that azide represents a transition state analog for the enzyme.[413]

As indicated above, substitution of cysteine for the selenocysteine of the molybdenum coordination sphere of formate dehydrogenase H results in a 300-fold decrease in k_{cat}, to $9\ s^{-1}$. This is due to a 1000-fold decrease in the rate constant for reduction of the enzyme by formate, which makes the reductive half-reaction essentially completely rate limiting. Under these circumstances it is found that the primary isotope effect on k_{cat} and k_{cat}/K_m become the same.[412] There is also a ~10-fold reduction in the rate of reoxidation of the enzyme by benzyl viologen (to 830 s^{-1}) and a 3-fold reduction in the K_m for formate (to 9 mM) upon substitution of cysteine for selenocysteine in formate dehydrogenase H. This substitution also has a very significant effect on the Mo(V) EPR signal exhibited by formate dehydrogenase H upon reduction by formate: the native enzyme has $g_{1,2,3} =$ 2.094, 2.001, 1.989 whereas the cysteine mutant has $g_{1,2,3} \approx$ 1.994, 1.987, 1.974.[149] (It is to be noted that *g* values for the cysteine mutant were not actually reported in this work; the values given here were calculated assuming an experimental microwave frequency comparable to that used in recording the EPR signal for wild-type enzyme, for which *g* values but not the microwave frequency were reported. For this reason there could be a substantial systematic error in the *g* values cited here for the cysteine mutant, but the inferred line shape accurately represents the experimental data.) The Mo(V) signal observed with wild-type formate dehydrogenase H exhibits no coupling to solvent-exchangeable protons and has the same basic form as the "very rapid" signal observed with xanthine oxidase, but with *g* values that are 0.04 to 0.07 higher. At present, a number of possibilities exist as to the structure of the signal-giving species, depending on whether the pterin cofactor coordination to the metal is stable or whether one of the two dithiolenes that may be inferred on the basis of the sequence similarity is labile. It appears most likely that the functional center remains *bis*(dithiolene) coordinated, with selenocysteine and Mo−OH or an anion from buffer also present. It is noteworthy that the EPR signal of the formate-reduced native enzyme resembles that exhibited by substrate-reduced nicotinate hydroxylase from *Clostridium barkeri* ($g_{1,2,3} =$ 2.067, 1.982, 1.974), another molybdenum-containing enzyme that possesses selenium coordinated to the active site metal.[307]

The formate dehydrogenases from *Methanobacterium formicicum*[409] and *Wolinella succinogenes*[410] exhibit considerable homology to the *E. coli* formate dehydrogenases (Figure 16), but possess a cysteine residue in place of the selenocysteine found in the *E. coli* proteins. The formate dehydrogenase from the archaeon *M. formicicum* is an $\alpha\beta$ dimer with subunits of 76 and 44 kDa possessing a cofactor constitution distinct from the other enzymes considered in the present section.[410] The larger subunit possesses considerable homology to the molybdenum-containing subunits of the formate dehydrogenases and nitrate reductases, but has a second Fe-S motif to the C-terminal side of the molybdenum-binding region that is not present in the other proteins. The smaller subunit has three 4Fe-4S binding motifs (rather than four), the N- and C-terminal of which are related to the clusters of the [4Fe-4S]x2 bacterial ferredoxins. FAD is also a redox cofactor for the *M. formicicum* formate dehydrogenase[414] and is required for hydride transfer to the physiological oxidant for the enzyme, the 5-deazaflavin cofactor F_{420} that is found in

methanogens (and which is used as the source of low-potential reducing equivalents to reduce CO_2 to methane).[414,416] It is not known which of the two subunits the FAD cofactor binds. The Mo(V) EPR signal seen upon reduction of the enzyme by formate is similar in line shape to that seen for the cysteine mutant of the *E. coli* formate dehydrogenase H discussed above, with $g_{1,2,3} = 2.0180, 2.0030, 1.9940$.[417] The EPR signal arising from the *M. formicicum* enzyme shows evidence for moderate coupling to a pair of $I = {}^1/_2$ nuclei, but the splitting is not fully resolved in the reported spectrum. The appearance and decay of this signal in the course of a potentiometric titration yields reduction potentials for the Mo(VI/V) and Mo(V/IV) couples of −330 and −470 mV, respectively.[417] It is thus clear that the molybdenum center of the *M. formicicum* formate dehydrogenase is operating in a considerably lower redox regime than is the case with other members of this family of molybdenum enzymes, comparable to that seen with members of the molybdenum hydroxylase family.

The formate dehydrogenase from *Wolinella succinogenes* (formerly genus *Vibrio*) bears a greater similarity to the *E. coli* enzyme than does the enzyme from *Methanobacterium formicicum*. The *Wolinella* enzyme is encoded by the *fdhABCD* operon, of which *fdhA*, *B*, and *C* represent the structural genes for the enzyme (101, 22, and 32 kDa, respectively); like the NarJ/W protein, FdhD presumably plays a role in the maturation of the functional enzyme.[410] Sequence identity between FdhA from *W. succinogenes* with other members of this family of molybdenum enzymes ranges from 40% with FdhF from *E. coli* to 17% for the *E. coli* NarG protein. As with the *M. formicicum* enzyme, the pterin cofactor is present as the guanine dinucleotide.[415] Sequence identity between *W. succinogenes* FdhB and *E. coli* DmsB is ∼35%. Somewhat surprisingly, no significant homology is observed between the *Wolinella* FdhC and any other component of other molybdenum-containing enzymes, although it is known to possess a *b*-type cytochrome[418] and thought to represent a membrane anchor as are the third subunits of the nitrate reductases and formate dehydrogenases. The formate dehydrogenase of *W. succinogenes* is oriented with respect to the inner membrane of the bacterium in such a way that the FdhAB catalytic dimer is exposed to the periplasmic space.[419]

In *Wolinella*, formate dehydrogenase is linked to either fumarate reductase or polysulfide reductase to generate a transmembrane proton gradient.[420] This last enzyme is also a molybdenum-containing protein closely related to other members of the DMSO reductase family of enzymes and is distinct from the periplasmic sulfide dehydrogenase of the organism.[421] With formate dehydrogenase, polysulfide reductase catalyzes the overall reaction shown in Scheme 30.

Scheme 30

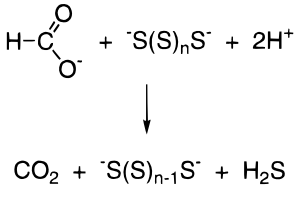

It appears that electron transfer between the two enzymes is direct, in all likelihood via diffusional electron transfer between the two membrane components and involving the low-potential cytochrome *b* of the formate dehydrogenase,[418] rather than mediated by the intramembrane quinone pools.[420] Polysulfide reductase is encoded by the *psrABC* gene locus, with *psrA* encoding a large (81 kDa) molybdenum-containing subunit with an inferred amino acid sequence that possesses 16−26% overall sequence identity with other members of this family of enzymes, particularly in the previously identified regions of conserved sequence.[422] Although the molybdenum-containing PsrA subunit possesses the N-terminal cysteine cluster for a putative 4Fe-4S cluster in common with the *E. coli* formate dehydrogenases, however, the highest degree of homology in the molybdenum-binding portion of the subunit is shared with the biotin-*S*-oxide reductase from *E. coli*, which lacks the iron−sulfur cluster. As with the formate dehydrogenase from *W. succinogenes*, the pterin cofactor of the molybdenum center in the organism's polysulfide reductase is found as the guanine dinucleotide.[415] The second and third genes of the *psr* operon encode a smaller (∼21 kDa) Fe-S-containing subunit and a membrane anchor possessing a *b*-type cytochrome (34 kDa), respectively,[420] entirely analogous to the dissimilatory nitrate reductases or formate dehydrogenases described above. On the basis of the existence of a putative leader sequence in common with FdhA from *W. succinogenes*, it is likely that polysulfide reductase is oriented in the inner membrane such that the PsrAB catalytic dimer faces into the periplasm rather than the cytoplasm.[422] As with the FdhC cytochrome *b*-containing subunit of the *W. succinogenes* formate dehydrogenase, the PsrC gene product does not possess significant sequence homology to the membrane anchors of other bacterial molybdenum enzymes[415] and indeed has not yet been established to possess a heme.

E. Formylmethanofuran Dehydrogenase

Formylmethanofuran dehydrogenase catalyzes the reversible oxidative dehydrogenation of formylmethanofuran to methanofuran ($\Delta E^{\circ\prime} = -497$ mV) (Scheme 31). The enzyme participates in methanogenesis in

Scheme 31

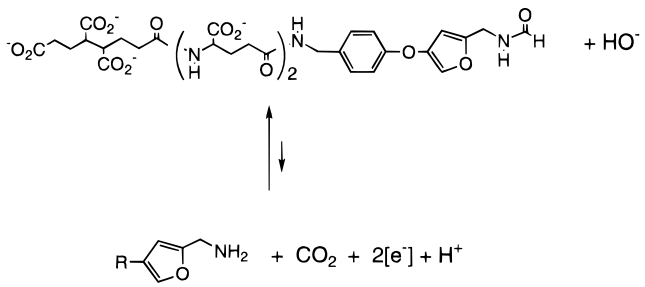

the archaeal sources in which it is found, with the enzyme operating in the reverse of the direction shown in Scheme 25 to catalyze the first step in CO_2 reduction to methane (the formyl group being transferred to tetrahydromethanopterin for subsequent reduction to methane).[423] The enzyme has been

characterized from *Methanosarcina barkeri, Methanobacterium thermoautotrophicum,* and *Methanobacterium wolfei,* and has been found as either a molybdenum- or tungsten-containing enzyme. In *M. thermoautotrophicum,* the molybdenum enzyme is an $\alpha\beta$ dimer, the product of the *fmdAB* gene locus, while the tungsten enzyme is an $\alpha\beta\gamma\delta$ tetramer whose subunits are encoded by the first four genes of the *fwdEFGDACB* operon.[424] The molybdenum-containing enzyme from *M. barkeri* is encoded by an analogous *fmdEFACDB* operon.[425] In all cases, the FmdA (or FmdB in the case of *M. barkeri*) and FwdB peptides are the Mo- or W-containing subunits, and in *M. wolfei* FmdA and FwdB possess identical amino termini;[426] the same has been reported for the enzyme from *M. thermoautotrophicum*.[424] The entire *fmd* and *fwd* operons been reported for *M. barkeri*[425] and *T. thermoautotrophicum*.[423]

The structural genes for the formylmethanofuran dehydrogenases are found to be *fwdABCD,* with *fwdE* and *fwdG* encoding a pair of 2x[4Fe-4S] iron−sulfur proteins (17.8 and 8.6 kDa, respectively).[424] *fwdF* encodes a 38.6 kDa iron−sulfur protein containing eight copies of a CxxCxxCxxxC motif that is reminiscent of the somewhat larger polyferredoxin from the same organisms. This polyferredoxin is not present in the as-isolated FwdABCD formylmethanofuran dehydrogenase from *M. thermoautotrophicum*,[427] but has recently been shown to be an integral subunit of the FmdABCD enzyme isolated from *M. barkeri*.[425] The tungsten-containing FwdB subunit is 47.4 kDa and shares 27% sequence identity with the corresponding molybdenum-containing formate dehydrogenase from *T. thermoautotrophicum,* including a putative N-terminal 4Fe-4S cluster and a cysteine at the metal-coordinating position homologous to Ser 147 residue of the *R. sphaeroides* DMSO reductase, strongly implicating similar structures for the active sites of these tungsten enzymes and the DMSO reductase family of molybdenum enzymes.[423] Sequence homology between the Mo- and W-containing subunits is largely restricted, however, to the N-terminal 210 residues (which includes the metal-binding portion of the sequence) and there may be substantive differences in overall protein folding patterns. There is negligible sequence homology between the *T. thermoautotrophicum* formylmethanofuran dehydrogenase and the tungsten-containing *Pyrococcus furiosus* aldehyde:ferredoxin oxidoreductase, no doubt due in part to the fact that the former binds one of several dinucleotide forms (MGD, MAD, MHD in the ratio 1.0/0.4/0.1) of the pterin cofactor[21] while the latter binds the mononucleotide form.[13] (The *M. barkeri* formylmethanofuran dehydrogenase, on the other hand, possesses exclusively the guanine dinucleotide form of the pterin cofactor.[428]) Evidence that the tungsten- and molybdenum-containing formylmethanofuran dehydrogenases are very closely related consists of the observation that the molybdenum enzyme of *M. wolfei* is expressed as a tungsten-containing form when the archaeon is grown on molybdenum-deficient medium,[429,430] and similarly the tungsten-containing enzyme from *T. thermoautotrophicum* can be isolated in a molybdenum-containing form.[145] The tungsten-substituted Mo-enzyme is functional, with only a ~25% decrease in k_{cat} compared to the molybdenum form of the enzyme in the reaction with formylmethanofuran.[430] On the other hand, the tungsten-substituted enzyme has only 1/100 the activity toward formate (an alternate substrate) compared to the native molybdenum-containing enzyme. These observations contrast with other work in which it has been shown that tungsten cannot substitute for molybdenum in the formylmethanofuran dehydrogenase from *M. barkeri*.[431]

The molybdenum-containing formylmethanofuran dehydrogenase from all three methanogens is strongly inhibited by cyanide, and in a manner that is reversible by sulfide,[145,426] and it is likely that the enzyme possesses a Mo=S group, as is found in at least some of the formate dehydrogenases. This behavior contrasts with that for the tungsten-substituted form of the enzyme, which is unaffected by cyanide.[145] At present it is not clear whether this is due to the presence of a W=O group substituting for a Mo=S, although such an interpretation is consistent with the data. The molybdenum center of the *M. thermoautotrophicum* enzyme exhibits a Mo(V) EPR signal with $g_{1,2,3} = 2.005, 1.979, 1.946$ when reduced with formylmethanofuran,[145] and the enzyme from *M. thermoautotrophicum* [145] and *M. wolfei* [426] exhibit comparable signals. In addition, all three enzymes exhibit a closely related Mo(V) signal that appears to arise from inactive enzyme.[145] Substitution of tungsten for molybdenum in the *M. wolfei* formylmethanofuran dehydrogenase gives rise to a W(V) signal with $g_{1,2,3} = 2.049, 2.012, 1.964$ that exhibits the characteristic hyperfine arising from the 24% natural abundance ^{173}W ($I = {}^1/_2$).[426] It is thus clear that the active sites of the DMSO reductase family of molybdenum enzymes and at least some of the tungsten enzymes are closely related.[18,429]

VI. Concluding Remarks

Study of the mononuclear molybdenum enzymes has entered a new stage in the development of our understanding of their structure and mechanism of action. The broad classification of these enzymes proposed here has been greatly facilitated by the development in the past five years of a substantial database of protein amino acid sequences inferred from cloned genes of an extremely diverse range of organisms. At the same time, the new crystal structures of the *Desulfovibrio gigas* aldehyde oxidoreductase and *Rhodobacter sphaeroides* DMSO reductase promise the ability to put this sequence information in a structural context, from the standpoint of both the structure of the active site molybdenum center and its relationship to other redox-active centers within a polypeptide of an increasingly well-understood folding pattern. The principal questions regarding the mechanism of action of these enzymes are now more clearly framed than ever before, and it can be expected that issues such as the resolution of the reaction mechanism of the molybdenum hydroxylases (*i.e.*, hydroxylation via the action of an electrophilic Mo=O or nucleophilic Mo−OH_2) will soon be experimentally addressed in a definitive way. Although only two molybdenum enzymes of the type considered here (formate dehydrogenase H from *E. coli* and the human sulfite oxidase) have been successfully overexpressed to any

satisfactory degree, the development of suitable expression systems can reasonably be expected in the near future. This will open the way for a more specific analysis of the mechanistic role of particular amino acid residues in the active site and a critical evaluation of the several mechanistic aspects of each of these enzymes that remain to be answered (concerning the mechanistic roles, for example, of those residues—serine, cysteine, selenocysteine—that presumably coordinate the molybdenum). Coupled with kinetic and spectroscopic techniques that are increasingly available for the study of these enzymes (EPR, XAS, resonance Raman, magnetic circular dichroism, electron spin echo, and ENDOR), the relationship of the physical and electronic structures of the active sites of these enzymes to their chemical reactivity and catalytic properties is expected to become increasingly well understood. Finally, it is to be anticipated that work in the near future will provide greater insight into the evolutionary and structural relationship of the molybdenum enzymes to those that possess tungsten in their active sites.

Acknowledgments

The author acknowledges the following for permission to reproduce previously published data: R. C. Bray, W. H. Campbell, R. Huber, K. V. Rajagopalan, and J. H. Weiner. In addition, the following are thanked for communication of data prior to publication: M. W. W. Adams, R. C. Bray, G. N. George, J. Enemark, R. Huber, D. Rees, R. A. Rothery, and J. H. Weiner. Thanks are also due to M. Brody, T. Conrads, L. Huang, A. Lazarev, K. Ratnam, and E. Wilson in the author's laboratory for help in preparing figures and tables presented in this review. Finally, the author acknowledges R. C. Bray, J. H. Enemark, and M. Kirk for their comments on a preliminary version of the manuscript. Work in the author's laboratory is supported by grants from the National Insititutes of Health (AR38917 and GM52322) and the National Science Foundation (MCB 94-20185).

Note Added in Proof

Pietsch and Hall (*Inorg. Chem.* **1996**, *35*, 1273) have recently conducted an important theoretical study of dioxomolybdenum complexes that is directly relevant to the reaction mechanism of the sulfite oxidase family of mononuclear molybdenum enzymes. Using a MoO_2 model system whose metal coordination sphere is completed by a pair of ammonia and thiolate ligands (in an octahedral coordination geometry), these workers have analyzed in detail oxygen atom transfer from the dioxo−Mo (VI) parent to trimethylphosphine using Møller−Plesset perturbation theory at the MP3 level. It is found that in order to optimize orbital overlap for efficient O−P bond formation (and also to populate the Mo d_{xy} orbital in the course of formal reduction of the metal), it is necessary that the attacking phosphine lone pair approach the complex normal to the MoO_2 plane with a Mo−O−P angle of approximately 130°. In order to facilitate release of the phosphine oxide subsequent to formation of the O−P bond of product, the system must pass through an intermediate in which the M−O bond is rotated by 90° such that the O−Mo−O−P unit is now coplanar. This rotation results in a weakening of the Mo−OPR_3 bond prior to dissociation of the phosphine oxide from the metal and at the same time a strengthening of the remaining ("spectator") metal oxo to give a formal Mo≡O triple bond. The spectator oxygen effect in this system (which possesses two thiolate ligands to the metal) thus plays a significant role in stabilizing this intermediate. Displacement of the phosphine oxide by water is found to proceed via an associative mechanism in which water binds to the molybdenum in the *xy* plane (the *z* axis being defined by the Mo≡O bond), transiently expanding the coordination number of the metal. The free energies of activation for the reaction of the $Mo^{VI}O_2$ complex with phosphine and subsequent displacement of the phosphine oxide from the $Mo^{IV}O$ complex by water are found to be quite modest, 15 and 19 kcal/mol, respectively, consistent with the established catalytic power of the MoO_2 complexes discussed here. These results demonstrate that in a theoretical model system which closely resembles the likely ligand coordination environment and geometry of the sulfite oxidase family the spectator oxo effect described by Rappé and Goddard plays a significant role in dictating the chemistry of the system.

References

(1) Howard, J. B.; Rees, D. C. *Chem. Rev.* **1996**, *96*, 2965 (this issue).
(2) Burgess, B. K.; Lowe, D. J. *Chem. Rev.* **1996**, *96*, 2983 (this issue).
(3) Holm, R. H. *Chem. Rev.* **1987**, *87*, 1401.
(4) Hille, R. *Biochim. Biophys. Acta* **1994**, *1184*, 143.
(5) Bray, R. C. In *The Enzymes*; Boyer, P. D., Ed.; **1975**, *12*, 299.
(6) Romão, M. J.; Archer, M.; Moura, I.; Moura, J. J. G.; LeGall, J.; Engh, R.; Schneider, M.; Hof, P.; Huber, R. *Science* **1995**, *270*, 1170.
(7) Schindelin, H.; Kisker, C.; Hilton, J.; Rajagopalan, K. V.; Rees, D. C. *Science* **1996**, *272*, 1615.
(8) Johnson, J. L.; Hainline, B. E.; Rajagopalan, K. V. *J. Biol. Chem.* **1980**, *255*, 1783.
(9) Johnson, J. L.; Rajagopalan, K. V. *Proc. Natl. Acad. Sci. U.S.A.* **1982**, *79*, 6856.
(10) Johnson, J. L.; Hainline, B. E.; Rajagopalan, K. V.; Arison, B. H. *J. Biol. Chem.* **1984**, *259*, 5414.
(11) Kramer, S. P.; Johnson, J. L.; Ribiero, A. A.; Millington, D. S.; Rajagopalan, K. V. *J. Biol. Chem.* **1987**, *262*, 16357.
(12) Taylor, E. C.; Reiter, L. A. *J. Am. Chem. Soc.* **1989**, *111*, 285.
(13) Taylor, E. C.; Ray, P. S.; Darwish, I. S. *J. Am. Chem. Soc.* **1989**, *111*, 7664.
(14) Chan, M. K.; Mukund, S.; Kletzin, A.; Adams, M. W. W.; Rees, D. C. *Science* **1995**, *267*, 1463.
(15) Johnson, J. L.; Rajagopalan, K. V.; Mukund, S.; Adams, M. W. W. *J. Biol. Chem.* **1993**, *268*, 4848.
(16) Burgmayer, S. J. N.; Stiefel, E. I. *J. Am. Chem. Soc.* **1986**, *108*, 8310.
(17) Fischer, B.; Schmalle, H.; Dubler, E.; Schäfer, A.; Visconti, M. *Inorg. Chem.* **1995**, *34*, 5726.
(18) Pilato, R. S.; Stiefel, E. I. In *Bioinorganic Catalysis*; Reedjik, J., Ed.; Dekker: New York, 1993; pp 131−188.
(19) Adams, M. W. W. *FEMS Microbiol Rev.* **1996**, *18*, 5.
(20) Johnson, J. L.; Bastian, N. R.; Rajagopalan, K. V. *Proc. Natl. Acad. Sci. U.S.A.* **1990**, *87*, 3190.
(21) Johnson, J. L.; Rajagopalan, K. V.; Meyer, O. *Arch. Biochem. Biophys.* **1990**, *283*, 542.
(22) Börner, G.; Karrasch, K.; Thauer, R. K. *FEBS Lett.* **1991**, *290*, 31.
(23) Pateman, J. A.; Cove, D. J.; Rever, B. M.; Roberts, D. B. *Nature* **1964**, *201*, 58.
(24) Rajagopalan, K. V. *Adv. Enzymol.* **1991**, *64*, 215.
(25) Rajagopalan, K. V.; Johnson, J. L. *J. Biol. Chem.* **1992**, *267*, 10199.
(26) Shanmugan, K. T.; Stewart, V.; Gunsalus, R. P.; Boxer, D. H.; Cole, J. A.; Chippaux, M.; DeMoss, J. A.; Giordano, G.; Lin, E. C. C.; Rajagopalan, K. V. *Mol. Microbiol.* **1992**, *6*, 3452.
(27) Plunkett, G., III; Burland, V.; Daniels, D. L.; Blattner, F. R. *Nucleic Acids Res.* **1993**, *21*, 3391.
(28) Palmer, T.; Vasishta, A.; Whitty, P. W.; Boxer, D. H. *Eur. J. Biochem.* **1994**, *222*, 687.
(29) Palmer, T.; Santini, C.-L.; Iobbi-Nivol, C.; Eaves, D. J.; Boxer, D. H.; Giordano, G. *Mol. Microbiol.* **1996**, *20*, 875.

(30) Johnson, J. L.; Indermauer, L. W.; Rajagopalan, K. V. *J. Biol. Chem.* **1991**, *266*, 12140.
(31) Miller, J. B.; Scott, D. J.; Amy, N. K. *J. Bacteriol.* **1987**, *169*, 1853.
(32) Johann, S.; Hinton, S. M. *J. Bacteriol.* **1987**, *169*, 1911.
(33) Rosentel, J. K.; Healy, F.; Maupin-Furlow, J. A.; Lee, J. H.; Shanmugan, K. T. *J. Bacteriol.* **1995**, *177*, 4857.
(34) Mouncy, N. J.; Mitchenall, L. A.; Pau, R. N. *J. Bacteriol.* **1995**, *177*, 5294.
(35) Rech, S.; Deppenmeier, U.; Gunsalus, R. P. *J. Bacteriol.* **1995**, *177*, 1023.
(36) Maupin-Furlow, J. A.; Rosentel, J. K.; Lee, J. H.; Deppenmeier, U.; Gunsalus, R. P.; Shanmugan, K. T. *J. Bacteriol.* **1995**, *177*, 4851.
(37) Rech, S.; Wolin, C.; Gunsalus, R. P. *J. Biol. Chem.* **1996**, *271*, 2557.
(38) Luque, F.; Mitchenall, L. A.; Chapman, M.; Christine, R.; Pau, R. N. *Mol. Microbiol.* **1993**, *7*, 447.
(39) Wang, G.; Angermüller, S.; Klipp, W. *J. Bacteriol.* **1993**, *175*, 3031.
(40) Rivers, S. L.; McNairn, E.; Blasco, F.; Giordano, G.; Boxer, D. H. *Mol. Microbiol.* **1993**, *8*, 1071.
(41) Hoff, T.; Schnorr, K. M.; Meyer, C.; Caboche, M. *J. Biol. Chem.* **1995**, *270*, 6100.
(42) Kamdar, K. P.; Shelton, M. E.; Finnerty, V. *Genetics* **1994**, *137*, 791.
(43) Lee, J. H.; Wendt, J. C.; Shanmugan, K. T. *J. Bacteriol.* **1990**, *172*, 2079.
(44) Aguilar, M.; Kalakoutskii, K.; Cádenas, J.; Fernández, E. *FEBS Lett.* **1992**, *307*, 162.
(45) Pitterle, D. M.; Rajagopalan, K. V. *J. Biol. Chem.* **1993**, *268*, 13499.
(46) Pitterle, D. M.; Johnson, J. L.; Rajagopalan, K. V. *J. Biol. Chem.* **1993**, *268*, 13506.
(47) Wuebbens, M. M.; Rajagopalan, K. V. *J. Biol. Chem.* **1993**, *268*, 13493.
(48) Johnson, J. L.; Wuebbens, M. M.; Rajagopalan, K. V. *J. Biol. Chem.* **1989**, *264*, 13440.
(49) Johnson, M. E.; Rajagopalan, K. V. *J. Bacteriol.* **1987**, *169*, 110.
(50) Doyle, W. A.; Burke, J. F.; Chovnick, A.; Dutton, F. L. Whittle; J. R. S.; Bray, R. C. *Eur. J. Biochem.* **1996**, *239*, 782.
(51) Irby, R. B.; Adair, W. L., Jr. *J. Biol. Chem.* **1994**, *269*, 23981.
(52) Wuebbens, M. M.; Rajagopalan, K. V. *J. Biol. Chem.* **1995**, *270*, 1082.
(53) Johnson, J. L.; Waud, W. R.; Rajagopalan, K. V.; Duran, M.; Beemer, F. A.; Wadman, S. K. *Proc. Natl. Acad. Sci. U.S.A.* **1980**, *77*, 3715.
(54) Johnson, J. L.; Wadman, S. K. In *Metabolic Basis of Inherited Disease*, 6th ed.; Scriver, C. R., Bandet, A. L., Sly, W. S., Valle, D., Eds.; McGraw-Hill: New York, 1989; Vol. 1, pp 1463−1475.
(55) Gardlik, S.; Rajagopalan, K. V. *J. Biol. Chem.* **1991**, *266*, 4889.
(56) Hille, R.; Massey, V. *J. Biol. Chem.* **1982**, *257*, 8898−8901.
(57) Huber, R.; Hof, P.; Duarter, R. O.; Moura, J. J. G.; Moura, I.; Liu, M.-Y.; LeGall, J.; Hille, R.; Archer, M.; Romão, M. *Proc. Natl. Acad. Sci. U.S.A.* **1996**, *93*, 8846.
(58) Eisenberg, R. Prog. *Inorg. Chem.* **1970**, *12*, 295.
(59) Stiefel, E. I.; Miller, K. F.; Bruce, A. E.; Corbin, J. L.; Berg, J. M.; Hodgson, K. O. *J. Am. Chem. Soc.* **1980**, *102*, 3624.
(60) Dance, I. G.; Wedd, A. G.; Boyd, I. W. *Aust. J. Biochem.* **1978**, *31*, 519.
(61) Tullius, T. D.; Kurtz, D. M., Jr.; Conradson, S. D.; Hodgson, K. O. *J. Am. Chem. Soc.* **1979**, *101*, 2776.
(62) Bordas, J.; Bray, R. C.; Garner, C. D.; Gutteridge, S.; Hasnain, S. *Biochem. J.* **1980**, *191*, 499.
(63) Cramer, S. P.; Hille, R. *J. Am. Chem. Soc.* **1985**, *107*, 8164.
(64) Cramer, S. P.; Wahl, R.; Rajagopalan, K. V. *J. Am. Chem. Soc.* **1981**, *103*, 7721.
(65) Massey, V.; Edmondson, D. E. *J. Biol. Chem.* **1970**, *245*, 6595.
(66) Stiefel, E. I. *Prog. Inorg. Chem.* **1977**, *21*, 1.
(67) George, G. N.; Hilton, J.; Rajagopalan, K. V. *J. Am. Chem. Soc.* **1996**, *118*, 1113.
(68) Hilton, J. C.; Rajagopalan, K. V. *Arch. Biochem. Biophys.* **1996**, *325*, 139.
(69) Mayer, J. M. *Inorg. Chem.* **1988**, *27*, 3899.
(70) Adams, M. W. W. Personal communication.
(71) Kletzin, A.; Mukund, S.; Kelley-Crouse, T. L.; Chan, M. K.; Rees, D. C.; Adams, M. W. W. *J. Bacteriol.* **1995**, *177*, 4817.
(72) Yamamoto, I.; Wada, N.; Ujiye, T.; Tachibana, M.; Matsuzaki, M.; Kajiwara, H.; Watanabe, Y.; Hirano, H.; Okubo, A.; Satoh, T.; Yamazaki, S. *Biosci. Biotechnol. Biochem.* **1995**, *59*, 1850.
(73) Barber, M. J.; van Valkenburgh, H.; Trimboli, A. J.; Pollock, V. V.; Neame, P. J.; Bastian, N. R. *Arch. Biochem. Biophys.* **1995**, *320*, 266.
(74) Hilton, J. C.; Rajagopalan, K. V. *Biochim. Biophys. Acta* **1996**, *1294*, 111.
(75) Cramer, S. P.; Gray, H. B.; Rajagopalan, K. V. *J. Am. Chem. Soc.* **1979**, *101*, 2772.
(76) Berg, J. M.; Hodgson, K. O.; Cramer, S. P.; Corbin, J. L.; Elsberry, A.; Periyadath, N.; Stiefel, E. I. *J. Am. Chem. Soc.* **1979**, *101*, 2774.
(77) George, G. N.; Kipke, C. A.; Prince, R. C.; Sunde, R. A.; Enemark, J. H.; Cramer, S. P. *Biochemistry* **1989**, *28*, 5075.
(78) Stiefel, E. I. *Proc. Natl. Acad. Sci. U.S.A.* **1973**, *70*, 988.
(79) Sullivan, E. P., Jr.; Hazzard, J. T.; Tollin, G.; Enemark, J. H. *Biochemistry* **1993**, *32*, 12465.
(80) Neame, P. J.; Barber, M. J. *J. Biol. Chem.* **1989**, *264*, 20894.
(81) Barber, M. J.; Neame, P. J. *J. Biol. Chem.* **1990**, *265*, 20912.
(82) Garde, J.; Kinghorn, J. R.; Tomsett, A. B. *J. Biol. Chem.* **1995**, *270*, 6644.
(83) Garrett, R. M.; Rajagopalan, K. V. *J. Biol. Chem.* **1996**, *271*, 7387.
(84) Hoffmüller, P.; Frunzke, K.; Meyer, O. *Bioforum* **1991**, *14*, 47.
(85) Meyer, O.; Frunzke, K.; Tachil, J.; Volk, M. In *Molybdenum Enzymes, Cofactors and Model Systems*; Stiefel, E. I., Coucouvanis, D., Newton, W. E., Eds.; ACS Symposium Series 535; American Chemical Society: Washington, DC, 19xx; p 50.
(86) Wootton, J. C.; Nicolson, R. E.; Cock, J. M.; Walters, D. E.; Burke, J. F.; Doyle, W. A.; Bray, R. C. *Biochim. Biophys. Acta* **1991**, *1057*, 157.
(87) Meyer, O. *J. Biol. Chem.* **1982**, *257*, 1333.
(88) Meyer, O.; Jacobity, S.; Kruger, B. *FEMS Microbiol. Rev.* **1986**, *39*, 161.
(89) Moura, J. J. G.; Xavier, A. V.; Bruschi, M.; LeGall, J.; Hall, D. O.; Cammack, R. *Biochem. Biophys. Res. Commun.* **1976**, *72*, 782.
(90) Ichida, K.; Amaya, Y.; Noda, K.; Minoshima, S.; Hosoya, T.; Sakai, O.; Shimizu, N.; Nishino, T. *Gene* **1993**, *133*, 279.
(91) Amaya, A.; Yamazaki, K.; Sato, M.; Noda, K.; Nishino, T.; Nishino, T. *J. Biol. Chem.* **1990**, *265*, 14170.
(92) Krüger, B.; Meyer, O. *Eur. J. Biochem.* **1986**, *157*, 121.
(93) Schübel, U.; Kraut, M.; Mörsdorf, G.; Meyer, O. *J. Bacteriol.* **1995**, *177*, 2197.
(94) Tshisuaka, B.; Kappl, R.; Hüttermann, J.; Lingens, F. *Biochemistry* **1993**, *32*, 12928.
(95) Peschke, B.; Lingens, F. *Biol. Chem. Hoppe-Seyler* **1991**, *372*, 1081.
(96) Schach, S.; Tshisuaka, B.; Fetzner, S.; Lingens, F. *Eur. J. Biochem.* **1995**, *232*, 536.
(97) Lehmann, M.; Tshisuaka, B.; Fetzner, S.; Röger, P.; Lingens, F. *J. Biol. Chem.* **1994**, *269*, 11254.
(98) Bauer, G.; Lingens, F. *Biol. Chem. Hoppe-Seyler* **1992**, *373*, 699.
(99) Fetzner, S.; Lingens, F. *Biol. Chem. Hoppe-Seyler* **1993**, *374*, 363.
(100) Sauter, M.; Tshisuaka, B.; Fetzner, S.; Lingens, F. *Biol. Chem. Hoppe-Seyler* **1993**, *374*, 1037.
(101) Dilworth, G. L. *Arch. Biochem. Biophys.* **1982**, *219*, 30.
(102) Nagel, M.; Andreesen, J. R. *Arch. Microbiol.* **1990**, *154*, 605.
(103) Freudenberg, W.; König, K.; Andreesen, J. R. *FEMS Microbiol Lett.* **1988**, *52*, 13.
(104) Grether-Beck, S.; Iglio, G. L.; Pust, S.; Schilz, E.; Decker, K.; Brandsch, R. *Mol. Microbiol.* **1994**, *13*, 929.
(105) Xiang, Q.; Edmondson, D. E. *Biochemistry* **1996**, *35*, 5441.
(106) Koenig, K.; Andreesen, J. R. *J. Bacteriol.* **1990**, *172*, 5999.
(107) Wright, R. M.; Vaitaitis, G. M.; Wilson, C. M.; Repine, T. B.; Terada, L. S.; Repine, J. E. *Proc. Natl. Acad. Sci. U.S.A.* **1993**, *90*, 10690.
(108) Glatigny, A.; Scazzocchio, C. *J. Biol. Chem.* **1995**, *270*, 3534.
(109) Xu, P.; Hueckstaedt, T. P.; Harrison, R.; Hoidal, J. R. *Biochem. Biophys. Res. Commun.* **1994**, *199*, 998.
(110) Turner, N. A.; Doyle, W. A.; Ventom, A. M.; Bray, R. C. *Eur. J. Biochem.* **1995**, *232*, 646.
(111) Li Calzi, M.; Raviolo, C.; Ghibaudi, E.; De Gioia, L.; Salmona, M.; Cazzaniga, G.; Kurosaki, M.; Terao, M.; Garattini, E. *J. Biol. Chem.* **1995**, *270*, 31037.
(112) Saksela, M.; Raivio, K. O. *Biochem. J.* **1996**, *315*, 235.
(113) Berglund, L.; Rasmussen, J. T.; Andersen, M. D.; Rasmussen, M. S.; Petersen, T. E. *J. Dairy Sci.* **1996**, *79*, 198.
(114) Cohen, H. J.; Fridovich, I. *J. Biol. Chem.* **1971**, *246*, 367.
(115) Kessler, D. L.; Rajagopalan, K. V. *J. Biol. Chem.* **1972**, *247*, 6566.
(116) McLeod, R. M.; Farkas, W.; Fridovich, I.; Handler, P. *J. Biol. Chem.* **1961**, *236*, 1841.
(117) Toghrol, F.; Southerland, W. M. *J. Biol. Chem.* **1983**, *258*, 6762.
(118) Cohen, H. J.; Fridovich, I. *J. Biol. Chem.* **1971**, *246*, 359.
(119) Cohen, H. J.; Fridovich, I.; Rajagopalan, K. V. *J. Biol. Chem.* **1971**, *246*, 374.
(120) Cohen, H. J.; Betcher-Lange, S.; Kessler, D. L.; Rajagopalan, K. V. *J. Biol. Chem.* **1972**, *247*, 7759.
(121) Garrett, R. M.; Bellissimo, D. B.; Rajagopalan, K. V. *Biochim. Biophys. Acta* **1995**, *1262*, 147.
(122) Solomonson, L. P.; Barber, M. J. *Annu. Rev. Plant Physiol. Plant Mol. Biol.* **1990**, *41*, 225.
(123) Crawford, N. M.; Smith, M.; Bellissimo, D.; Davis, R. W. *Proc. Natl. Acad. Sci. U.S.A.* **1988**, *85*, 5006.
(124) Karplus, P. A.; Walsh, K. A.; Herriott, J. R. *Biochemistry* **1984**, *23*, 6576.
(125) Karplus, P. A.; Daniels, M. J.; Herriott, J. R. *Science* **1991**, *251*, 60.
(126) Ozols, J.; Korza, G.; Heinemann, F. S.; Hediger, M. A.; Strittmatter, P. *J. Biol. Chem.* **1985**, *260*, 11953.
(127) Yubisui, T.; Miyata, T.; Iwanaga, S.; Tamura, M.; Yoshida, S.; Takeshita, M.; Nakajima, H. *J. Biochem.* **1984**, *96*, 579.
(128) Nóbrega, F. G.; Ozols, J. *J. Biol. Chem.* **1971**, *246*, 1706.

(129) Johnson, J. L.; Rajagopalan, K. V. *J. Biol. Chem.* **1977**, *252*, 2017.
(130) Southerland, W. M.; Winge, D. R.; Rajagopalan, K. V. *J. Biol. Chem.* **1978**, *253*, 8747.
(131) Kubo, Y.; Ogura, N.; Nakagawa, H. *J. Biol. Chem.* **1988**, *263*, 19684.
(132) Kay, C. J.; Solomonson, L. P.; Barber, M. J. *J. Biol. Chem.* **1986**, *261*, 5799.
(133) Cannons, A. C.; Iida, N.; Solomonson, L. P. *Biochem. J.* **1991**, *278*, 203.
(134) Hyde, G. E.; Campbell, W. H. *Biochem. Biophys. Res. Commun.* **1990**, *168*, 1285.
(135) Campbell, W. H. *Plant Physiol.* **1992**, *99*, 693.
(136) Satoh, T.; Kurihara, F. N. *J. Biochem. (Tokyo)* **1987**, *102*, 191.
(137) McEwan, A. G.; Ferguson, S. J.; Jackson, J. B. *Biochem. J.* **1991**, *274*, 305.
(138) del Campillo-Campbell, A.; Campbell, A. *J. Bacteriol.* **1982**, *149*, 469.
(139) Weiner, J. H.; MacIsaac, D. P.; Bishop, R. E.; Bilous, P. T. *J. Bacteriol.* **1988**, *170*, 1505.
(140) Weiner, J. H.; Rothery, R. A.; Sambasivarao, D.; Trieber, C. A. *Biochim. Biophys. Acta* **1992**, *1102*, 1.
(141) Blasco, F.; Iobbi, C.; Giordano, G.; Chippaux, M.; Bonnefoy, V. *Mol. Gen. Genet.* **1989**, *218*, 249.
(142) Clegg, R. A. *Biochem. J.* **1976**, *153*, 533.
(143) Cammack, R.; Weiner, J. H. *Biochemistry* **1990**, *29*, 8410.
(144) Brito, F.; DeMoss, J. A.; Dubourdeau, M. *J. Bacteriol.* **1995**, *177*, 3728.
(145) Bertram, P. A.; Karrasch, M.; Schmitz, R. A.; Böcher, R.; Albracht, S. P. J.; Thauer, R. K. *Eur. J. Biochem.* **1994**, *220*, 477.
(146) Barber, M. J.; May, H. D.; Ferry, J. G. *Biochemistry* **1986**, *25*, 8150.
(147) Schmitz, R. A.; Richter, M.; Linder, D.; Thauer, R. K. *Eur. J. Biochem.* **1992**, *207*, 559.
(148) Axley, M. J.; Grahame, D. A.; Stadtman, T. C. *J. Biol. Chem.* **1990**, *265*, 18213.
(149) Gladyshev, V. N.; Khangulov, S. V.; Axley, M. J.; Stadtman, T. C. *Proc. Natl. Acad. Sci. U.S.A.* **1994**, *91*, 7708.
(150) Jones, J. B, Stadtman, T. C. *J. Biol. Chem.* **1981**, *256*, 656−663.
(151) Dilworth, G. L. *Arch. Biochem. Biophys.* **1983**, *221*, 565.
(152) Gladyshev, V. N.; Khangulov, S. V.; Stadtman, T. C. *Proc. Natl. Acad. Sci. U.S.A.* **1994**, *91*, 232.
(153) Gladyshev, V. N.; Khangulov, S. V.; Stadtman, T. C. *Biochemistry* **1996**, *35*, 212.
(154) Sommer, S.; Reichenbacher, W.; Schink, B.; Kroneck, P. M. H. *J. Inorg. Biochem.* **1995**, *59*, 729.
(155) Reichenbacher, W.; Rüdiger, A.; Kroneck, P. M. H.; Schink, B. *Eur. J. Biochem.* **1996**, *237*, 406.
(156) Thoenes, U.; Flores, O. L.; Neves, A.; DeVreese, B.; van Beeumen, J. J.; Huber, R.; Romão, M. J.; LeGall, J.; Moura, J. J. G.; Rodrigues-Pousada, C. *Eur. J. Biochem.* **1994**, *220*, 901.
(157) Bray, R. C.; Turner, N. A.; LeGall, J.; Barata, B. A. S.; Moura, J. J. G. *Biochem. J.* **1991**, *280*, 817.
(158) Palmer, G.; Massey, V. *J. Biol. Chem.* **1969**, *244*, 2614.
(159) Hille, R.; Hagen, W. R.; Dunham, W. R. *J. Biol. Chem.* **1985**, *260*, 10569.
(160) Barber, M. J.; Bray, R. C.; Lowe, D. J.; Coughlan, M. P. *Biochem. J.* **1976**, *153*, 297.
(161) Lowe, D. J.; Lynden-Bell, R. M.; Bray, R. C. *Biochem. J.* **1972**, *130*, 239.
(162) Lowe, D. J.; Bray, R. C. *Biochem. J.* **1978**, *169*, 471.
(163) Coffman, R. E.; Buettner, G. R. *J. Phys. Chem.* **1979**, *83*, 2392.
(164) Bertrand, P.; More, C.; Guigliarelli, B.; Fournel, A.; Bennett, B.; Howes, B. *J. Am. Chem. Soc.* **1994**, *116*, 3078.
(165) Komai, H.; Massey, V.; Palmer, G. *J. Biol. Chem.* **1969**, *244*, 1692.
(166) Ryan, M. G.; Ratnam, K.; Hille, R. *J. Biol. Chem.* **1995**, *270*, 19209.
(167) Hille, R.; George, G. N.; Eidsness, M. K.; Cramer, S. P. *Inorg. Chem.* **1989**, *28*, 4018.
(168) Turner, N. A.; Bray, R. C.; Diakun, G. P. *Biochem. J.* **1989**, *260*, 563.
(169) Morpeth, F. F.; George, G. N.; Bray, R. C. *Biochem. J.* **1984**, *220*, 235.
(170) Morpeth, F. F. *Biochim. Biophys. Acta* **1983**, *744*, 328.
(171) Turner, N. A.; Barata, B.; Bray, R. C.; Deistung, J.; Legall, J.; Moura, J. J. G. *Biochem. J.* **1987**, *243*, 755.
(172) Bray, R. C.; Vänngård, T. *Biochem. J.* **1969**, *114*, 725.
(173) Bray, R. C. *Q. Rev. Biophys.* **1988**, *21*, 299.
(174) Pick, F. M.; Bray, R. C. *Biocehm. J.* **1969**, *114*, 735.
(175) Hille, R.; Kim, J. H.; Hemann, C. *Biochemistry* **1993**, *32*, 3973.
(176) Murray, K. N.; Watson, J. G.; Chaykin, S. *J. Biol. Chem.* **1966**, *241*, 4798.
(177) Hille, R.; Sprecher, H. *J. Biol. Chem.* **1987**, *262*, 10914.
(178) Holm, R. H. *Coord. Chem. Rev.* **1990**, *100*, 183.
(179) Caradonna, J. P.; Reddy, P. R.; Holm, R. H. *J. Am. Chem. Soc.* **1988**, *110*, 2139.
(180) Shelton, K. R.; Clarke, J. M, Jr. *Biochemistry* **1967**, *6*, 2735.
(181) Bray, R. C.; Gutteridge, S.; Stotter, D. A.; Tanner, S. J. *Biochem. J.* **1979**, *177*, 357.
(182) D'Ardenne, S. C.; Edmondson, D. E. *Biochemistry* **1990**, *29*, 9046.
(183) McWhirter, R. B.; Hille, R. *J. Biol. Chem.* **1991**, *266*, 23724.
(184) Greenwood, R. J.; Wilson, G. L.; Pilbrow, J. R.; Wedd, A. G. *J. Am. Chem. Soc.* **1993**, *115*, 5385.
(185) Lister, J. H. In *The Chemistry of Hetyerocyclic Compounds: Fused Purines*; Brown, D. J., Ed.; Wiley Interscience: New York, 1971; Part II, Chapter 6.
(186) Skibo, E. B.; Gilchrist, J. H.; Lee, C. H. *Biochemistry* **1987**, *26*, 3032.
(187) Coucouvanis, D.; Toupadakis, A.; Lane, J. D.; Koo, S. M.; Kim, C. G.; Hadjikyriacou, A. *J. Am. Chem. Soc.* **1991**, *113*, 5271.
(188) Howes, B. D.; Bray, R. C.; Richards, R. L.; Turner, N. A.; Bennett, B.; Lowe, D. J. *Biochemistry* **1996**, *35*, 1432.
(189) Rappé, A. K.; Goddard, W. A., III. *Nature* **1980**, *285*, 311.
(190) Rappé, A. K.; Goddard, W. A., III. *J. Am. Chem. Soc.* **1982**, *104*, 448.
(191) Kim, J. H.; Ryan, M. G.; Knaut, H.; Hille, R. *J. Biol. Chem.* **1996**, *271*, 6771.
(192) Albert, A.; Brown, D. J. *J. Chem. Soc.* **1954**, 4350.
(193) Davis, M. D.; Olson, J. S.; Palmer, G. *J. Biol. Chem.* **1982**, *257*, 14730.
(194) Davis, M. D.; Olson, J. S.; Palmer, G. *J. Biol. Chem.* **1984**, *259*, 3526.
(195) Oertling, W. A.; Hille, R. *J. Biol. Chem.* **1990**, *265*, 17446.
(196) Hille, R.; Stewart, R. C. *J. Biol. Chem.* **1984**, *259*, 1570.
(197) Kim, J. H.; Hille, R. *J. Biol. Chem.* **1993**, *268*, 44.
(198) Bray, R. C.; George, G. N. *Biochem. Soc. Trans.* **1985**, *13*, 560.
(199) Bray, R. C.; Palmer, G.; Beinert, H. *J. Biol. Chem.* **1964**, *239*, 2667.
(200) Palmer, G.; Bray, R. C.; Beinert, H. *J. Biol. Chem.* **1964**, *239*, 2657.
(201) Edmondson, D.; Ballou, D.; van Heuvelen, A.; Palmer, G.; Massey, V. *J. Biol. Chem.* **1973**, *248*, 6135.
(202) Olson, J. S.; Ballou, D. P.; Palmer, G.; Massey, V. *J. Biol. Chem.* **1974**, *249*, 4363.
(203) Olson, J. S.; Ballou, D. P.; Palmer, G.; Massey, V. *J. Biol. Chem.* **1974**, *249*, 4342.
(204) Hille, R.; Massey, V. *J. Biol. Chem.* **1981**, *256*, 9090.
(205) Porras, A. G.; Olson, J. S.; Palmer, G. *J. Biol. Chem.* **1981**, *256*, 9096.
(206) Symons, M. C. R.; Taiwo, F. A.; Peterson, R. L. *J. Chem. Soc., Faraday Trans.* **1989**, *85*, 4063.
(207) Tanner, S.; Bray, R. C.; Bergmann, F. *Biochem. Soc. Trans.* **1978**, *6*, 1328.
(208) Wahl, R. C.; Rajagopalan, K. V. *J. Biol. Chem.* **1982**, *257*, 1354.
(209) Malthouse, J. P. G.; Bray, R. C. *Biochem. J.* **1980**, *191*, 265.
(210) Malthouse, J. P. G.; George, G. N.; Lowe, D. J.; Bray, R. C. *Biochem. J.* **1981**, *199*, 629.
(211) Gutteridge, S.; Bray, R. C. *Biochem. J.* **1980**, *189*, 615.
(212) George, G. N.; Bray, R. C. *Biochemistry* **1988**, *27*, 3603.
(213) Dowerah, D.; Spence, J. T.; Singh, R.; Wedd, A. G.; Wilson, G. L.; Farchione, F.; Enemark, J. H.; Kristofzski, J.; Bruck, M. *J. Am. Chem. Soc.* **1987**, *109*, 5655.
(214) Wilson, G. L.; Greenwood, R. J.; Pilbrow, J. R.; Spence, J. T.; Wedd, A. G. *J. Am. Chem. Soc.* **1991**, *113*, 6803.
(215) Lorigan, G. A.; Britt, R. D.; Kim, J. H.; Hille, R. *Biochim. Biophys. Acta* **1994**, *1185*, 284.
(216) Lowe, D. J.; Barber, M. J.; Pawlik, R. T.; Bray, R. C. *Biochem. J.* **1976**, *155*, 81.
(217) Howes, B. D.; Pinhal, N. M.; Turner, N. A.; Bray, R. C.; Anger, G.; Ehrenberg, A.; Raynor, J. B.; Lowe, D. J. *Biochemistry* **1990**, *29*, 6120.
(218) Howes, B. D.; Bennett, B.; Bray, R. C.; Richards, R. L.; Lowe, D. J. *J. Am. Chem. Soc.* **1994**, *116*, 11624.
(219) Davis, M. D.; Edmondson, D. E.; Müller, F. *Eur. J. Biochem.* **1984**, *145*, 237.
(220) Johnson, J. L.; London, R. E.; Rajagopalan, K. V. *Proc. Natl. Acad. Sci. U.S.A.* **1989**, *86*, 6493.
(221) Howes, B. D.; Bennett, B.; Koppenhöfer, A.; Lowe, D. J.; Bray, R. C. *Biochemistry* **1991**, *30*, 3969.
(222) Gutteridge, S.; Tanner, S. J.; Bray, R. C. *Biochem. J.* **1978**, *175*, 869.
(223) Gutteridge, S.; Tanner, S. J.; Bray, R. C. *Biochem. J.* **1978**, *175*, 887.
(224) Malthouse, J. P. G.; Bray, R. C. *Biochem. J.* **1983**, *215*, 101.
(225) Mondal, M. S.; Mitra, S. *Biochemistry* **1994**, *33*, 10305.
(226) Bray, R. C.; Barber, M. J.; Lowe, D. J. *Biochem. J.* **1978**, *171*, 653.
(227) Tsopanakis, A. D.; Tanner, S. J.; Bray, R. C. *Biochem. J.* **1978**, *175*, 879.
(228) Bray, R. C.; Gutteridge, S. *Biochemistry* **1982**, *21*, 5992.
(229) Babcock, G. T.; Vickery, L. E.; Palmer, G. *J. Biol. Chem.* **1978**, *253*, 2400.
(230) Cammack, R.; Barber, M. J.; Bray, R. C. *Biochem. J.* **1976**, *157*, 469.
(231) Hille, R.; Massey, V. *J. Biol. Chem.* **1991**, *266*, 17401.
(232) Palmer, G.; Olson, J. S. In *Molybdenum Chemistry of Biological Significance*; Coughlan, M., Ed.; Pergamon: Elmsford, NY, 1980; p 187.
(233) Porras A. G.; Palmer, G. *J. Biol. Chem.* **1982**, *257*, 11617.
(234) Barber, M. J.; Siegel, L. M. *Biochemistry* **1982**, *21*, 1638.

(235) Spence, J. T.; Barber, M. J.; Siegel, L. M. *Biochemistry* **1982**, 21, 1656.
(236) Bhattacharyya, A.; Tollin, G.; Davis, M.; Edmondson, D. E. *Biochemistry* **1983**, *22*, 5270.
(237) Walker, M. C.; Hazzard, J. T.; Tollin, G.; Edmondson, D. E. *Biochemistry* **1991**, *30*, 5912.
(238) Hille, R.; Massey, V. *J. Biol. Chem.* **1986**, *261*, 1241.
(239) Anderson, R. F.; Hille, R.; Massey, V. *J. Biol. Chem.* **1986**, *261*, 15870.
(240) Hille, R.; Anderson, R. F. *J. Biol. Chem.* **1991**, *266*, 5608.
(241) Buxton, G. V. In *The Study of Fast Processes and Transient Species by Electron Pulse Radiolysis*; Baxendale, J. H., Busi, F., Eds.; D. Reidel Publishing Co.: Dordrecht, Holland, 1982; p 241.
(242) Hille, R. *Biochemistry* **1991**, *30*, 8522.
(243) Mizzer, J. P.; Thorpe, C. *Biochemistry* **1981**, *20*, 4965.
(244) Gorelick, R. J.; Schopfer, L. M.; Ballou, D. P.; Massey, V.; Thorpe, C. *Biochemistry* **1985**, *24*, 6830.
(245) Della Corte, E.; Stirpe, F. *Biochem. J.* **1972**, *126*, 739.
(246) Battelli, M. G.; Lorenzoni, E.; Stirpe, F. *Biochem. J.* **1973**, *131*, 191.
(247) Nakamura, M.; Yamazaki, I. *J. Biochem.* **1982**, *92*, 1279.
(248) Nishino, T.; Nishino, T.; Schopfer, L. M.; Massey, V. *J. Biol. Chem.* **1989**, *264*, 2518.
(249) Waud, W. R.; Rajagopalan, K. V. *Arch. Biochem. Biophys.* **1976** *172*, 354.
(250) Waud, W. R.; Rajagopalan, K. V. *Arch. Biochem. Biophys.* **1976** *172*, 365.
(251) Hunt, J.; Massey, V. *J. Biol. Chem.* **1992**, *267*, 21479.
(252) Sato, A.; Nishino, T.; Noda, K.; Amaya, Y.; Nishino, T. *J. Biol. Chem.* **1995**, *270*, 2818.
(253) Bray, R. C.; Bennett, B.; Burke, J. F.; Chovnick, A. *Biochem. Soc. Trans.* **1996**, *24*, 99.
(254) Ratnam, K.; Brody, M.; Hille, R. *Prep. Biochem.* **1996**, *26*, 143.
(255) Schopfer, L. M.; Massey, V.; Nishino, T. *J. Biol. Chem.* **1988**, *263*, 13528.
(256) Hunt, J.; Massey, V. *J. Biol. Chem.* **1994**, *269*, 18904.
(257) Nishino, T.; Nishino,T. *Biochemistry* **1987**, *26*, 3068.
(258) Nishino, T.; Nishino, T. *J. Biol. Chem.* **1989**, *264*, 5468.
(259) Massey, V.; Schopfer, L. M.; Nishino, T.; Nishino, T. *J. Biol. Chem.* **1989**, *264*, 10567.
(260) Saito, T.; Nishino, T.; Massey, V. *J. Biol. Chem.* **1989**, *264*, 15930.
(261) Barber, M. J.; Bray, R. C.; Cammack, R.; Coughlan, M. P. *Biochem. J.* **1977**, *163*, 279.
(262) Hunt, J.; Massey, V.; Dunham, W. R.; Sands, R. H. *J. Biol. Chem.* **1993**, *268*, 18685.
(263) Ratnam, K.; Hille, R. *Biochem. Biophys. Res. Commun.* **1993**, *194*, 1097.
(264) Kobayashi, K.; Miki, M.; Okamoto, K, Nishino, T. *J. Biol. Chem.* **1993**, *268*, 24642.
(265) Rajagopalan, K. V.; Fridovich, I.; Handler, P. *J. Biol. Chem.* **1962**, *237*, 922.
(266) Knox, W. E.; Grossman, W. I. *J. Biol. Chem.* **1946**, *166*, 391.
(267) Krenitsky, T. A.; Neil, S. M.; Elion, G. B.; Hitchings, G. H. *Arch. Biochem. Biophys.* **1972**, *150*, 585.
(268) Tatsumi, K.; Kitamura, S.; Yamada, H. *Biochim. Biophys. Acta* **1983**, *747*, 86.
(269) Branzoli, U.; Massey, V. *J. Biol.Chem.* **1974**, *249*, 4346.
(270) Palmer, G. *Biochim. Biophys. Acta* **1962**, *56*, 444.
(271) Tomita, S.; Tsujita, M.; Ichikawa, Y. *FEBS Lett.* **1993**, *336*, 272.
(272) Branzoli, U.; Massey, V. *J. Biol. Chem.* **1974**, *249*, 4339.
(273) Bray, R. C.; George, G. N.; Gutteridge, S.; Norlander, L.; Stell, J. G. P.; Stubley, C. *Biochem. J.* **1982**, *203*, 263.
(274) Barber, M. J.; Coughlan, M. P.; Rajagopalan, K. V.; Siegel, L. M. *Biochemistry* **1982**, *21*, 3561.
(275) Coughlan, M. P.; Rajagopalan, K. V.; Handler, P. *J. Biol. Chem.* **1969**, *244*, 2658.
(276) Rajagopalan, K. V.; Handler, P.; Palmer, G.; Beinert, H. *J. Biol. Chem.* **1968**, *243*, 3784.
(277) Rajagopalan, K. V.; Handler, P.; Palmer, G.; Beinert, H. *J. Biol. Chem.* **1968**, *243*, 3797.
(278) Coughlan, M. P.; Johnson, J. L.; Rajagopalan, K. V. *J. Biol. Chem.* **1980**, *255*, 2694.
(279) Koshiba, T.; Saito, E.; Ono, N.; Yamamoto, N.; Sato, M. *Plant Physiol.* **1996**, *110*, 781.
(280) Lamy, M. T.; Gutteridge, S.; Bray, R. C. *Biochem. J.* **1980**, *185*, 397.
(281) Bray, R. C.; Gutteridge, S.; Lamy, M. T.; Wilkinson, T. *Biochem. J.* **1983**, *211*, 227.
(282) George, G. N. *J. Magn. Res.* **1985**, *64*, 384.
(283) Cramer, S. P.; Johnson, J. L.; Rajagopalan, K. V.; Sorrell, T. N. *Biochem. Biophys. Res. Commun.* **1979**, *91*, 434.
(284) Bray, R. C.; Lamy, M. T.; Gutteridge, S.; Wilkinson, T. *Biochem. J.* **1982**, *201*, 241.
(285) George, G. N.; Prince, R. C.; Kipke, C. A.; Sunde, R. A.; Enemark, J. H. *Biochem. J.* **1988**, *256*, 307.
(286) Gutteridge, S.; Lamy, M. T.; Bray, R. C. *Biochem. J.* **1980**, *191*, 285.
(287) Berg, J. M.; Holm, R. H. *J. Am. Chem. Soc.* **1984**, *106*, 3035.
(288) Berg, J. M.; Holm, R. H. *J. Am. Chem. Soc.* **1985**, *107*, 917.
(289) Berg, J. M.; Holm, R. H. *J. Am. Chem. Soc.* **1985**, *107*, 925.
(290) Gheller, S. F.; Schultz, B. E.; Scott, M. J.; Holm, R. H. *J. Am. Chem. Soc.* **1992**, *114*, 6934.
(291) Roberts, S. A.; Young, C. G.; Kipke, C. A.; Cleland, W. E., Jr.; Yamanouchi, K.; Carducci, M. D.; Enemark, J. H. *Inorg. Chem.* **1990**, *29*, 3650.
(292) Xiao, Z.; Young, C. G.; Enemark, J. H.; Wedd, A. G. *J. Am. Chem. Soc.* **1992**, *114*, 9194.
(293) Schultz, B. E.; Holm, R. H. *Inorg. Chem.* **1993**, *32*, 4244.
(294) Schultz, B. E.; Gheller, S. F.; Muetterties, M. C.; Scott, M. J.; Holm. R. H. *J. Am. Chem. Soc.* **1993**, *115*, 2714.
(295) Holm, R. H.; Donahue, J. P. *Polyhedron* **1993**, *12*, 571.
(296) Ortiz de Montellano, P. R. *Cytochrome P-450. Structure Mechanism and Biochemistry*, 2nd ed.; Plenum Press: New York, 1994.
(297) Enemark, J. H.; Young, C. G. *Adv. Inorg. Chem.* **1993**, *40*, 1.
(298) Brody, M. S.; Hille, R. *Biochim. Biophys. Acta* **1995**, *1253*, 133.
(299) Cramer, S. P.; Gray, H. B.; Scott, N. S.; Barber, M.; Rajagopalan, K. V. In *Molybdenum Chemistry of Biological Significance*; Newton, W. E., Otsuka, S., Eds.; Plenum Press: New York, 1980; pp 157−168.
(300) Spence, J. T.; Kipke, C. A.; Enemark, J. H.; Sunde, R. A. *Inorg. Chem.* **1991**, *30*, 3011.
(301) Kipke, C. A.; Cusanovich, M. A.; Tollin, G.; Sunde, R. A.; Enemark, J. H. *Biochemistry* **1988**, *27*, 2918.
(302) Sullivan, E. P., Jr.; Hazzard, J. T.; Tollin, G.; Enemark, J. H. *J. Am. Chem. Soc.* **1992**, *114*, 9662.
(303) Basu, P.; Raitsimring, A. M.; LaBarre, M. J.; Dhawan, I. K.; Weibrecht, J. L.; Enemark, J. H. *J. Am. Chem. Soc.* **1994**, *116*, 7166.
(304) Basu, P.; Shokhirev, N. V.; Enemark, J. H.; Walker, F. A. *J. Am. Chem. Soc.* **1995**, *117*, 9042.
(305) Wray, J. L.; Kinghorn, J. R. *Molecular and Genetic Aspects of Nitrate Assimilation*; Oxford University Press: New York, 1989.
(306) Solomonson, L. P.; Barber, M. J.; Robbins, A. P.; Oaks, A. *J. Biol. Chem.* **1986**, *261*, 11290.
(307) Cannons, A. C.; Barber, M. J.; Solomonson, L. P. *J. Biol. Chem.* **1993**, *268*, 3268.
(308) Lu, G.; Campbell, W. H.; Schneider, G.; Lindqvist, Y. *Structure* **1994**, *2*, 809.
(309) Schulz, G. E. *Curr. Opin. Struct. Biol.* **1992**, *2*, 61.
(310) Correll, C. C.; Batie, C. J.; Ballou, D. P.; Ludwig, M. L. *Science* **1992**, *258*, 1604.
(311) Lu, G.; Lindqvist, Y.; Schneider, G.; Dwivedi, U.; Campbell, W. H. *J. Mol. Biol.* **1995**, *248*, 931.
(312) Xia, Z.-X.; Mathews, F. S. *J. Mol. Biol.* **1990**, *212*, 837.
(313) Dwivedi, U. N.; Shiraishi, N.; Campbell, W. H. *J. Biol. Chem.* **1994**, *269*, 13785.
(314) Ratnam, K.; Shiraishi, N.; Campbell, W. H.; Hille, R. *J. Biol. Chem.* **1995**, *270*, 24067.
(315) Cramer, S. P.; Solomonson, L. P.; Adams, M. W. W.; Mortenson, L. E. *J. Am. Chem. Soc.* **1984**, *106*, 1467.
(316) Solomonson, L. P.; Barber, M. J.; Howard, W. D.; Johnson, J. L.; Rajagopalan, K. V. *J. Biol. Chem.* **1984**, *259*, 849.
(317) Kay, C. J.; Barber, M. J. *Biochemistry* **1989**, *28*, 5750.
(318) Kay, C. J.; Barber, M. J.; Solomonson, L. J.; Kau, D.; Cannons, A. C.; Hipkin, C. R. *Biochem. J.* **1990**, *272*, 545.
(319) Gutteridge, S.; Bray, R. C.; Notton, BA.; Fido, R. J.; Hewitt, E. J. *Biochem. J.* **1983**, *213*, 137.
(320) Kay, C. J.; Barber, M. J.; Solomonson, L. P. *Biochemistry* **1988**, *27*, 6142.
(321) Kay, C. J.; Solomonson, L. P.; Barber, M. J. *Biochemistry* **1990**, *29*, 10823.
(322) Spence, J. T.; Barber, M. J.; Solomonson, L. P. *Biochem. J.* **1988**, *250*, 921.
(323) Kay, C. J.; Barber, M. J.; Notton, B. A.; Solomonson, L. P. *Biochem. J.* **1989**, *263*, 285.
(324) Douglas, P.; Morrice, N.; MacKintosh, C. *FEBS Lett.* **1995**, *377*, 113.
(325) Abo, M.; Tachibana, M.; Okubo, A.; Yamazaki, S. *Bioorg. Med. Chem.* **1995**, *3*, 109.
(326) Bastian, N. R.; Kay, C. J.; Barber, M. J.; Rajagopalan, K. V. *J. Biol. Chem.* **1991**, *266*, 45.
(327) Gruber, S.; Kilpatrick, L.; Bastian, N. R.; Rajagopalan, K. V.; Spiro, T. G. *J. Am. Chem. Soc.* **1990**, *112*, 8179−8180.
(328) Kilpatrick, L.; Rajagopalan, K. V.; Hilton, J.; Bastian, N. R.; Stiefel, E. I.; Pilato, R. S.; Spiro, T. G. *Biochemistry* **1995**, *34*, 3032.
(329) Benson, N.; Farrar, J. A.; McEwan, A. G.; Thomson, A. J. *FEBS Lett.* **1992**, *307*, 169.
(330) Finnegan, M. G.; Hilton, J.; Rajagopalan, K. V.; Johnson, M. K. *Inorg. Chem.* **1993**, *32*, 2616−2617.
(331) Subramanian, P.; Burgmayer, S.; Richards, S.; Szalai,V.; Spiro, T. G. *Inorg. Chem.* **1990**, *29*, 3849.
(332) Carducci, M. D.; Brown, C.; Solomon, E. I.; Enemark, J. H. *J. Am. Chem. Soc.* **1994**, *116*, 11856.
(333) Schultz, B. E.; Hille, R.; Holm, R. H. *J. Am. Chem. Soc.* **1995**, *117*, 827.
(334) Bennett, B.; Benson, N.; McEwan, A. G.; Bray, R. C. *Eur. J. Biochem.* **1994**, *223*, 321.
(335) del Campillo-Campbell, A.; Dykhuizen, D.; Cleary, P. P. *Methods Enzymol.* **1979**, *62*, 379.

(336) Pierson, D. E.; Campbell, A. *J. Bacteriol.* **1990**, *172*, 2194.
(337) Pollock, V. V.; Barber, M. J. *Arch. Biochem. Biophys.* **1995**, *318*, 322.
(338) del Campillo-Campbell, A.; Campbell, A. *J. Mol. Evol.* **1996**, *42*, 85.
(339) Minetti, G.; Balduini, C.; Brovelli, A. *Ital. J. Biochem.* **1994**, *43*, 273.
(340) Rahman, M. A.; Brot, N.; Weissbach, H. *Cell. Mol. Biol.* **1992**, *38*, 529.
(341) Brot, N.; Rahman, M. A.; Moskovitz, J.; Weissbach, H. *Methods Enzymol.* **1995**, *251*, 462.
(342) Bilous, P. T.; Weiner, J. H. *J. Bacteriol.* **1985**, *163*, 369.
(343) Loosmore, S. M.; Shortreed, J. M.; Coleman, D. C.; England, D. M.; Klein, M. H. *Gene* **1996**, *169*, 137.
(344) Lorenzen, J.; Steinwachs, S.; Unden, G. *Arch. Microbiol.* **1994**, *162*, 277.
(345) Rothery, R.; Simala Grant, J. L.; Johnson, J. L.; Rajagopalan, K. V.; Weiner, J. H. *J. Bacteriol.* **1995**, *177*, 2057.
(346) Trieber, C. A.; Rothery, R. A.; Weiner, J. H. *J. Biol. Chem.* **1994**, *269*, 7103.
(347) Trieber, C. A.; Rothery, R. A.; Weiner, J. H. *J. Biol. Chem.* **1996**, *271*, 4620.
(348) Bilous, P. T.; Cole, S. T.; Anderson, W. F.; Weiner, J. H. *Mol. Microbiol.* **1988**, *2*, 785.
(349) Rothery, R. A.; Weiner, J. H. *Biochemistry* **1991**, *30*, 8296.
(350) Rothery, R. A.; Weiner, J. H. *Biochemistry* **1996**, *35*, 3247.
(351) Sambasivarao, D.; Scraba, D. G.; Trieber, C.; Weiner, J. H. *J. Bacteriol.* **1990**, *172*, 5938.
(352) Rothery, R. A.; Weiner, J. H. *Biochemistry* **1993**, *32*, 5855.
(353) Weiner, J. H.; Shaw, G.; Turner, R. J.; Trieber, C. A. *J. Biol. Chem.* **1993**, *268*, 3238.
(354) Guerrero, M. G.; Vega, J. M.; Losada, M. *Annu. Rev. Plant Physiol.* **1981**, *32*, 169.
(355) Jones, R. W.; Lamont, A.; Garland, P. B. *Biochem. J.* **1980**, *190*, 79.
(356) Iobbi, C.; Santini, C.-L.; Bonnefoy, V.; Giordano, G. *Eur. J. Biochem.* **1987**, *168*, 451.
(357) Blasco, F.; Iobbi, C.; Ratouchniak, J.; Bonnefoy, V.; Chippaux, M. *Mol. Gen. Genet.* **1990**, *222*, 104.
(358) Sodergren, E. J.; DeMoss, J. A. *J. Bacteriol.* **1988**, *170*, 1721.
(359) Sodergren, E. J.; Hsu, P.-Y.; DeMoss, J. A. *J. Biol. Chem.* **1988**, *263*, 16156.
(360) Dubourdieu, M.; DeMoss, J. A. *J. Bacteriol.* **1992**, *174*, 867.
(361) Blasco, F.; Pommier, J.; Augier, V.; Chippaux, M.; Giordano, G. *Mol. Microbiol.* **1992**, *6*, 221.
(362) Ruiz-Herrera, J.; DeMoss, J. A. *J. Bacteriol.* **1969**, *99*, 720.
(363) Enoch, H. G.; Lester, R. L. *Biochem. Biophys. Res. Commun.* **1974**, *61*, 1234.
(364) MacGregor, C. H. *J. Bacteriol.* **1975**, *121*, 1111.
(365) Chaudhry, G. R.; MacGregor, C. H. *J. Biol. Chem.* **1983**, *258*, 5819.
(366) Forget, P. *Eur. J. Biochem.* **1974**, *42*, 325.
(367) Vincent, S. P.; Bray, R. C. *Biochem. J.* **1978**, *171*, 639.
(368) Enoch, H. G.; Lester, R. L. *J. Biol. Chem.* **1975**, *250*, 6693.
(369) Morpeth, F. F.; Boxer, D. H. *Biochemistry* **1985**, *24*, 40.
(370) MacGregor, C. H.; Schnaitman, C. A.; Normansell, D. E.; Hodgins, M. G. *J. Biol. Chem.* **1974**, *249*, 5321.
(371) Adams, M. W. W.; Mortenson, L. E. *J. Biol. Chem.* **1982**, *257*, 1791.
(372) George, G. N.; Turner, N. A.; Bray, R. C.; Morpeth, F. F.; Boxer, D. H.; Cramer, S. P. *Biochem. J.* **1989**, *259*, 693.
(373) George, G. N.; Bray, R. C.; Morpeth, F. F.; Boxer, D. H. *Biochem. J.* **1985**, *227*, 925.
(374) Johnson, M. K.; Bennett, D. E.; Morningstar, J. E.; Adams, M. W. W.; Mortenson, L. E. *J. Biol. Chem.* **1985**, *260*, 5456.
(375) Emptage, M. H.; Kent, T. A.; Huynh, B. H.; Rawlings, J.; Orme-Johnson, W. H.; Münck, E. *J. Biol. Chem.* **1980**, *255*, 1793.
(376) Huynh, B. H.; Moura, J. J. G.; Moura, I.; Kent, T. A.; LeGall, J.; Xavier, A. V.; Münck, E. *J. Biol. Chem.* **1980**, *255*, 3242.
(377) Hille, R.; Yoshida, T.; Tarr, G. E.; Williams, C. H., Jr.; Ludwig, M. L.; Fee, J. A.; Kent, T. A.; Hyunh, B. H.; Münck, E. *J. Biol. Chem.* **1983**, *258*, 13008.
(378) Godfrey, C.; Greenwood, C.; Thomson, A. J.; Bray, R. C.; George, G. N. *Biochem. J.* **1984**, *224*, 601.
(379) Vincent, S. P. *Biochem. J.* **1979**, *177*, 757.
(380) Guigliarelli, B.; Asso, M.; More, C.; Augier, V.; Blasco F.; Pommier, J.; Giordano, G.; Bertrand, P. *Eur. J. Biochem.* **1992**, *207*, 61.
(381) Augier, V.; Guigliarelli, B.; Asso, M.; Bertrand, P.; Frixon, C.; Giordano, G.; Chippaux, M.; Blasco, F. *Biochemistry* **1993**, *32*, 2013.
(382) Augier, V.; Asso, M.; Guigliarelli, B.; More, C.; Bertrand, P.; Santini, C.-L.; Blasco, F.; Chippaux, M.; Giordano, G. *Biochemistry* **1993**, *32*, 5099.
(383) Guigliarelli, B.; Magalin, A.; Asso, M.; Bertrand, P.; Frixon, C.; Giordano, G.; Blasco, F. *Biochemistry* **1996**, *35*, 4828.
(384) Buc, J.; Santini, C.-L.; Blasco, F.; Giordani, R.; Cárdena, M. L.; Chippaux, M.; Cornish-Bowden, A.; Giordano, G. *Eur. J. Biochem.* **1995**, *234*, 766.
(385) Berks, B. C.; Richardson, D. J.; Robinson, C.; Reilly, A.; Aplin, R. T.; Ferguson, S. J. *Eur. J. Biochem.* **1994**, *220*, 117.
(386) Ludwig, W.; Mittenhuber, G.; Friedrich, C. G. *Int. J. Syst. Bacteriol.* **1993**, *43*, 363.
(387) Siddiqui, R. A.; Warnecke-Eberz, U.; Hengsberger, A.; Schneider, B.; Kostka, S.; Friedrich, B. *J. Bacteriol* **1993**, *175*, 5867.
(388) Satoh, T. *Plant Cell Physiol.* **1981**, *22*, 443.
(389) Reyes, F.; Roldán, M. D.; Klipp, W.; Castillo, F.; Moreno-Vivián, C. *Mol. Microbiol.* **1996**, *19*, 1307.
(390) McEwan, A. G.; Wetzstein, H. G.; Meyer, O.; Jackson, J. B.; Ferguson, S. J. *Arch. Microbiol.* **1987**, *147*, 340.
(391) Richardson, D. J.; McEwan, A. G.; Page, M. D.; Jackson, J. B.; Ferguson, S. J. *Eur. J. Biochem.* **1990**, *194*, 263.
(392) Breton, J.; Berks, B. C.; Reilly, A.; Thomson, A. J.; Ferguson, S. J.; Richardson, D. J. *FEBS Lett.* **1994**, *345*, 76.
(393) Berks, B. C.; Richardson, D. J.; Reilly, A.; Willis, A. C.; Ferguson, S. J. *Biochem. J.* **1995**, *309*, 983.
(394) Choe, M.; Reznikoff, W. S. *J. Bacteriol.* **1993**, *175*, 1165.
(395) Grove, J.; Tanapongpipat, S.; Thomas, G.; Griffiths, T. L.; Crooke, H.; Cole, J. *Mol. Microbiol.* **1996**, *19*, 467.
(396) Bennett, B.; Berks, B. C.; Ferguson, S. J.; Thomson, A. J.; Richardson, D. J. *Eur. J. Biochem.* **1994**, *226*, 789.
(397) Sears, H. J.; Bennett, B.; Spiro, S.; Thomson, A. J.; Richardson, D. J. *Biochem. J.* **1995**, *310*, 311.
(398) Jollie, D. R.; Lipscomb, J. D. *J. Biol. Chem.* **1991**, *266*, 21853.
(399) Yamamoto, I.; Saiki, T.; Liu, S.-M.; Ljungdahl, L. G. *J. Biol. Chem.* **1983**, *258*, 1826.
(400) Adams, M. W. W.; Mortenson, L. E. In *Molybdenum Enzymes*; Spiro, T. G., Ed.; Wiley-Interscience: New York, 1985; p 519.
(401) Zinoni, F.; Birkmann, A.; Stadtman, T. C.; Böck, A. *Proc. Natl. Acad. Sci. U.S.A.* **1986**, *83*, 4650.
(402) Berg, B. L.; Stewart, V. *Genetics* **1990**, *125*, 691.
(403) Berg, B. L.; Li, J.; Heider, J.; Stewart, V. *J. Biol. Chem.* **1991**, *266*, 22380.
(404) Stewart, V. *Microbiol Rev.* **1988**, *52*, 190.
(405) Abaibou, H.; Pommier, J.; Benoit, S.; Giordano, G.; Mandrand-Berthelot, M.-A. *J. Bacteriol.* **1995**, *177*, 7141.
(406) Blattner, F. R.; Burland, V. D.; Plunkett, G., III; Sofia, H. J.; Daniels, D. L. *Nucleic Acids Res.* **1993**, *21*, 5408.
(407) Sawers, G.; Heider, J.; Zehelein, E.; Böck, A. *J. Bacteriol.* **1991**, *173*, 4983.
(408) Zinoni, F.; Birkmann, A.; Leinfelder, W.; Böck, A. *Proc. Natl. Acad. Sci. U.S.A.* **1987**, *84*, 3156.
(409) Shuber, A. P.; Orr, E. C.; Recny, M. A.; Schendel, P. F.; May, H. D.; Schauer, N. L.; Ferry, J. G. *J. Biol. Chem.* **1986**, *261*, 12942.
(410) Bokranz, M.; Gutmann, M.; Körner, C.; Kojro, E.; Fahrenholz, F.; Lauterbach, F.; Kröger, A. *Arch. Microbiol.* **1991**, *156*, 119.
(411) Gladyshev, V. N.; Boyington, J. C.; Khangulov, S. V.; Grahame, D. A.; Stadtman, T. C.; Sun, P. C. *J. Biol. Chem.* **1996**, *271*, 8095.
(412) Axley, M. J.; Böck, A.; Stadtman, T. C. *Proc. Natl. Acad. Sci. U.S.A.* **1991**, *88*, 8450.
(413) Axley, M. J.; Grahame, D. A. *J. Biol. Chem.* **1991**, *266*, 13731.
(414) Schauer, N. L.; Ferry, J. G. *J. Bacteriol.* **1986**, *165*, 405.
(415) Jankielewicz, A.; Schmitz, R. A.; Klimmek, O.; Kröger, A. *Arch. Microbiol.* **1994**, *162*, 238.
(416) Schauer, N. L.; Ferry, J. G. *J. Bacteriol.* **1983**, *155*, 467.
(417) Barber, M. J.; Siegel, L. M.; Schauer, N. L.; May, H. D.; Ferry, J. G. *J. Biol. Chem.* **1983**, *258*, 10839.
(418) Unden, G.; Kröger, A. *Biochim. Biophys. Acta* **1983**, *725*, 325.
(419) Kröger, A.; Dorrer, E.; Winkler, E. *Biochim. Biophys. Acta* **1980**, *589*, 118.
(420) Jankielewicz, A.; Klimmek, O.; Kröger, A. *Biochim. Biophys. Acta* **1995**, *1231*, 157.
(421) Kotzian, S.; Kreis-Kleinschmidt; Krafft, T.; Klimmek, O.; Macy, J. M.; Kröger, A. *Arch. Microbiol.* **1966**, *165*, 65.
(422) Krafft, T.; Bokranz, M.; Klimmek, O.; Schröder, I.; Fahrenholz, F.; Kojro, E.; Köger, A. *Eur. J. Biochem.* **1992**, *206*, 503.
(423) DiMarco, A. A.; Bobik, T. A.; Wolfe, R. S. *Annu. Rev. Biochem.* **1990**, *59*, 355.
(424) Hochheimer, A.; Schmitz, R. A.; Thauer, R. K.; Hedderich, R. *Eur. J. Biochem.* **1995**, *234*, 910.
(425) Vorholt, J. A.; Vaupel, M.; Thauer, R. K. *Eur. J. Biochem.* **1996**, *236*, 309.
(426) Schmitz, R. A.; Albracht, S. P. J.; Thauer, R. K. *Eur. J. Biochem.* **1992**, *209*, 1013.
(427) Reeve, J. N.; Beckler, G. S.; Cram, D. S.; Hamilton, P. T.; Brown, J. W.; Krzycki, J. A.; Kolodziej, A. F.; Alex, L.; Orme-Johnson, W. H.; Walsh, C. T. *Proc. Natl. Acad. Sci. U.S.A.* **1989**, *86*, 3031.
(428) Karrasch, M.; Börner, G.; Thauer, R. K. *FEBS Lett.* **1990**, *274*, 48.
(429) Bertram, P. A.; Schmitz, R. A.; Linder, D.; Thauer, R. K. *Arch. Microbiol.* **1994**, *161*, 220.
(430) Schmitz, R. A.; Albracht, S. P. J.; Thauer, R. K. *FEBS Lett.* **1992**, *309*, 78.
(431) Schmitz, R. A.; Bertram, P. A.; Thauer, R. K. *Arch. Microbiol.* **1994**, *161*, 528.

CR950061T